FINAL REPORT

FHWA/IN/JTRP-2001/10-II

FATIGUE BEHAVIOR OF BEAM DIAPHRAGM CONNECTIONS WITH INTERMITTENT FILLET WELDS

PART II: BRITTLE FRACTURE EXAMINATION OF THE I-64 BLUE RIVER BRIDGE

By

Mark D. Bowman
Professor of Civil Engineering

Purdue University
School of Civil Engineering

Joint Transportation Research Project
Project No: C-36-56KK
File No: 7-4-37
SPR-2113

Prepared in Cooperation with the
Indiana Department of Transportation and
the U.S. Department of Transportation
Federal Highway Administration

Purdue University
West Lafayette, IN 47907-1284
March 2002

TECHNICAL REPORT STANDARD TITLE PAGE

1. Report No.	2. Government Accession No.	3. Recipient's Catalog No.
FHWA/IN/JTRP-2001/10-II		

4. Title and Subtitle	5. Report Date
Fatigue Behavior of Beam Diaphragm Connections With Intermittent Fillet Welds Part II: Brittle Fracture Examination of the I-64 Blue River Bridge	March 2002
	6. Performing Organization Code
7. Author(s) Mark D. Bowman	8. Performing Organization Report No. FHWA/IN/JTRP-2001/10-II
9. Performing Organization Name and Address Joint Transportation Research Program 1284 Civil Engineering Building Purdue University West Lafayette, Indiana 47907-1284	10. Work Unit No.
	11. Contract or Grant No. SPR-2113
12. Sponsoring Agency Name and Address Indiana Department of Transportation State Office Building 100 North Senate Avenue Indianapolis, IN 46204	13. Type of Report and Period Covered Final Report
	14. Sponsoring Agency Code

15. Supplementary Notes

Prepared in cooperation with the Indiana Department of Transportation and Federal Highway Administration.

16. Abstract

This report is the third of a two-part, three volume final report presenting the findings of the research work that was undertaken to evaluate the behavior of Indiana highway bridges with diaphragm members welded directly to the web of the primary beams and girders. Fatigue cracks have been observed at several bridges that utilize the welded diaphragm connection. The seriousness of the cracking and the corresponding potential risk on the integrity of the bridge superstructure were assessed. Inspection and repair guidelines for bridges with welded diaphragm connections were also developed as part of the research effort. This volume presents the results of an evaluation of a brittle fracture crack that was discovered in one of the welded plate girder members of the I-64 Blue River Bridge in Harrison County of southern Indiana. The crack, which nearly severed the exterior girder on the northern side of the east-bound structure, was located in the middle span of the three-span bridge structure. The crack extended for most of the plate girder depth before it was arrested in the compression region near the top of the girder and the concrete deck. The primary purpose of the research study was to examine the causes of the brittle fracture of the I-64 Blue River Bridge girder. In addition to understanding the reasons for the brittle fracture, possible repair and retrofit procedures were formulated to improve the fracture resistance of bridges with details similar to the Blue River Bridge.

The titles of the three volumes (Report Number in parentheses) are listed below:

Part I, Volume 1: Field Evaluation (FHWA/IN/JTRP-2001/10-I-1)
Part I, Volume 2: Laboratory Fatigue Evaluation (FHWA/IN/JTRP-2001/10-I-2)
Part II: Brittle Fracture Examination of the I-64 Blue River Bridge (FHWA/IN/JTRP-2001/10-II)

17. Key Words	18. Distribution Statement
brittle fracture, crack, fatigue, bridge, steel, girder, attachment plate, gusset plate, web gap, differential displacement, inspection, weld repair	No restrictions. This document is available to the public through the National Technical Information Service, Springfield, VA 22161

19. Security Classif. (of this report)	20. Security Classif. (of this page)	21. No. of Pages	22. Price
Unclassified	Unclassified	129	

Form DOT F 1700.7 (8-69)

ACKNOWLEDGMENTS

The research project was financially supported by the Federal Highway Administration and the Indiana Department of Transportation through the auspices of the Joint Transportation Research Program. The author would like to express his grateful acknowledgment for this sponsorship.

The valuable suggestions and comments provided by the Study Advisory Committee are sincerely appreciated. The members of the Study Advisory Committee include Mr. William Dittrich, Mr. James Karr and Mr. Joseph Torkos from Indiana Department of Transportation, and Mr. Don Johnson from Federal Highway Administration.

Sincere thanks are also due to Mr. Albert Kovacs of Purdue University who oversaw the preparation and testing of the specimens for the materials evaluation. Appreciation is also extended to a number of individuals from Purdue University who provided enthusiastic and timely help for various aspects of the experimental and analytical portions of the study. Among them, in particular, are Mr. Harry Tidrick, Ms. Jodi Enderson, Dr. Hung-I Wu, Dr. Keith Bowman, and Janet Lovell.

INDOT Research

TECHNICAL *Summary*

Technology Transfer and Project Implementation Information

TRB Subject Code: 25-01 Bridge Design and Performance *March 2002*
Publication No.: FHWA/IN/JTRP-2001-10-II *Final Report*

Brittle Fracture Examination of the I-64 Blue River Bridge Part II of Fatigue Behavior of Beam Diaphragm Connections with Intermittent Fillet Welds

Introduction

Fatigue cracking caused by differential distortion has become quite common in steel bridge structures throughout the United States. This type of cracking is typically caused by out-of-plane bending stresses that occur when non-uniform deformations occur. Vehicles crossing the bridge will often cause one girder to deform more than another adjacent girder, resulting in a non-uniform - or differential - deformation. Cracking occurs when the out-of-plane bending stress and the normal in-plane bending stress combine to produce a stress range that is large enough to result in fatigue cracking, when repeated often enough.

Problems developed in a number of bridges throughout the United States have demonstrated that certain details are particularly susceptible to fatigue cracking from differential deformation. Two different general types of details that have exhibited this behavior in plate girder webs are cracks developed in the gap region at the end of vertical connection plates and in the gap region between a vertical stiffener and a horizontal gusset plate. Cracks developed at the end of a vertical connection plate often occur when a floor beam or a diagonal cross frame is attached to the vertical plate and causes an out-of-plane deformation to occur in the web gap region between the end of the vertical plate and the flange plate. Cracks can also occur in the web gap region at the intersection of a vertical stiffener and a horizontal gusset plate, which is typically used to attach horizontal bracing members to the bridge girder. Cracks at the end of a vertical connection plate are often horizontal and, initially, are not particularly detrimental. However, cracks in the web gap region between a vertical stiffener and a horizontal gusset plate are typically perpendicular to the primary bending stress as soon as they initiate. This orientation means that fatigue cracks in the web gap between vertical and horizontal plates are often quite serious.

The research study reported herein was undertaken to evaluate the brittle fracture that occurred on the I-64 Blue River Bridge in Harrison County of southern Indiana. The fracture occurred in the middle span of a three span structure at a location where both a lateral diaphragm and a horizontal bracing members framed into a vertical and horizontal plate, respectively. The study involved experimental studies to evaluate the material performance and behavior of the bridge steel and analytical studies to assess the fracture resistance and susceptibility to brittle fracture. Recommendations for retrofit and repair of similar bridge details were formulated to decrease the fracture susceptibility from distortion related fatigue cracking.

Findings

Visual inspection confirmed that a brittle fracture of the I-64 Blue River Bridge occurred in the northern most girder of the east-bound structure. Features related to the brittle fracture were studied by experimental testing and analytical modeling. The primary observations from the investigation are summarized in the following:

(1) Visual inspection of the brittle fracture surface indicated that the brittle fracture initiated in the girder web near the intersection of a vertical connection plate and a horizontal gusset plate. Moreover, it is believed that the crack initiated as a fatigue crack in the web gap region immediately adjacent to the weld toe of the web-to-vertical stiffener weld.

(2) It is believed that the brittle fracture occurred during a period of extremely cold weather in January 1994. The measured temperatures at a site near the bridge during this period were as low as –30 ^{o}C (-22 ^{o}F). Low temperature values are known to produce fracture toughness values in structural steel that approach a minimum lower shelf level.

(3) Charpy V-notch testing demonstrated that the flange and web plate steel have fracture toughness levels that satisfy those required by AASHTO for non-fracture critical members. Also, an analysis of the steel chemistry was used to compute the carbon equivalent value for both the web and flange plates and it was found that both steels were well suited for welding

(4) Elastic fracture mechanics was used to evaluate the fracture susceptibility of the web plate. It was found that an elliptical crack with a one-to-four aspect ratio could develop a stress-intensity factor equivalent to the estimated fracture toughness of the steel (at a low temperature) prior to propagation of a crack through the thickness of the web plate.

Four factors are believed to have elevated the stresses in the gusset-to-stiffener connection welds: lack of positive attachment between the horizontal gusset plate and the vertical diaphragm, a small lateral gap distance between the toes of the horizontal and vertical fillet welds, loose bolts in the horizontal bracing to gusset plate connection, and impact forces introduced into the web via the horizontal bracing members.

Implementation

A number of different factors were responsible for the brittle fracture of the I-64 Blue River Bridge girder. It is believed that a number of the factors can be addressed through corrective maintenance and repair. Consequently, it is suggested that the following recommendations for inspection and repair be implemented on lateral bracing details similar to that of the I-64 Blue River Bridge to minimize the likelihood of future brittle fracture events:

(1) Inspect lateral bracing connections to determine if the horizontal attachment (gusset) plate has fractured. Fracture, or even a partial fracture, must be repaired to ensure a positive connection between the gusset plate and the vertical stiffener.

(2) Inspect the girder web for evidence of fatigue cracking in the immediate vicinity of the region where the lateral gusset plates and the vertical stiffener intersect.

(3) Drill holes through the lateral gusset plate to produce a gap between the weld toes that is at least four times the web thickness or 51 mm (2 in).

Tighten or replace all loose bolts that are used to connect the horizontal bracing members to the lateral gusset plate. Also, all conditions that may introduce excessive impact should be corrected to minimize damaging longitudinal forces.

Contact

For more information:

Prof. Mark D. Bowman
Principal Investigator
School of Civil Engineering
Purdue University
West Lafayette IN 47907
Phone: (765) 494-2220
Fax: (765) 496-1105

Indiana Department of Transportation
Division of Research
1205 Montgomery Street
P.O. Box 2279
West Lafayette, IN 47906
Phone: (765) 463-1521
Fax: (765) 497-1665

Purdue University
Joint Transportation Research Program
School of Civil Engineering
West Lafayette, IN 47907-1284
Phone: (765) 494-9310
Fax: (765) 496-1105

TABLE OF CONTENTS

LIST OF TABLES

LIST OF FIGURES

IMPLEMENTATION REPORT

Fatigue cracking caused by differential distortion has become quite common in steel bridge structures throughout the United States. Problems developed in a number of bridges throughout the United States have demonstrated that certain details are particularly susceptible to fatigue cracking from differential deformation. The type of distress that was studied in this investigation involved the development of a crack in the web gap region between a vertical stiffener and a horizontal gusset plate.

A horizontal gusset plate is commonly used to attach horizontal bracing members to the bridge girder. A chamfer of the gusset plate is often used to prevent direct intersection of the vertical stiffener-to-web fillet welds and the web-to-gusset welds. Forces developed in the bracing members, as well as differential displacement of the bridge girders, can introduce distortion in the web gap region. Repetitive loading can cause fatigue cracking in the web gap region, especially when the web gap is small and if there is no positive attachment between the vertical and horizontal plates.

Minimizing or eliminating the formation of fatigue cracks at stiffener to gusset plate intersections offers several advantages that affect both the safety and serviceability of a bridge. Brittle fracture often is precipitated by the stable growth of a fatigue crack. If fatigue cracking can be effectively eliminated, then most future brittle fracture events will also be addressed. Moreover, the cost required to retrofit or repair the bridges with gusset-to-stiffener details that have not yet developed serious distress will eventually be offset by

the additional service life that will be obtained by the modified bridges, and it should help to avoid costly major repairs encountered when a brittle fracture occurs.

The research study reported herein was undertaken to evaluate the brittle fracture that occurred on the I-64 Blue River Bridge in Harrison County of southern Indiana. The fracture occurred in the middle span of a three span structure at a location where both a lateral diaphragm and a horizontal bracing members framed into a vertical and horizontal plate, respectively. The study involved experimental studies to evaluate the material performance and behavior of the bridge steel and analytical studies to assess the fracture resistance and susceptibility to brittle fracture. Recommendations for retrofit and repair of similar bridge details were formulated to decrease the fracture susceptibility from distortion related fatigue cracking.

The primary observations from the investigation are summarized in the following:

(1) Visual inspection confirmed that brittle fracture of the I-64 Blue River Bridge occurred in the northern-most girder of the eastbound structure. The fracture initiated in the girder web near the intersection of a vertical connection plate and a horizontal gusset plate. Moreover, it is believed that the crack initiated as a fatigue crack in the web gap region immediately adjacent to the weld toe of the web-to-vertical stiffener weld.

(2) It is believed that the brittle fracture occurred during a period of extremely cold weather in January 1994. The measured temperatures at a site near the bridge during this period were as low as –30 ^{o}C (-22 ^{o}F).

(3) Charpy V-notch testing demonstrated that the flange and web plate steel have fracture toughness levels that satisfy those required by AASHTO for non-fracture critical members.

(4) Elastic fracture mechanics was used to evaluate the fracture susceptibility of the web plate. It was found that an elliptical crack with a one-to-four aspect ratio could develop a stress-intensity factor equivalent to the estimated fracture toughness of the steel (at a low temperature) prior to propagation of a crack through the thickness of the web plate.

(5) Four factors are believed to have elevated the stresses in the gusset-to-stiffener connection welds: lack of positive attachment between the horizontal gusset plate and the vertical diaphragm, a small lateral gap distance between the toes of the horizontal and vertical fillet welds, loose bolts in the horizontal bracing to gusset plate connection, and impact forces introduced into the web via the horizontal bracing members.

A number of different factors were responsible for the brittle fracture of the I-64 Blue River Bridge girder. It is believed that a number of the factors can be addressed through corrective maintenance and repair. Consequently, it is suggested that the following recommendations for inspection and repair be implemented on lateral bracing details similar to that of the I-64 Blue River Bridge to minimize the likelihood of future brittle fracture events:

(1) Inspect lateral bracing connections to determine if the horizontal attachment (gusset) plate has fractured. Fracture, or even a partial fracture, must be repaired to ensure a positive connection between the gusset plate and the vertical stiffener.

(2) Inspect the girder web for evidence of fatigue cracking in the immediate vicinity of the region where the lateral gusset plates and the vertical stiffener intersect.

(3) If necessary, holes should be drilled through the lateral gusset plate to produce a web gap between the weld toes that is at least four times the web thickness or 51 mm (2 in).

(4) Tighten or replace all loose bolts that are used to connect the horizontal bracing members to the lateral gusset plate. Also, all conditions that may introduce excessive impact should be corrected to minimize damaging longitudinal forces.

CHAPTER 1 INTRODUCTION

Sometime after a routine inspection during the Fall of 1993, the Interstate 64 highway bridge over the Blue River in southern Indiana suffered a severe brittle fracture in one of the outside girders. The fracture, shown in Figure 1.1, severed the bottom flange and all but 25 mm (1 in) of the 1778 mm (70 in.) deep web plate. The bridge was supported by the three remaining girders until an Indiana Department of Transportation maintenance crew discovered the fracture in May 1994. This report details subsequent research conducted at Purdue University to evaluate the causes of the fracture and to formulate recommendations concerning repairs for similarly designed bridges in Indiana.

The I-64 Blue River bridge, which crosses the Blue River and Blue Road, is located 6.67 km (4.1 mi) west of SR 337 in Harrison County, Indiana. The bridge was built in 1974 and is a three-span continuous structure, with spans of 36,271 mm (119 ft) – 45,110 mm (148 ft) – 36,271 mm (119 ft). Separate superstructures were built for the east and west bound lanes of traffic. Each structure carries two lanes of traffic and is supported by four steel plate girder members, as shown in the cross section in Figure 1.2.

The girders are spaced at 3658 mm (12 ft) and are fabricated from ASTM A36 steel. The girder cross section is composed of a 1778 mm (70 in) x 13 mm (0.5 in) web plate that is welded to 559 mm (22 in) wide flange plates that vary in thickness from 19 mm (0.75 in) to 63.5 mm (2 ½ in). The girder cross section at the location where the fracture occurred is shown in Figure 1.3.

The bridge structure is listed on the plans as non-composite. The bridge deck is 241 mm (9 ½ in) thick, with 457 mm (18 in) coping. The two interior piers have fixed bearings, while the outside abutments have expansion bearings.

Lateral bracing members, drawn schematically in Figure 1.4, are connected to the girder webs at about 305 mm (12 in) from the bottom flange through a horizontal attachment (gusset) plate as shown in Figure 1.5. These horizontal attachment plates wrap around vertical stiffeners, as shown in Figure 1.5. Moreover, the vertical stiffeners are used to connect horizontal and diagonal cross-frame diaphragm members to the web, as illustrated in Figure 1.4.

The fracture occurred near the center of the 45,110 mm (148 ft) middle span in the northern exterior girder of the (southern) east-bound bridge structure. The drawings in Figures 1.4 and 1.5 and the photographs in Figures 1.6 through 1.7 reveal the location of the crack that formed in the attachment plate, bottom flange, and web. The fracture severed the horizontal attachment plate and propagated downward through the tension flange and upward into the girder web. Figures 1.8 and 1.9 of the girder tension flange reveal that very little ductile tearing of the flange occurred and that the fracture was brittle in nature. The crack was arrested in the web shortly before it propagated into the top flange plate. It is also evident from Figures 1.6 to 1.9 that the path of the web crack was not perfectly vertical. The crack curves away from the attachment plate both above and below the gusset plate. Below the gusset plate, however, the curvature of the fracture path changes and the crack curves back towards the vertical stiffener.

Figures 1.10 and 1.11 illustrate the nature of the crack in the horizontal gusset plate. It is evident that the direction of the gusset plate crack changed as it propagated beyond the vertical stiffener. Initially, the crack parallels the vertical stiffener. It then swerves around the stiffener, but the direction changes abruptly and again becomes perpendicular to the girder web.

A location of particular interest is the portion of the girder where the vertical stiffener and the horizontal gusset plate intersect. Note how the crack passes through the region of the web, hereafter called the web gap, bounded by the vertical stiffener and a chamfered corner of the horizontal attachment plate (see Figure 1.5). The photographs in Figures 1.12 and 1.13 reveal that at this corner the crack just touches the protruding toe of the fillet weld that runs along the bottom of the horizontal attachment plate and connects the plate to the web. The brittle fracture clearly emanated from this web gap region.

Determination of the crack origin only begins to answer questions concerning the girder failure. Many other important questions are raised concerning the fracture. For example, what role does the geometry of the attachment plate connection detail play as a possible cause for the brittle fracture? What role, if any, did fatigue play in the Blue River bridge fracture? How large did the fatigue crack grow before fracture occurred? Did cold weather reduce the fracture toughness of the bridge steel to a critical level? Did the fracture occur because of an overload, or could an ordinary truck loading trigger the event? Did factors unique to the Blue River bridge, such as missing lateral bolts at an adjacent lateral connection and excessive impact at the bridge approach, contribute significantly to the failure? Conditions such as poor weld quality and construction errors may or may not exist in similar details. What role did they play in the Blue River bridge fracture? This report will address these and other questions concerning the reasons behind the Blue River bridge girder fracture.

Figure 1.1 View of brittle fracture in the outside girder of the I-64 Blue River Bridge

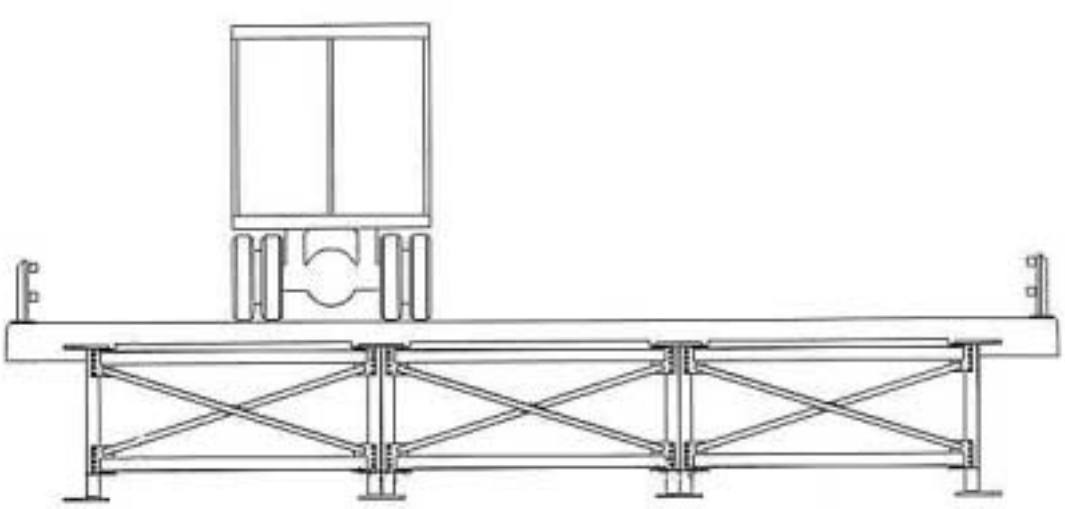

Figure 1.2 Cross section of four-girder bridge structure

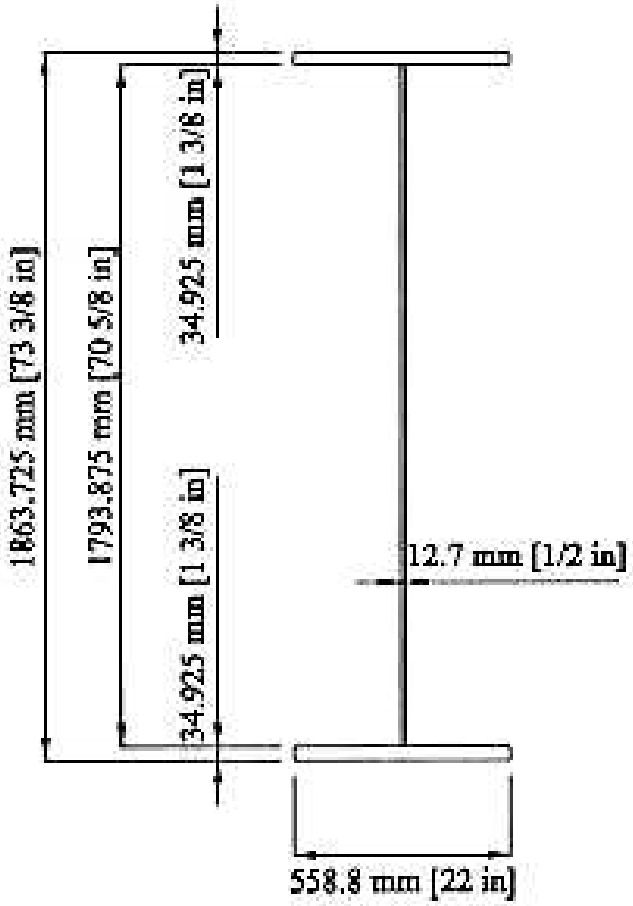

Figure 1.3 Sketch of girder cross section at brittle fracture location

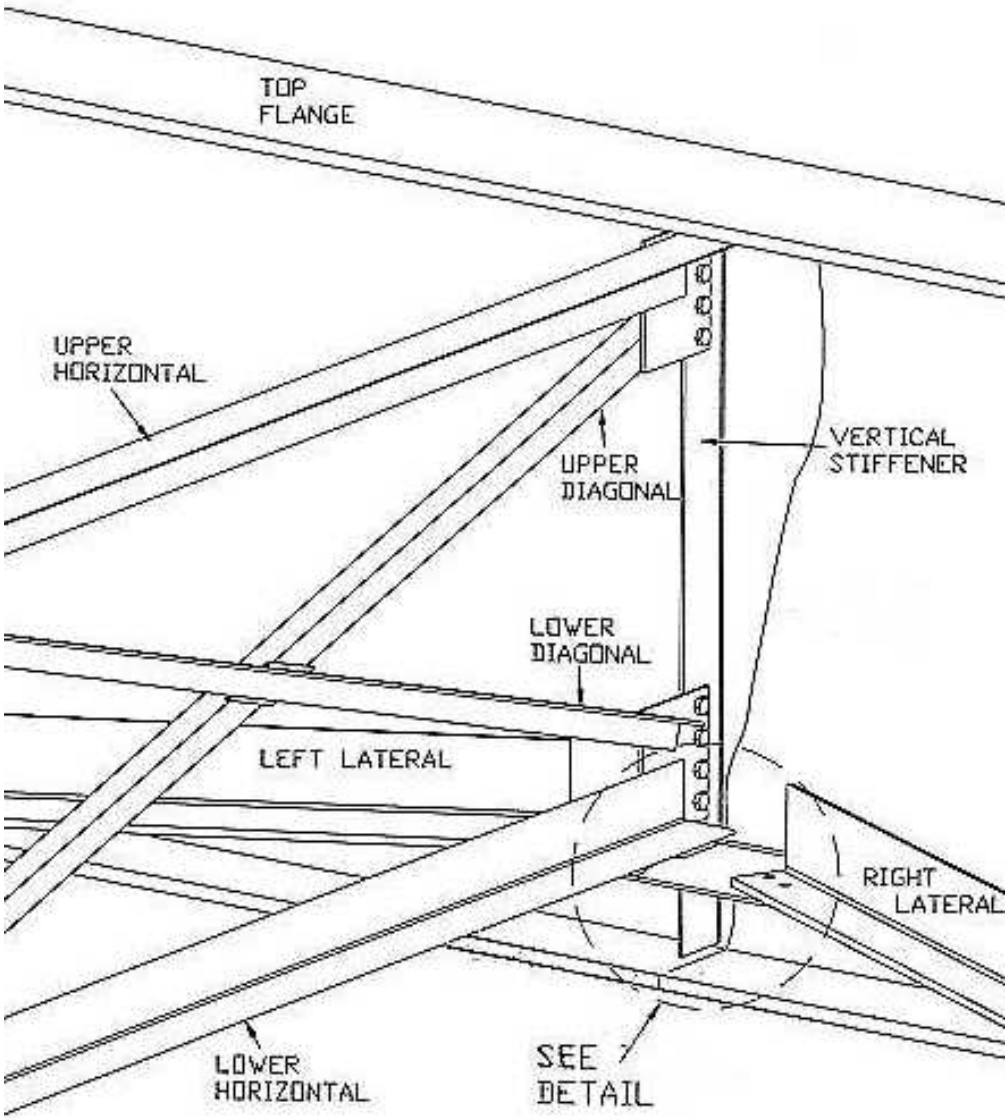

Figure 1.4 Sketch of connection detail at the brittle fracture location

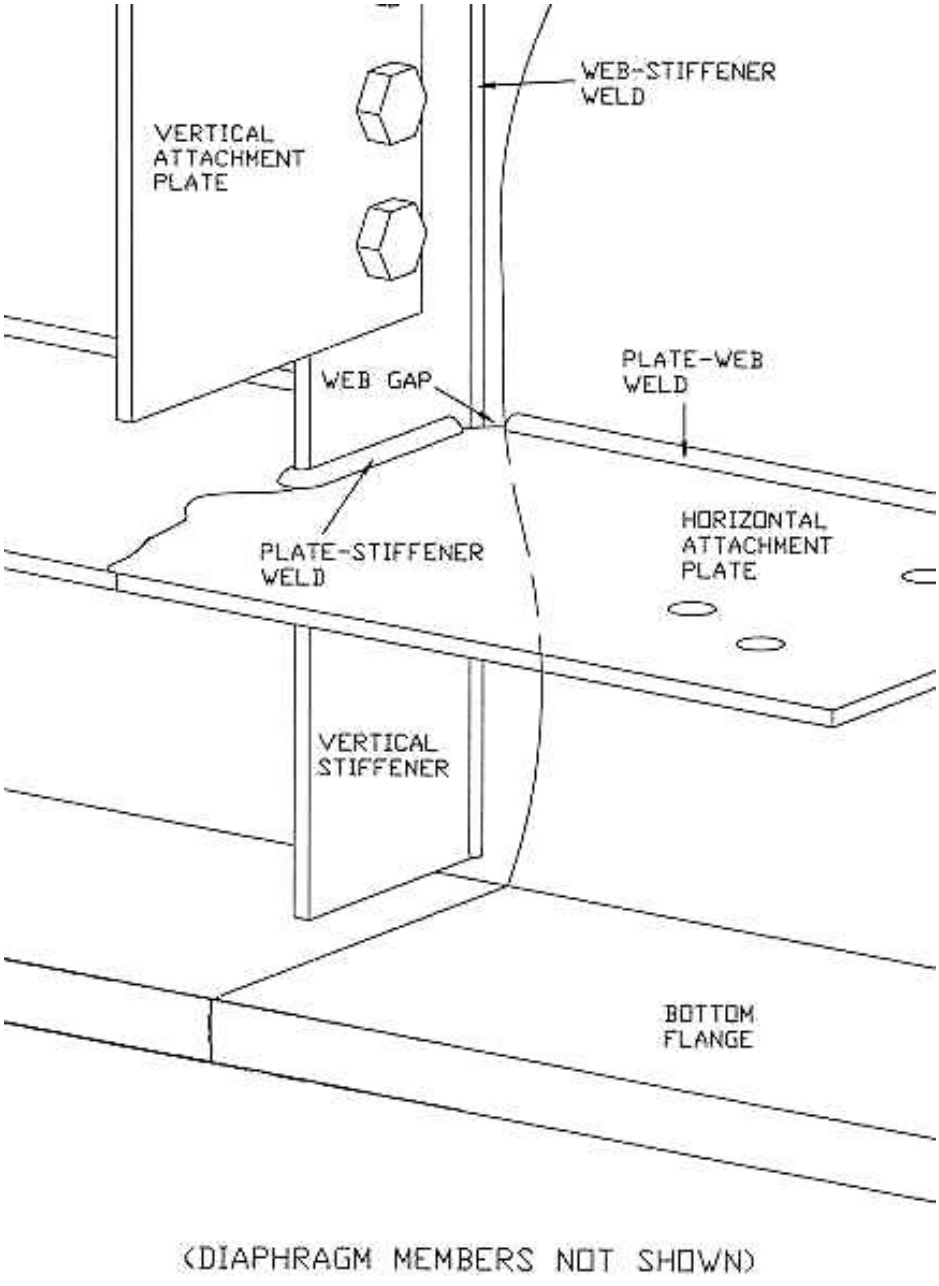

Figure 1.5 Close-up view of crack position relative to the vertical stiffener and the horizontal attachment plate

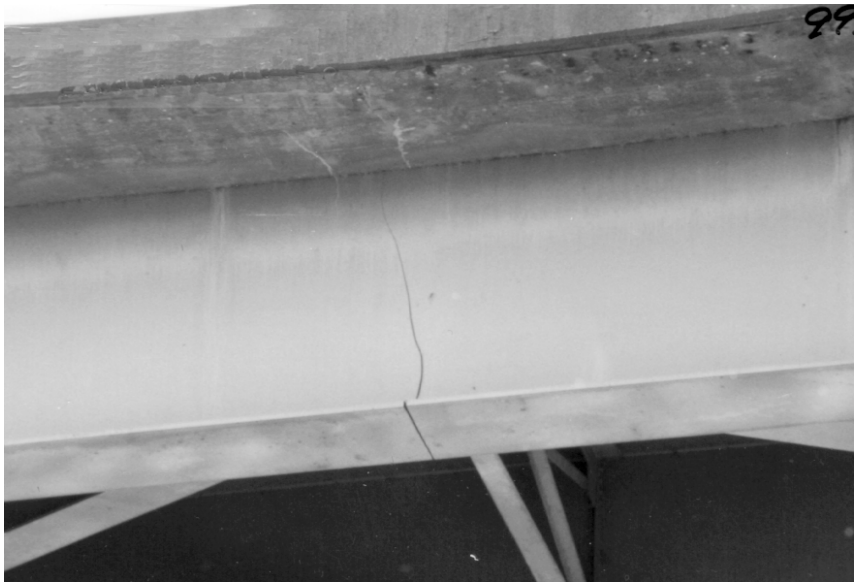

Figure 1.6 View of brittle fracture in the outside plate girder

Figure 1.7 View of crack through the flange, web and gusset plate

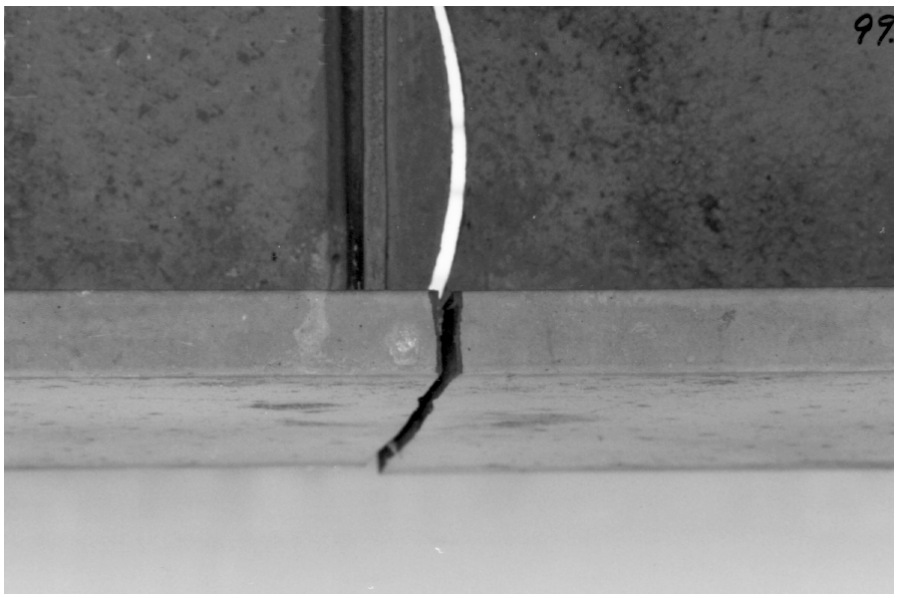

Figure 1.8 View of fracture through the bottom flange of the girder

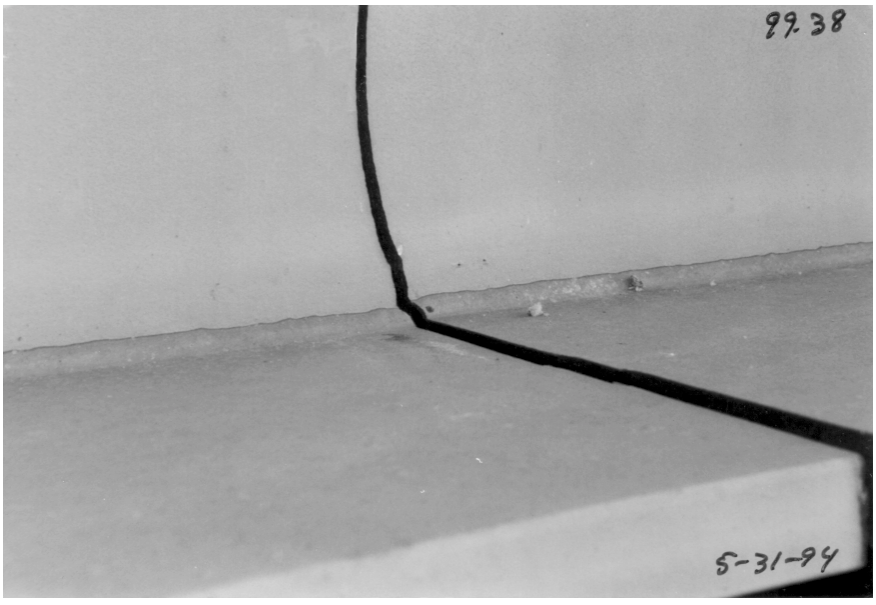

Figure 1.9 View of fracture from the top surface of the bottom flange

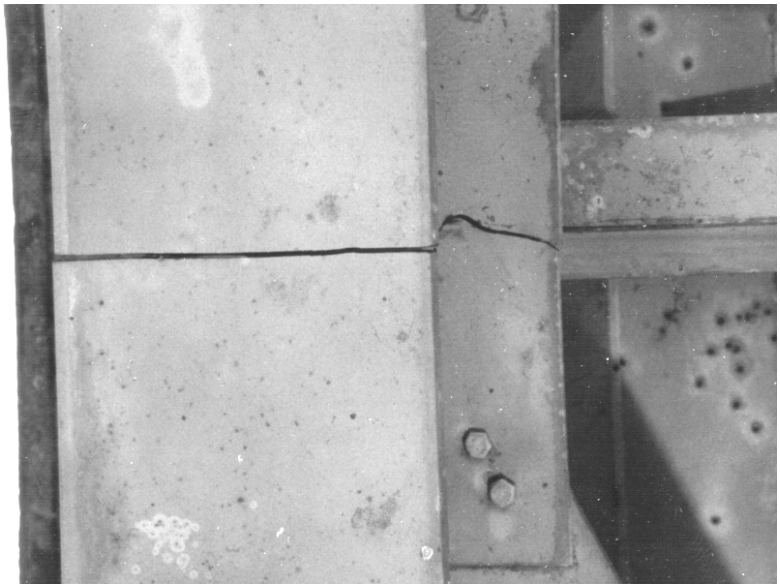

Figure 1.10 View of botttom flange and outside region of attachment plate

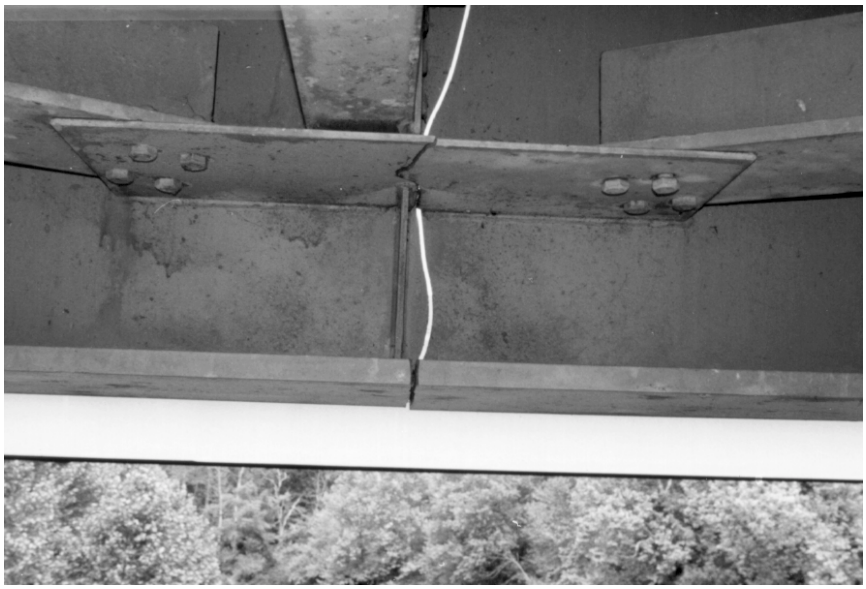

Figure 1.11 View of fracture at bottom connection detail

Figure 1.12 Close-up view of fracture through the attachment plate

Figure 1.13 View of crack at the weld toe at the chamfered edge of the horizontal gusset plate

CHAPTER 2

LITERATURE REVIEW

2.1 Introduction and Background

A number of case histories have been documented where cracks formed near web connection plates. Examples include the Lafayette Street Bridge in St. Paul, Minnesota (Fisher et al., 1977), two dual interstate girder bridges in West Virginia (Demers and Fisher, 1990), and the Canoe Creek Bridge in Clarion County, Pennsylvania (Demers and Fisher, 1990). Although the type of cracking developed in each of these bridges is different, some generalizations related to structural behavior are possible. Horizontal and vertical connection plates interrupt the otherwise continuous girder webs, causing stress concentrations within the webs. The plates are typically welded to the girder webs. The welding procedure, by its very nature, creates residual stresses and inevitably leaves some flaws in the weld material from which fatigue cracks may originate. Moreover, the plates also deliver forces from the diaphragm and lateral members directly to the relatively thin girder webs, resulting in out-of-plane bending stresses and other secondary stresses in the web. For these reasons, fatigue and fracture problems at web connection plates are not uncommon.

Most web connections consist of a horizontal attachment plate that is notched to fit around a vertical attachment plate. The horizontal attachment plate connects lateral braces to the girder web and will hereafter be referred to as a lateral gusset. A vertical web stiffener usually doubles as the vertical attachment plate. It connects diaphragm members to the web. However, many variations of this basic detail exist. The lateral

gusset, for example, may consist of a single plate that is notched to fit around the vertical plate or it may consist of two separate plates, one on each side of the vertical plate. Some lateral gussets are welded to both the web and the vertical plate, but the lower diaphragm members may be attached instead to the lateral gusset or to both the lateral gusset and a vertical plate. Finally, connection plate geometry, bolting patterns, and welding patterns also vary among connections.

All of these differences cause variation in the manner in which cracks originate and propagate. Fisher et al (1990) suggested that the severity of a lateral detail could be classified on the basis of the structural variables that influence the degree of distortion induced cracking and the nature and geometry of the detail.

Two subsets of the many lateral gusset plate details that result in fatigue cracking involve cases in which the welds for the vertical and lateral members either interset or do not interset. For example, in the Lafayette Street Bridge (Fisher et al, 1977) the cracks started in the lateral gusset and propagated through the intersecting welds into the web. In other bridges, however, the lateral gusset is not welded to the vertical attachment plate. The Canoe Creek Bridge falls into this latter category. The reduced restraint provided to the lateral gusset results in high out-of-plane bending stresses in the web. Consequently, the cracks start in the web itself.

The Blue River Bridge matches neither of these cases. Its lateral gusset is welded to the vertical attachment plate, but the welds do not intersect the web welds. Despite an extensive search, a published case study of fatigue or fracture cracking could not be found for connection details that identically match those of the Blue River Bridge.

Nevertheless, published case studies offer considerable insight into the possible behavior of the Blue River Bridge.

The following sections will review case studies that involved lateral bracing fractures. The results of appropriate experimental studies will also be reviewed.

2.2 Lafayette Street Bridge

The Lafayette Street Bridge over the Mississippi River Bridge in St. Paul, Minnesota is a three span structure with two main exterior plate girders (Fisher et al, 1977). Longitudinal stringers, which support the bridge deck, rest upon floor beams that frame into the main girders. Lateral members are connected to the main girder through a gusset plate, which wraps around the vertical stiffener near the bottom flange. The lateral gusset is groove welded to both the main girder and the vertical stiffener, with the welds intersecting. In addition to the lateral bracing, the diaphragm lower horizontal member is also bolted to the lateral gusset plate.

On May 7, 1975, a crack, which passed through the lateral gusset detail, was discovered in one of the main girders – see Figure 2.1. The fracture was discovered after a 190 mm (7-1/2 in) difference in level of medians of the two adjacent structures was observed near the fracture. (Previously, on March 20, 1975, a 64 mm (2-1/2 in) difference in the level of medians had been observed.) Moreover, the web fracture surface was observed to be shiny metal from a position 100-150 mm (4-6 in) above the gusset to the end of the crack.

After careful analysis, Fisher and his associates concluded that a lack of weld fusion gap between the lateral gusset and the vertical stiffener provided the initial crack-

like flaw from which a fatigue crack started. A single bevel groove weld was used to connect the gusset plate to the transverse stiffener and the girder web. The groove weld, however, did not penetrate to the backup bar on the root of the weld preparation. The size of the lack of fusion flaw varied from 3.8 mm (0.15 in) at the vertical stiffener edge to 9.65 mm (0.38 in) near the girder web.

Since the lack of fusion flaw was oriented perpendicular to the primary bending stress, it acted as a crack built into the structure. Growth of the crack from the fusion weld flaw to the final state is depicted in Figure 2.2. Initially, the crack grew until it passed through the intersection of the gusset-stiffener weld with the stiffener-web weld and into the web. The crack then propagated up and down the web to a small but critical size. Brittle fracture of the lower web and flange ensued. Some additional fatigue crack growth eventually led to brittle fracture of the remaining web. The top flange and part of the lateral gusset remained intact. The dates related to the difference in level of the median and absence of corrosion on the upper portion of the crack surface confirms that the fracture involved a combination of fatigue crack growth and brittle fracture.

2.3 Canoe Creek Bridge

The Canoe Creek Bridge on I-80 is located in Clarion County, Pennsylvania (Demers and Fisher, 1990). The bridge has identical structures that each carry two lanes of traffic, one eastbound and the other westbound. The structures have five continuous spans with two longitudinal girders, multiple stringers and transverse floor beams.

Lateral gusset plates were used to attach the lateral cross bracing and the floor beam bottom flange to the web of the plate girder. The lateral gusset plates are bolted to 100

mm by 19 m by 559 mm long (4 in by ¾ in by 22 in long) lateral tabs, which are fillet welded to the girder web. A small 38 mm (1-1/2 in) gap exists between the end of the lateral tabs and the transverse connection plate (Fisher et al, 1990). Also, the lateral gusset plates were not positively attached to the transverse stiffener. A sketch of the detail is shown in Figure 2.3.

In October 1985, cracks were detected on the outside girder web face along the transverse stiffener weld toe at the level of the lateral gusset plate. Fractographic examination of cores removed from the eastbound and westbound structures revealed that small fatigue cracks had also developed at the lateral tab weld toe in the horizontal web gap. Based on measured strains, it was shown that larger stress ranges were developed on the outside girder web face near the weld toe of the vertical stiffener and on the inside face of the web gap near the weld toe of the lateral tab termination.

Demers and Fisher (1990) suggest that the lateral cross-bracing acting out-of-plane caused the gusset plate and lateral tab to rotate, in spite of the positive attachment of the lateral gusset plate to the floor beam bottom flange and girder web. This rotation caused out-of-plane distortion of the girder web at the lateral gusset plate level. The superposition of out-of-plane web bending stresses combined together with in-plane bending stresses resulted in stress range values in excess of the Category E level.

The lateral gusset cracking was retrofitted by drilling holes at the ends of existing cracks and replacing the welded lateral tab plate with a bolted angle connection. Moreover, the horizontal web gap was increased from 38 mm (1-1/2 in) to 100 mm (4-in).

2.4 Big Sandy Creek Bridge

The 2682 bridges on I-79 cross the Big Sandy Creek north of Charleston, West Virginia (Demers and Fisher, 1990). The bridges were opened for traffic in 1972. Parallel curved structures carry north and south bound traffic over three continuous spans. Each structure has two longitudinal girders, with floorbeams and stringers used to transfer the deck loading to the main girders.

The floorbeams webs are bolt connected to a transverse connection plate that is fillet welded to the girder web. Lateral braces are framed to a horizontal gusset plate that is also fillet welded to the girder web – see Figure 2.4. The gusset plate contains a tapered cope so that it can fit around the transverse connection plate, resulting in a horizontal web gap of 6 to 25 mm (1/4 to 1 in.) between the gusset plate and the transverse stiffener. Moreover, there was a lack of positive attachment between the transverse connection plate and the gusset plate.

Cracks were detected in August 1984, in the inside face web gap locations created by the lateral gusset plates and the transverse connection plates. The crack location is shown in Figure 2.5. Cracks were found in both positive and negative moment locations. Most of the cracks were not particularly long when they were detected: 102 mm (4 in) was the longest crack length (Kulicki et al, 1986).

Strain gages were placed on the structure to evaluate the stress levels and the locations where cracking had been discovered; stresses were inferred from strain values measured as the result of random truck traffic. Stresses due to out-of-plane distortion in

the web gap between the lateral gusset plate and transverse connection plate were measured on the girder outside face. The stress range near the stiffener fillet weld toe was larger than the fatigue limit for a Category C detail.

Retrofit of the cracks in the horizontal web gap involved two measures. First, 51 mm (2 in) diameter retrofit holes were drilled through the girder web along the web stiffener weld toes. Holes were located roughly 51 mm (2 in) above and below the horizontal gusset plate. Second, the lateral bracing system was removed. Rather than trying to accommodate the out-of-plane bending by absorbing it with a larger portion of the web, the displacement could be eliminated by removing the lateral system. After verifying that the facia girders could resist the additional forces due to wind forces, it was recommended that the lateral bracing system be removed, including connection plates and the welds (Kulicki et al, 1986).

2.5 Experimental Research

A significant NCHRP research study was conducted by Fisher, et. al. (1990) to examine distortion-induced fatigue cracking. This goal of this NCHRP study was to develop recommended criteria for designing steel girders so that distortion-induced fatigue cracking problems are minimized. Both transverse connection plate and lateral gusset plate details were studied. Experimental tests of specimens that simulated details used in practice were conducted to evaluate the structural behavior.

The investigators classified the severity of a lateral gusset plate according to a few key variables. Included in these are the following five factors: the in-plane stress range at the lateral gusset plate, the horizontal web gap geometry, the manner of gusset plate

attachment and corresponding physical displacement, the magnitude of the transverse forces, and the secondary stress range induced within the web plate by lateral displacement. To study these variables, six full-scale girders were tested with lateral gusset plates attached to the girder webs.

Three different gusset plate connection configurations were examined. As shown in Figure 2.6, the three different connections utilized different web gap geometries and gusset plate attachment schemes. For detail type A, the gusset plate was coped 51 mm (2 in.) and welded to both the girder web and the transverse stiffener. In detail B, the gusset plate was cut to fit around the transverse stiffener and welded to the girder web. A positive attachment to the gusset plate and the vertical stiffener was provided by bolting a WT section to both plates. For detail C, a 152 mm (6 in.) deep rounded gap was cut in the gusset plate to fit around the vertical stiffener. No positive attachment was provided between the gusset plate and the vertical stiffener. Web gaps of both 25 mm and 76 mm (1 in. and 3 in.) were examined.

A number of observations were made from the cyclic testing program. First, the stress gradient for the web gap region varied significantly and produced larger stresses at the transverse connection plate weld toe than at the lateral gusset plate weld toe. Second, for an in-plane stress range of 41.4 MPa (6 ksi), no cracking was detected for details A and B after 10,000,000 cycles of loading. Third, fatigue cracks did develop at the weld toe of the transverse stiffener opposite the gusset plate for detail C, where there was not a positive attachment of the lateral gusset plate to the transverse stiffener. Fourth, when the data were plotted on an S-N curve, with the stress plotted on the basis of the sum of the in-plane flexural stress plus the estimated out-of-plane bending stress, then all of the data

exceeded the AASHTO category C level. Fifth, drilled holes at the crack tips were found to arrest the crack growth when the stress range levels did not exceed 138 MPa (20 ksi); higher stress levels require a positive attachment between the gusset plate and the transverse stiffener, even for large web gaps.

A couple of additional comments in this study are worth noting. They mention that fitting gusset plates around a transverse stiffener without a direct attachment does not appear to be desirable. Moreover, even with a positive attachment, the web gap between the weld toes should be at least four times the web thickness. Large stress gradients can occur in the gap region, even for very small gaps. Lastly, it is stated that the intersection of the gusset longitudinal weld and the transverse stiffener weld must be avoided. Weld shrinkage strains will produce severe restraint and contribute to the possibility of weld discontinuities and inclusions at the weld intersection.

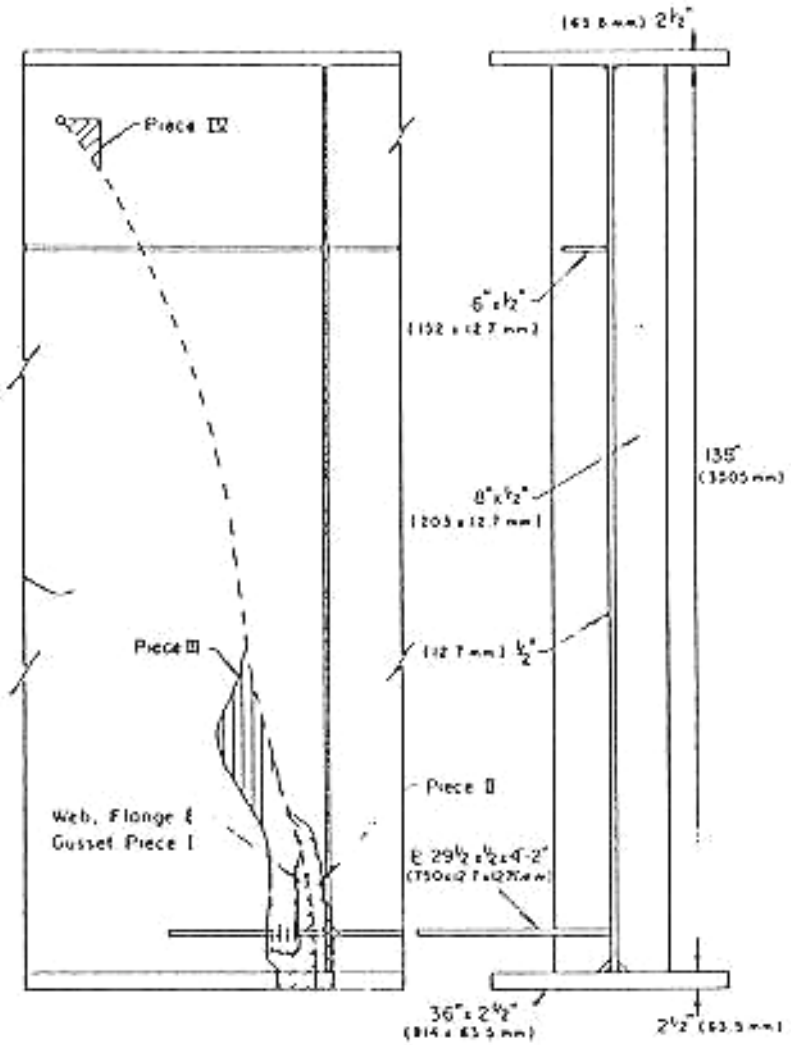

Figure 2.1 Cross sectional view of Lafayette Street Bridge girder and view of crack after brittle fracture (Fisher et al, 1977)

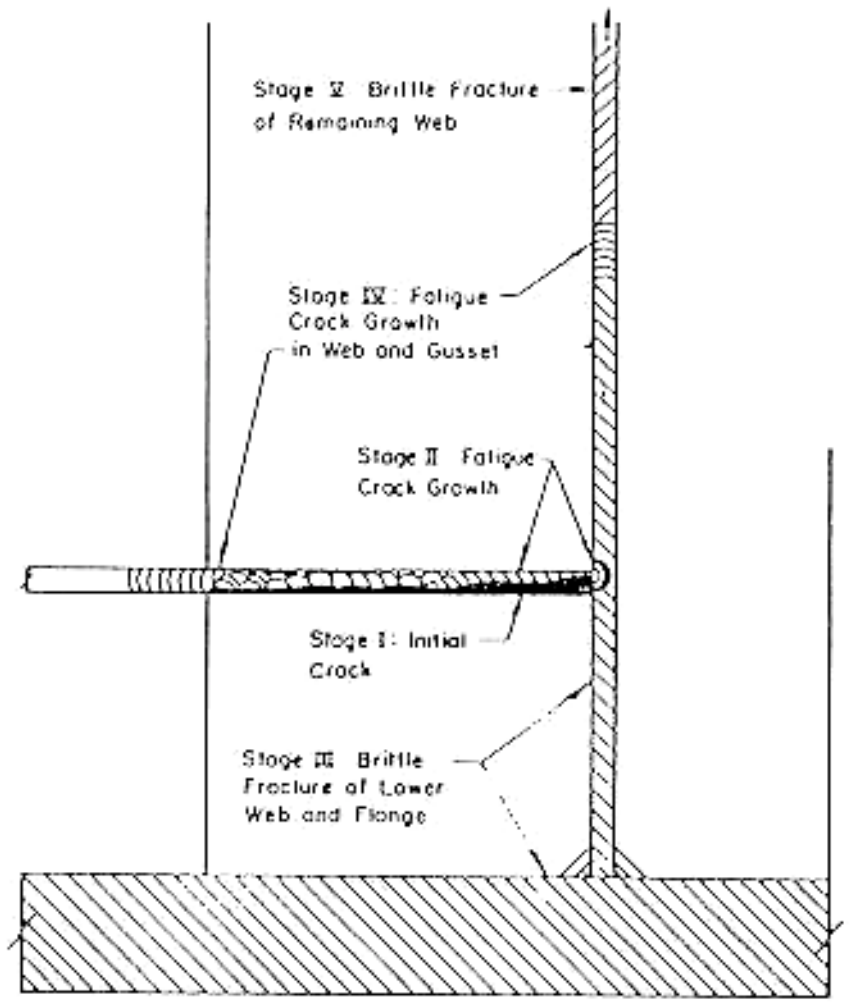

Figure 2.2 Position of crack in Lafayette Street Bridge (Fisher et al, 1977)

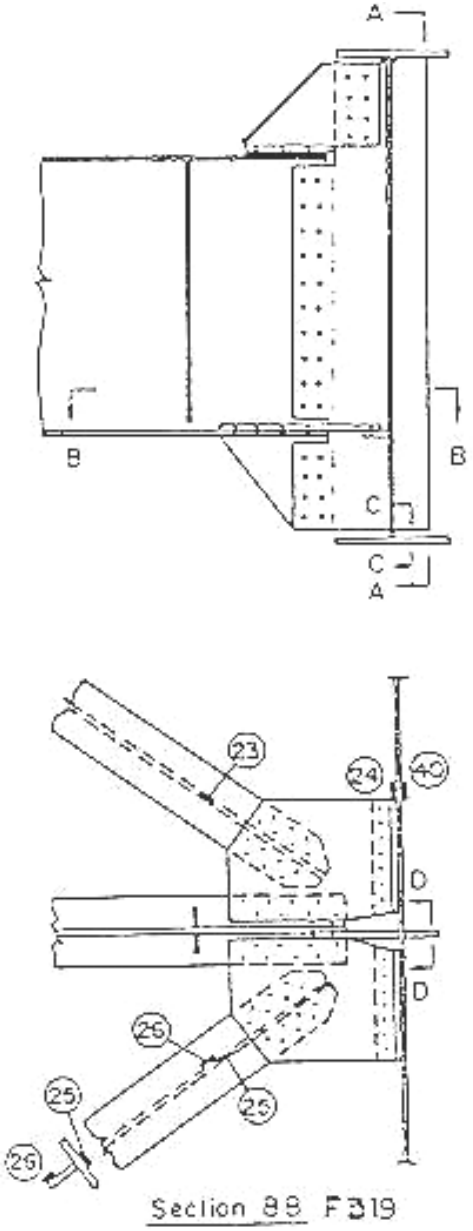

Figure 2.3 Horizontal attachment plate for lateral bracing members and floor beam bottom flange in the Canoe Creek Bridge (Demers and Fisher, 1990)

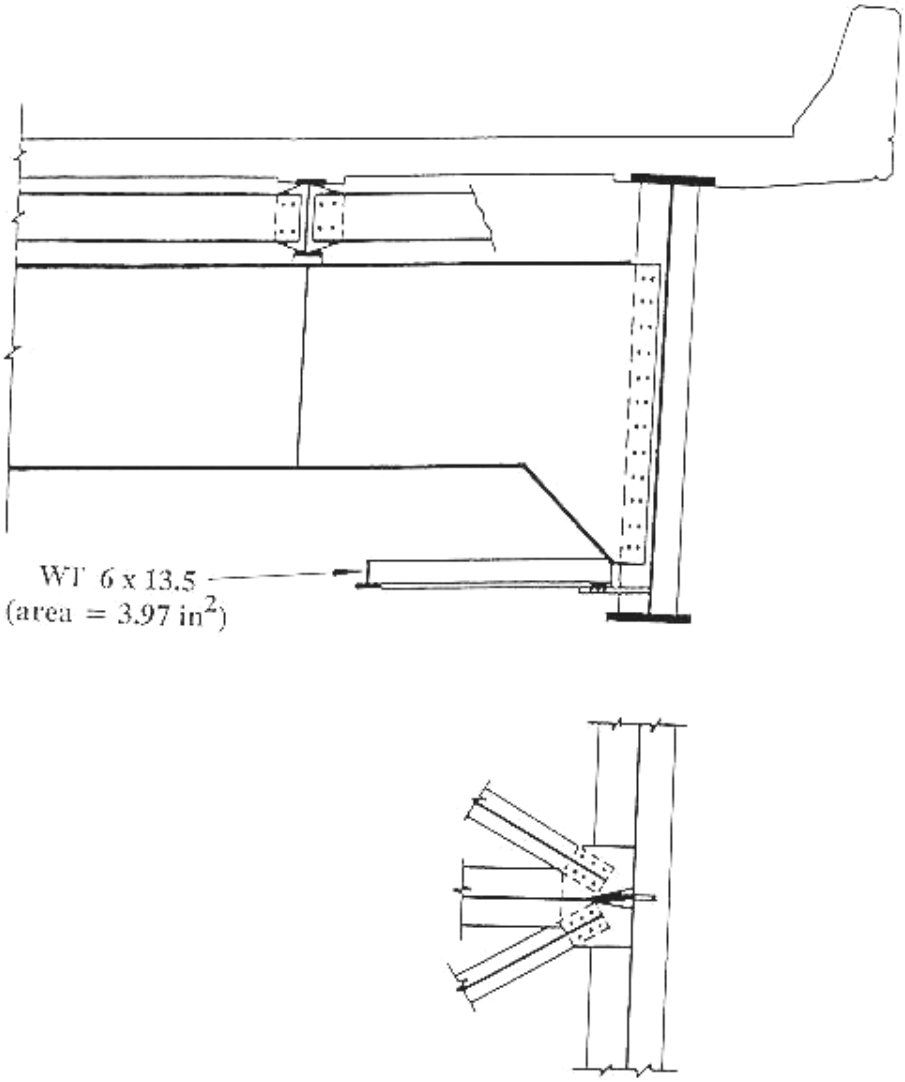

Figure 2.4 Floorbeam and lateral cross bracing connections in the Big Sandy Creek Bridge (Demers and Fisher, 1990)

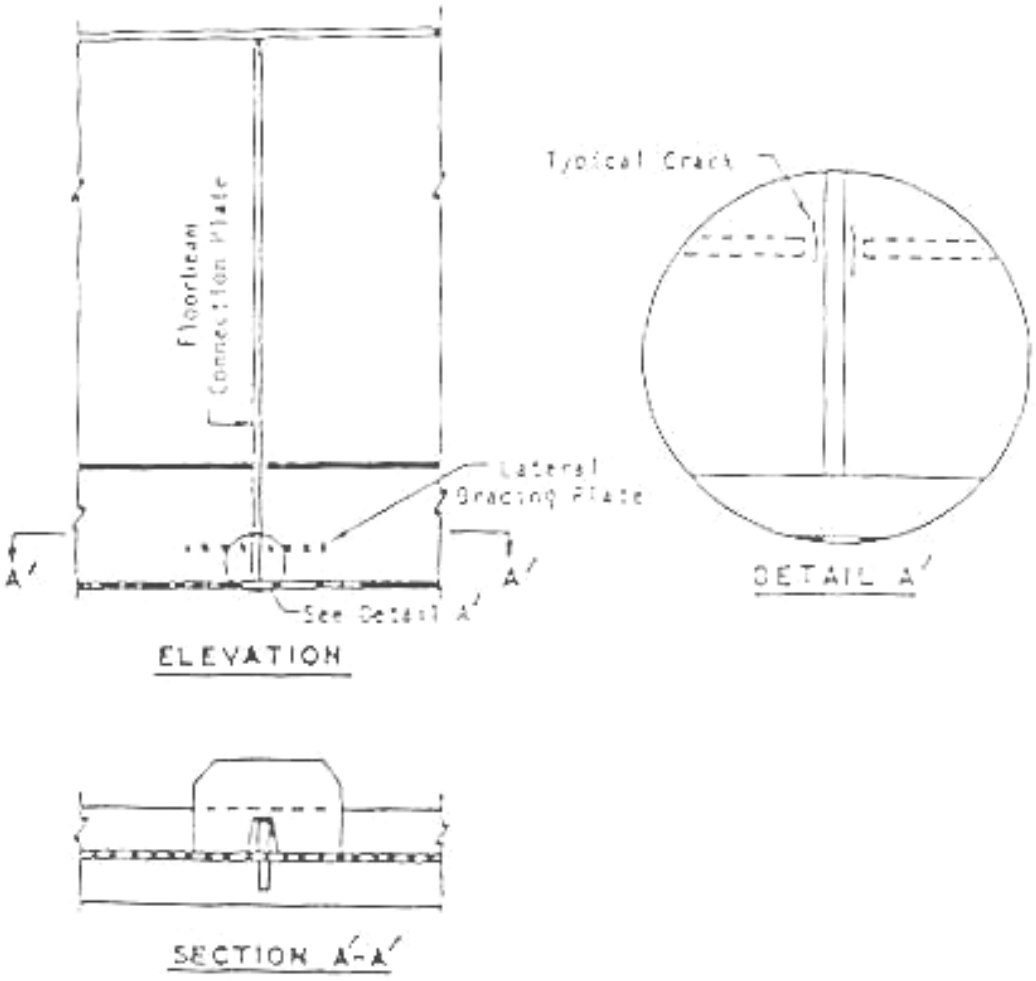

Figure 2.5 Floorbeam and lateral cross bracing connections in the Big Sandy Creek Bridge (Demers and Fisher, 1990)

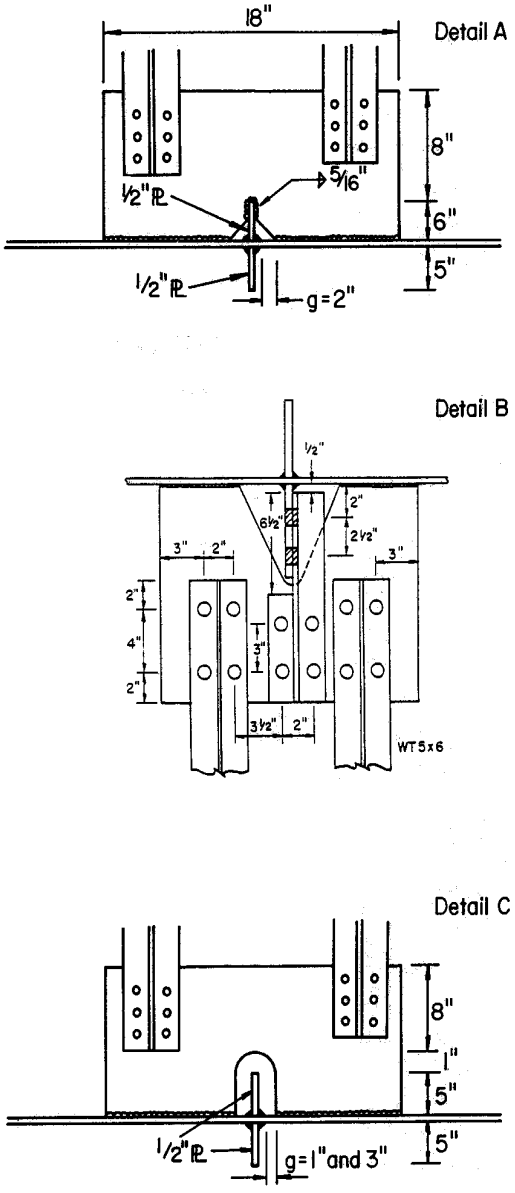

Figure 2.6 Details from experimental test program to study distortion-induced fatigue cracking in girders with horizontal web gaps (Fisher et al, 1990)

CHAPTER 3

I-64 BLUE RIVER BRIDGE FRACTURE

Brittle fracture does not generally occur unless several mitigating factors simultaneously work to reduce the resistance to rapid crack extension. Included among these factors are the geometry of the structural detail, the fracture toughness and strength of the steel, the stress level, and other bridge environment related factors. The geometry and related environmental factors are discussed in this chapter. Material strength and fracture toughness will be reviewed in Chapter 4, and the stress level and related analysis will be examined in Chapter 5.

3.1 Circumstances Related to the Fracture

A number of circumstances that are possibly related to the brittle fracture of the Blue River Bridge are discussed in this section. Included among these factors are recorded traffic levels, various bridge geometrical factors, and air temperature readings during the 1993-94 winter season.

3.1.1 Traffic Levels

The average daily traffic level during 1994, the year that the fracture was discovered, was collected for I-64 at a site near the bridge. The total average daily traffic (ADT) for both eastbound and westbound structures was found to be 9678 vehicles. Traffic count data were broken down into thirteen different vehicle classes, including cars, motorcycles, buses and various sizes and types of trucks according to the number of axles. The average mix for light and heavy weight vehicles was found to be 54.4 percent

for cars, motorcycles and two axle vehicles and 45.6 percent for trucks and all other vehicles. Hence, by using the latter number to represent truck traffic, the average daily truck traffic (ADTT) on both structures would be 4417 vehicles.

The traffic measurements were itemized further, with ADT values reported for each direction of traffic and for each lane. For the northern (westbound) structure, the ADT and ADTT are 4736 and 2141 vehicles, respectively, for both lanes. These numbers are broken down further into the ADT and ADTT for each lane of traffic for the westbound structure: 3925 and 1965 for lane 1 (right side), and 811 and 176 for lane 2 (left side). For the southern (eastbound) structure, the ADT and ADTT vehicle counts are 4943 and 2275, respectively, for both lanes. The corresponding vehicle count breakdowns per lane are 4245 and 2120 for lane 1 (right), and 698 and 155 for lane 2 (left). A summary of the traffic count data for the various lanes is shown in Figure 3.1.

The fracture occurred in the exterior (northern) girder of the eastbound (southern) structure. This would place the critical girder nearest to lane 2, which has a much lighter traffic volume than lane 1. If the ADTT of 155 vehicles per day is used along with a three percent growth factor for increase in traffic volume, then the total number of truck counts can be calculated. Based upon these assumptions, the total number of truck vehicles that lane 2 would experience between 1974 and the end of 1993 would be 867,000 trucks. The corresponding traffic level in lane 1, which is further removed from the girder that fractured, would be 11,860,000 trucks. It should be noted that there is a significant variation in the weight of the various trucks. Also, these numbers are very approximate and represent only the total number of trucks passages and not the stress developed in the girder as a result of a truck passage. The latter quantity, used in

conjunction with the number of truck passages, would be used to develop a measure of the fatigue damage.

3.1.2 Impact

Loads larger than the conventional gravity loads can be caused by a variety situations. For example, an uneven road surface can generate an additional inertial force. The magnitude of the force will vary significantly due to the vehicle weight, travel speed, and the vehicle suspension system, as well as the change in elevation of the roadway surface. Significant impact forces can also be generated when the wheels encounter a geometric discontinuity, such as a pothole in the deck or a bridge expansion joint.

Little specific information has been gathered on bridge impact effects for the Blue River Bridge. INDOT engineers, however, report that some significant impacts were occurring on the bridge due to a slight dip in the roadway just before the vehicles encounter the bridge. It was reported that the impact generated by the trucks coming onto the bridge was clearly perceivable when standing on the bridge deck.

It is difficult to quantify the truck impact effect since no field measurements were conducted to determine the dynamic forces generated in the Blue River Bridge. Undoubtedly, a dynamic force induced near the end of the bridge would primarily affect the end span, especially since fixed bearings are located at the two interior piers. However, some of the dynamic force generated near the bridge end would also be transmitted to the adjacent spans. Distribution of this force is dependent upon the stiffness of the deck, superstructure and substructure. Since the input dynamic force is

unknown, it is difficult to accurately predict the impact effect at the middle of the bridge where the brittle fracture occurred.

3.1.3 Loose Bolt at Gusset Plate

The bolts for one of the horizontal bracing members that framed into the horizontal gusset plate were found to be loose. One bolt, in fact, was so loose that the bolt head was no longer in contact with the gusset plate. This can clearly be seen in the right-side gusset connection shown in Figure 3.2, as well as in Figure 1.11.

It is difficult to accurately model the effect that one loose bolt – or even several partially loose bolts – would have on the structure. It is fairly certain, however, that the loose connection would cause some additional out-of-plane bending of the girder web. If both bracing members are rigidly attached to the horizontal gusset plate, then the connection will remain relatively stiff and transfer the force in one brace to the next with a minimum of out-of-plane web distortion. With a rigid bracing connection on one side only, however, then the force in the rigidly connected brace will be transferred (either fully or a significant portion thereof) through the gusset plate to the girder web. This will result in additional out-of-plane bending stresses.

It should be mentioned that the combination of a significant horizontal force generated by impact, coupled with a loose connection for one of the bracing members, could be partially responsible for the Blue River Bridge fracture. Although it is difficult to quantify these two factors, they may have played some role in the fracture. It is believed, however, that other factors were also significant and contributed to the brittle fracture to a greater extent.

3.1.4 Low Temperature Exposure

The fracture toughness of steel is directly related to temperature. The fracture toughness, or resistance to fracture, of most structural steels increases as the temperature increases. Furthermore, for many steels there is a transition region in which the fracture toughness changes drastically. In fact, in the Charpy V-notch test reference is often made to a transition region between a lower-shelf and upper-shelf notch toughness.

The I-64 Blue River Bridge is located in the southern portion of Indiana. Although more moderate than northern Indiana, the bridge is located in a region that would be classified as Zone 2 for evaluation of the fracture toughness of the bridge steel. In this temperature zone, the lowest anticipated service temperature (LAST) range is –17.8 ^{o}C (0^{o}F) to –34.4 ^{o}C (-30 ^{o}F).

During the winter of 1993-94, Indiana experienced a brief period with some very cold temperatures. Temperature data collected at a site near the Blue River Bridge indicated that temperatures in the lower third of the LAST were achieved. The high and low temperature records for most of December 1993 through February 1994 are shown in Figure 3.3. The coldest portion of that record occurred during January 1994, as shown in Figure 3.4. A low temperature of –30 ^{o}C (-22 ^{o}F) was recorded on January 19, 1994. Moreover, the low temperature was below –20 ^{o}C (-4^{o}F) during three days of a four day period (January 18-21, 1994). Those record low temperatures, which result in low fracture toughness levels, may very well have played a key role in the Blue River Bridge fracture.

3.2 Crack Surface Examination

A great deal may be learned about a fracture by examining the crack surface. The presence of shear lips, for example, indicates slow, ductile yielding. A herringbone pattern carved into the crack surface, on the other hand, indicates rapid, brittle fracture. Oxide build up and other forms of weathering sometimes reveal the chronology of events leading to final failure.

In order to examine fracture surfaces of the Blue River Bridge, a portion of the girder that contained the brittle fracture was removed from the bridge and shipped to Purdue University. To stabilize the girder during shipping, splice plates were bolted to the web of the fractured girder. The crack surfaces had to be separated to facilitate careful examination. Consequently, a cutting torch was used to remove the top portion of the girder by cutting through the web just below the top flange. The cut also passed through the end of the brittle fracture. A view of the girder after the top flange was cut off is shown in Figure 3.5. After arriving at the laboratory, the remaining girder was separated into the two halves pictured in Figure 3.6. Figure 3.7 schematically divides the left half into crack surface regions A through F, and the right half into corresponding regions A' through F' for reference purposes.

3.2.1. Visual Inspection of the Attachment Plate Crack

The web and flange plate crack surfaces appear essentially flat and uniform indicating that the girder crack formed almost entirely during a single brittle fracture event. The horizontal attachment plate deviates from this description. Crack surface

parts E and E’ pass through the top and bottom fillet welds that connect the horizontal plate to the vertical stiffener – see Figures 3.8 to 3.11. Significant amounts of oxide and rust in this area suggests that the 150 mm (6-in.) portion of attachment plate adjacent to the vertical stiffener cracked long before the final fracture occurred.

The peculiar appearance of parts E and E’ requires further explanation. As shown in Figures 3.10 and 3.11, part E of the attachment plate crack surface remains recessed between adjacent fillet welds. The relatively rough and rib-shaped surface of its counterpart (E’), shown in Figure 3.9, strongly resembles a flame cut edge.

Figure 3.12 summarizes the details of the attachment plate construction. A 12.7 mm (1/2 in) wide by 150 mm (6-in) deep notch had been designated to allow the attachment plate to fit around the 9.5 mm (3/8-in) thick vertical stiffener. This left a 1.6 mm (1/16-in) gap between each side of the vertical stiffener and the attachment plate. Actual measurements, however, indicate that the center of the attachment plate lies at least 3.2 mm (1/8-in.) to the left of the vertical stiffener centerline. Only the widening of the attachment plate notch could have enabled this circumstance. Faced with an extremely tight fit in the field, it is suspected that a cutting torch was used to enlarge the notch. The gaps between the stiffener and attachment plate were then filled in with weld metal. However, the weld metal did not fill the gap uniformly and resulted in lack of weld fusion in many regions. This procedure produced poor quality, oversized fillet welds and the rough surface appearance in regions E and E’.

In order to further confirm suspicions about the weld flaws, a section that passed through the attachment plate and vertical stiffener was extracted for further examination. The section was cut down to contain only the intersecting plates and welds and was then

polished. A view of the section appears in Figure 3.13. The image corresponds to cross-section B of Figure 3.11. Lack of fusion gaps clearly appear adjacent to each side of the vertical stiffener. The attachment plate crack grew from a similar lack of fusion gap adjacent to the inside edge of the horizontal attachment plate notch. Furthermore, the surface etching clearly reveals that to the right of the vertical stiffener only weld metal exists in the extracted section. This proves that the horizontal attachment plate notch was widened and filled with weld metal, creating serious flaws from which fatigue cracks could develop.

The crack follows an unusual, curved path just past the intersection of the attachment plate and the vertical stiffener. Most likely, non-uniform out-of-plane bending caused the principal crack opening stresses to deviate from the normal direction. The crack swerved sharply at this point as it extended across the attachment plate. Moreover, an unequal distribution of forces transferred through the large ST 9WF48 horizontal braces as a result of loose bolts on one side – see Figures 1.11 and 3.2 – would also contribute to the development of non-uniform stresses in the attachment plate.

The remaining attachment plate crack surfaces, labeled as parts F and F' in Figure 3.7, appear flat, uniform and mostly featureless. The crack appeared to return mostly to its original direction, thereby creating a significant bump in the crack path. Rather than propagating perpendicular to the longitudinal direction of the beam, however, the crack followed a skewed path but left a smooth fracture surface in the horizontal attachment plate that extended to the end of the attachment plate. A slight shear lip at the very end of the attachment plate is evident in the side view photograph in Figure 1.12.

3.2.2 Visual Inspection of the Web Crack

Like the latter part of the attachment plate crack discussed above, the web crack created a flat, uniform, and mostly featureless fracture surface. Shear lips and other evidence of ductile fracture do not exist. The degree of corrosion remains constant over the entire web crack surface. All these facts indicated that the web failed in a single brittle fracture event.

One exception to the uniformity, however, occurs on the crack surface. Close-up photographs of the web crack surface – reproduced in Figures 3.14 and 3.15 – reveal a herringbone pattern. The pattern extends from the region nearest the attachment plate (labeled parts A and A') downward into the bottom flange and upward about 300 mm (12-in) from the same region. Herringbone or chevron-type patterns on the fracture surface point towards the fracture origin (Hertzberg, 1976). In this case, the pattern points to the web crack region nearest the horizontal attachment plate. The tip of the longitudinal fillet weld that runs between the web and the underside of the horizontal attachment plate intersects the web crack in this region. Upon close visual inspection, the herringbone pattern nearly converges on this small point. The pattern adds to evidence already described and clearly indicates that the web failed primarily through brittle fracture. It also supports the hypothesis that the fracture originated in the region near the horizontal attachment plate which contains high stress concentrations.

The case study of the brittle fracture for the Lafayette Street Bridge, presented in the previous chapter, states that the crack propagated slowly by fatigue from an initial flaw until brittle fracture rapidly extended it. Visual inspection of the web crack surface for the Blue River Bridge suggests that the portion of the crack created by fatigue was

very small. As described above, the herringbone patterns appear to nearly touch the probable crack origin from which they extend. It is difficult to determine precisely where the herringbone patterns stop as they converge on the crack origin. The patterns fade gradually rather than abruptly, but they clearly leave no more than 38 mm (1 ½-in) of flat surface between them. Since herringbone patterns appear only on brittle fracture surfaces, the fatigue portion of the crack could not have extended more than about 38 mm (1 ½-in).

Rust and other forms of weathering also suggest that fatigue damage was fairly limited. The outside face of the exterior girder that fractured undoubtedly suffered exposure to rain, snow and other harsh elements. Had the fatigue crack propagated through the web thickness, its surfaces would have been exposed to the same corrosive environment. Since fatigue cracks typically grow very slowly, oxide build-up should appear to be relatively heavy near the crack origin and diminish gradually near the crack tips. No such variation, however, may be seen in the web crack. Brittle fracture probably occurred either before or shortly after the fatigue crack penetrated the exterior web surface. Considering that the crack length-depth ratio did not likely exceed four to one, the above observations imply that the fatigue crack did not grow beyond four times the girder web thickness in length, or 51 mm (2-in).

3.2.3 Microscopic Analysis of the Web Crack

To the naked eye, fatigue crack surfaces appear almost perfectly flat and featureless. When viewed under a high power microscope, however, lines called

striations may be seen on the crack surface. Striations form a pattern of closely spaced parallel lines which lie perpendicular to the crack surface.

The web plate fracture surface for the Blue River Bridge near the toe of the fillet weld that attached the horizontal gusset plate and the girder web was examined to detect evidence of fatigue crack growth. A scanning electron microscope in the School of Materials Engineering at Purdue University was used to conduct the examination of the fracture surface.

No evidence of fatigue striations was found in the region suspected to be the origin of the fracture. Although this may indicate that very little fatigue crack growth occurred, it is believed, instead, that the iron oxide layer on the fracture surface masked the striations. In any event, the microscopic examination of the fracture surface proved to be inconclusive.

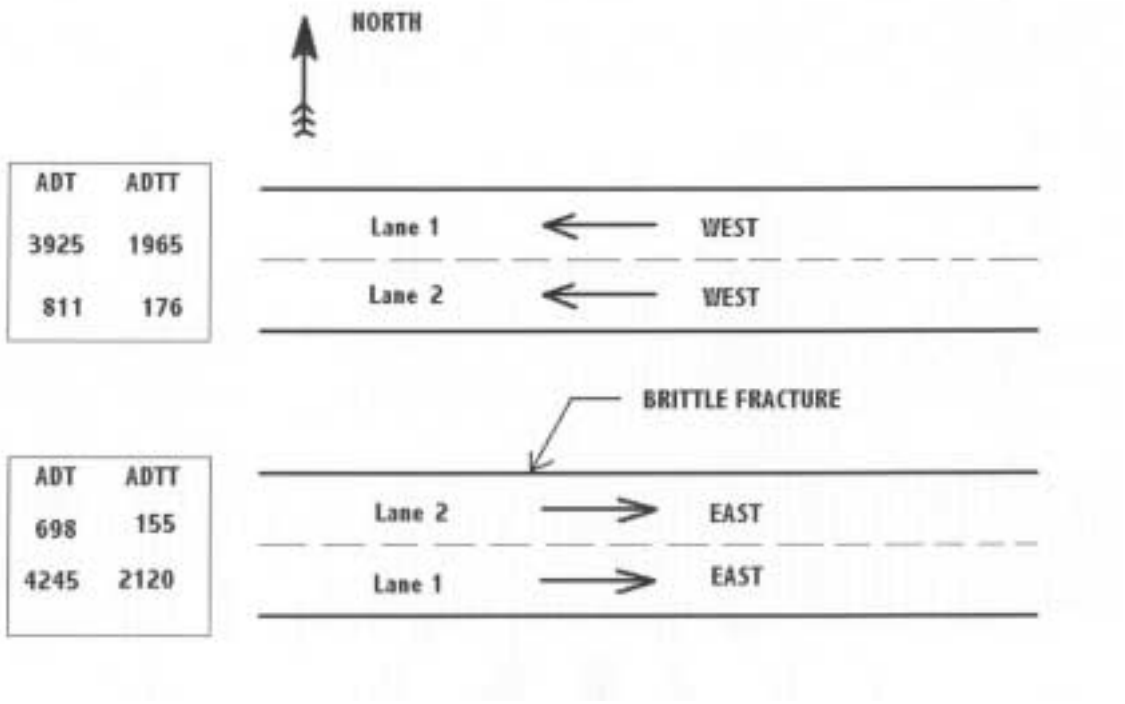

Figure 3.1 Traffic count data for all four lanes of the Blue River Bridge.

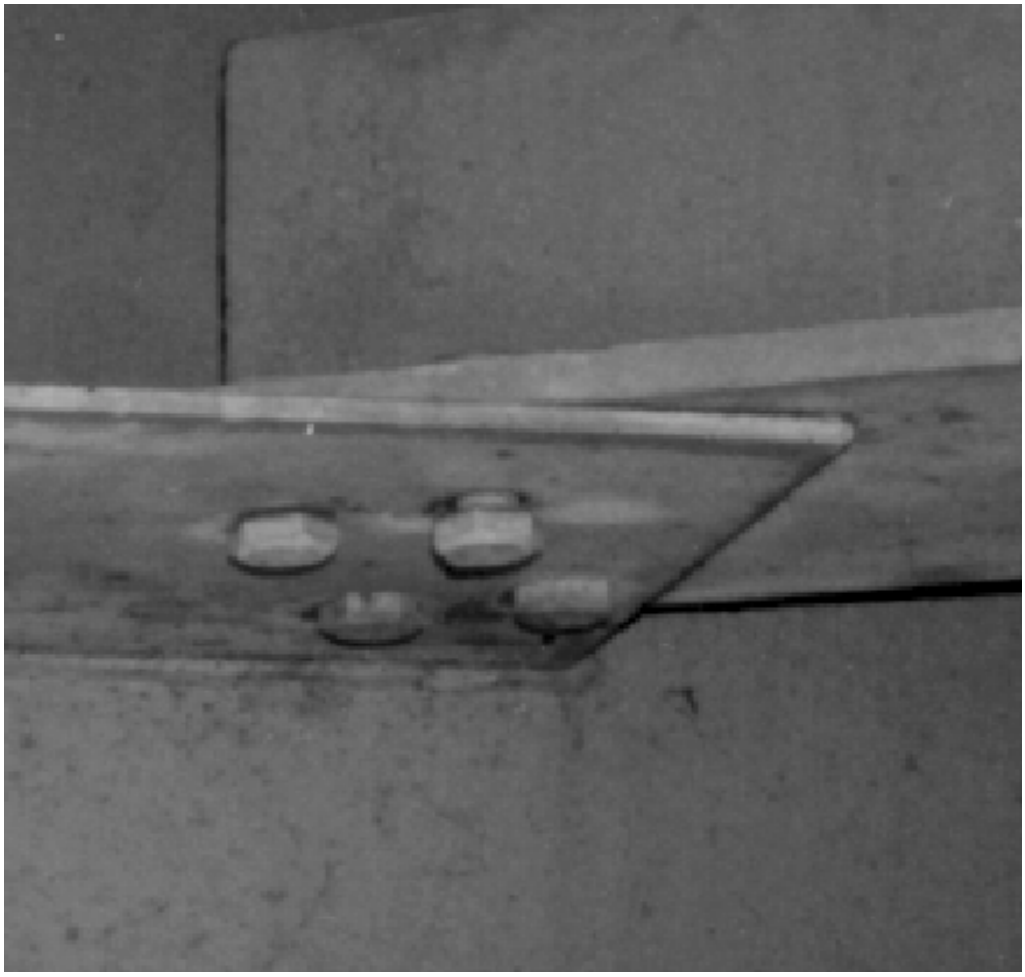

Figure 3.2 View of loose bolt at lateral brace to gusset plate connection

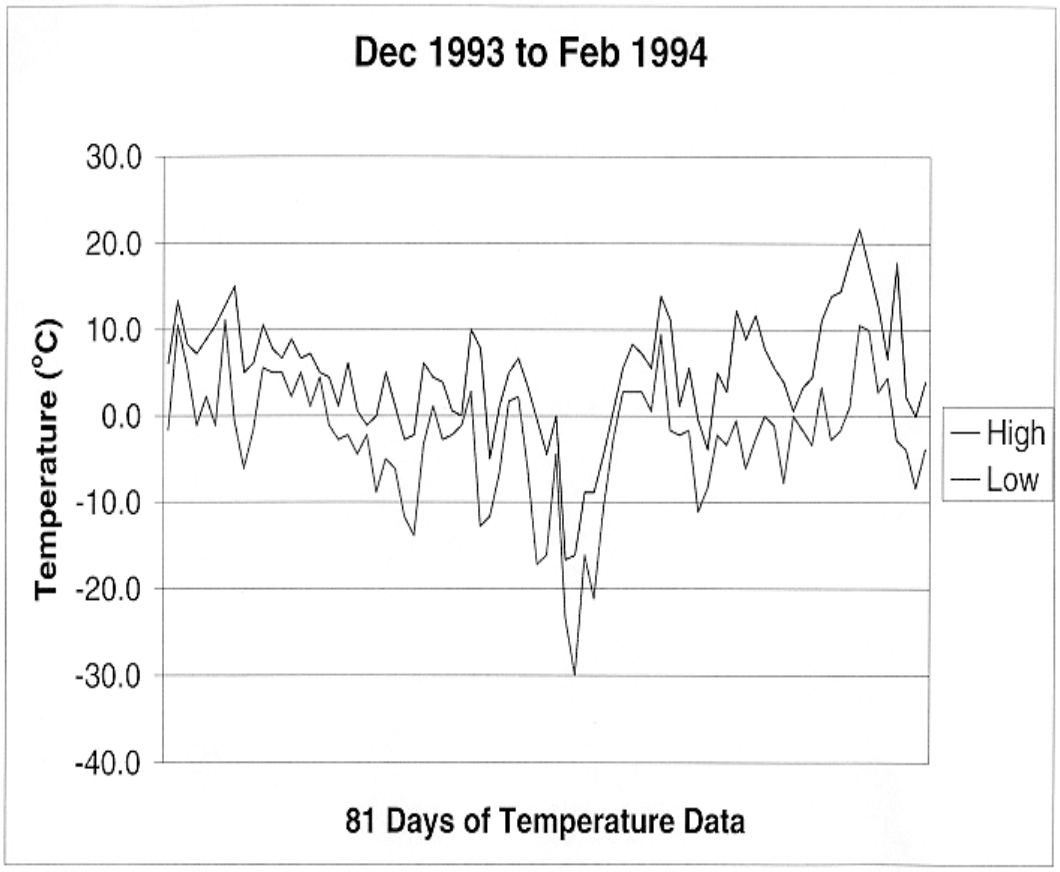

Figure 3.3 High and low temperatures during the winter of 1993-94

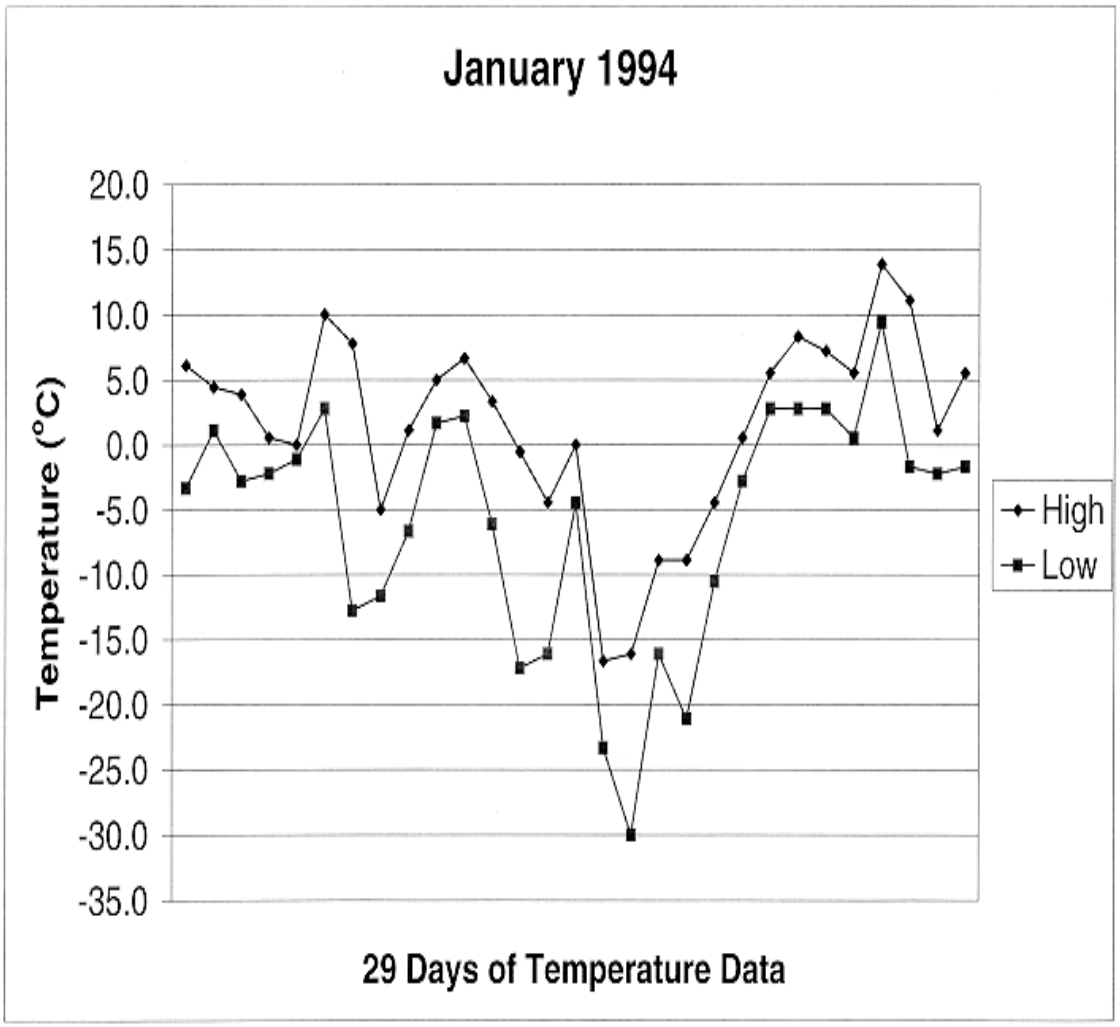

Figure 3.4 High and low temperatures during January 1994

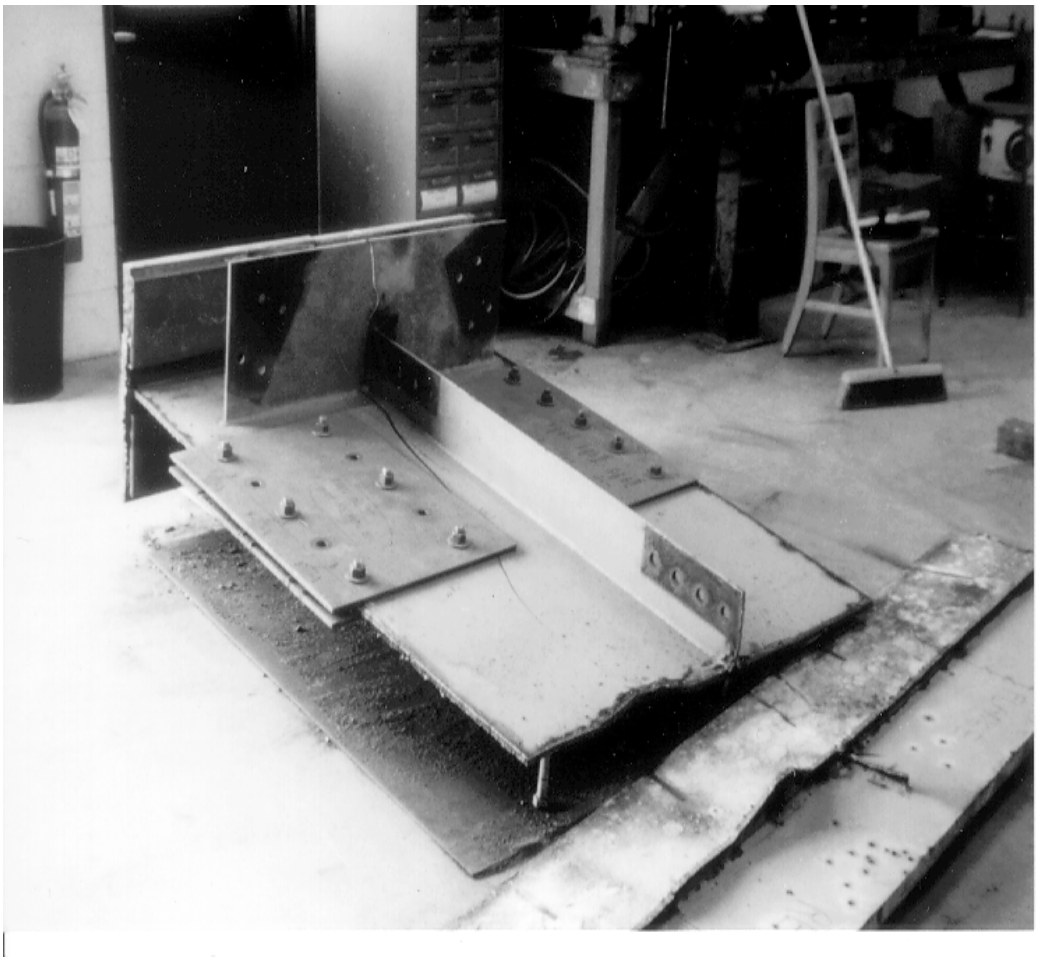

Figure 3.5 Top flange removal for crack surface examination

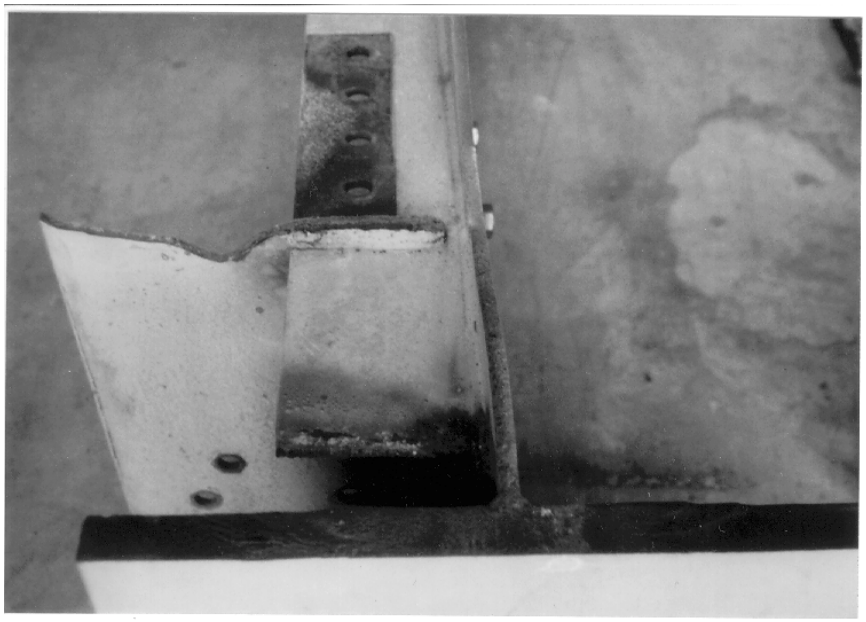

(a) View of left side crack surface

(b) View of right side crack surface

Figure 3.6 Two sides of the fracture surface after separation of girder web

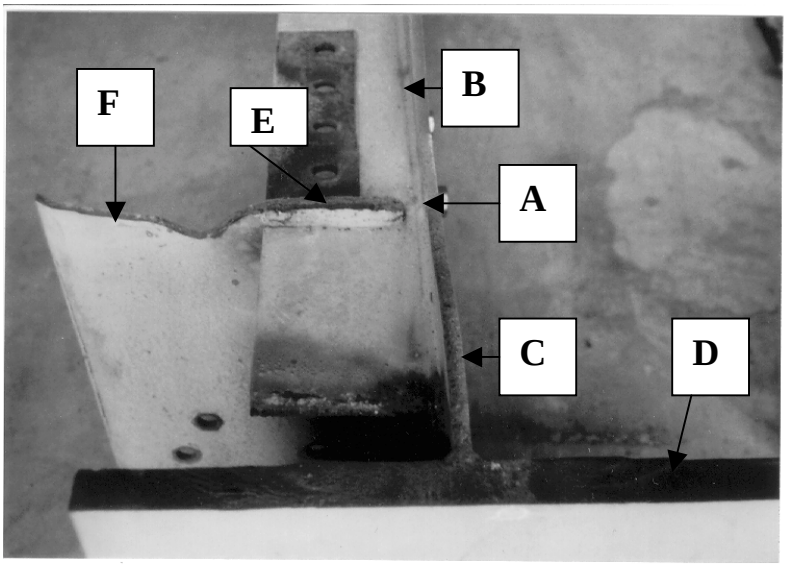

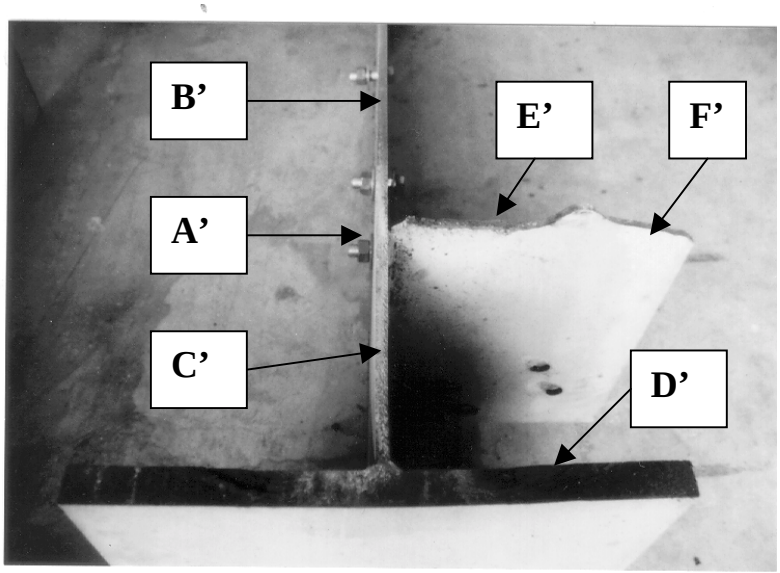

Figure 3.7 Schematic view of two crack surfaces with identification marks.

Figure 3.8 Crack surface at Part E

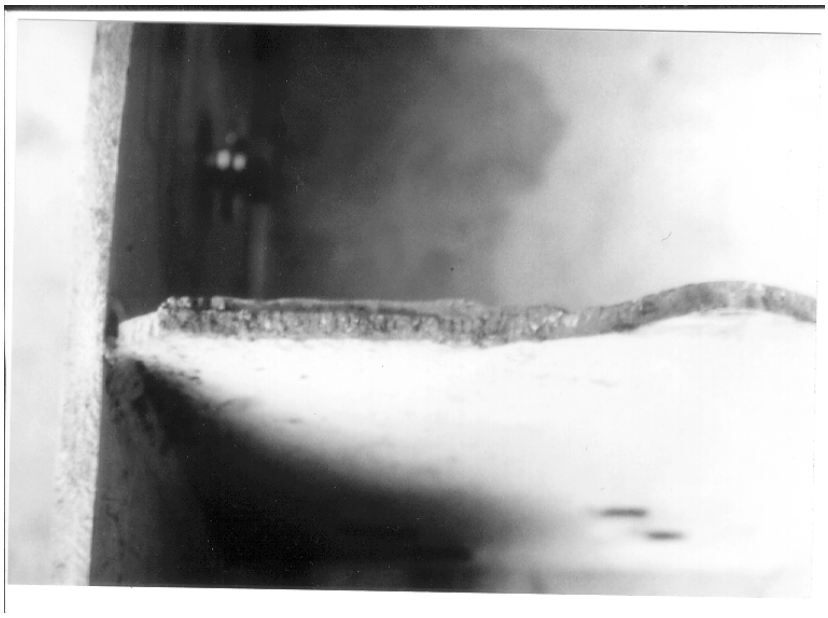

Figure 3.9 Crack surface at Part E’

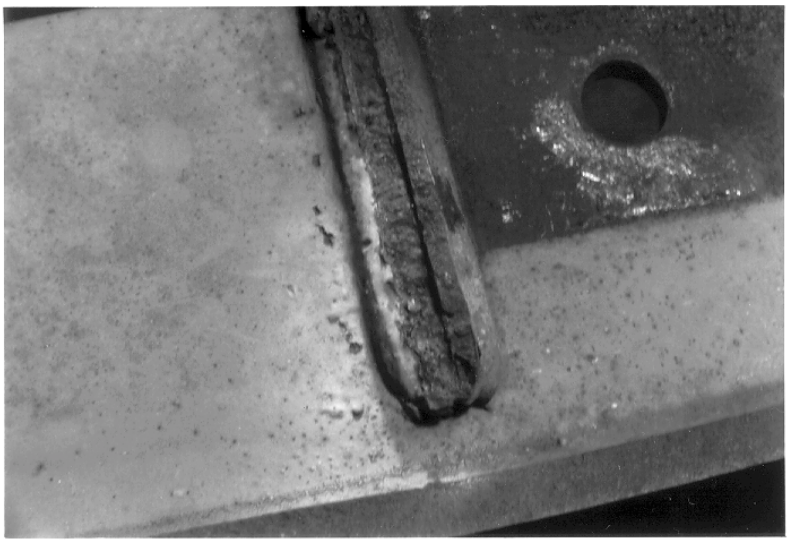

Figure 3.10 Close-up view of Part E crack surface

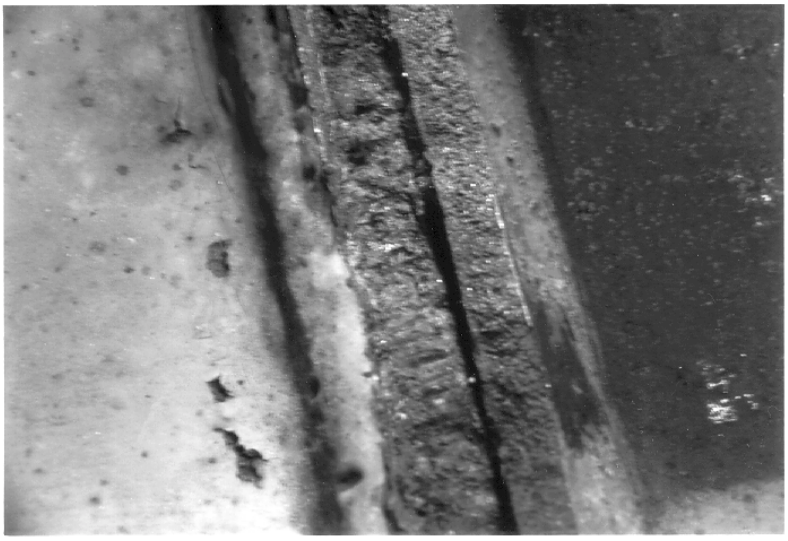

Figure 3.11 Magnified close-up view of Part E crack surface

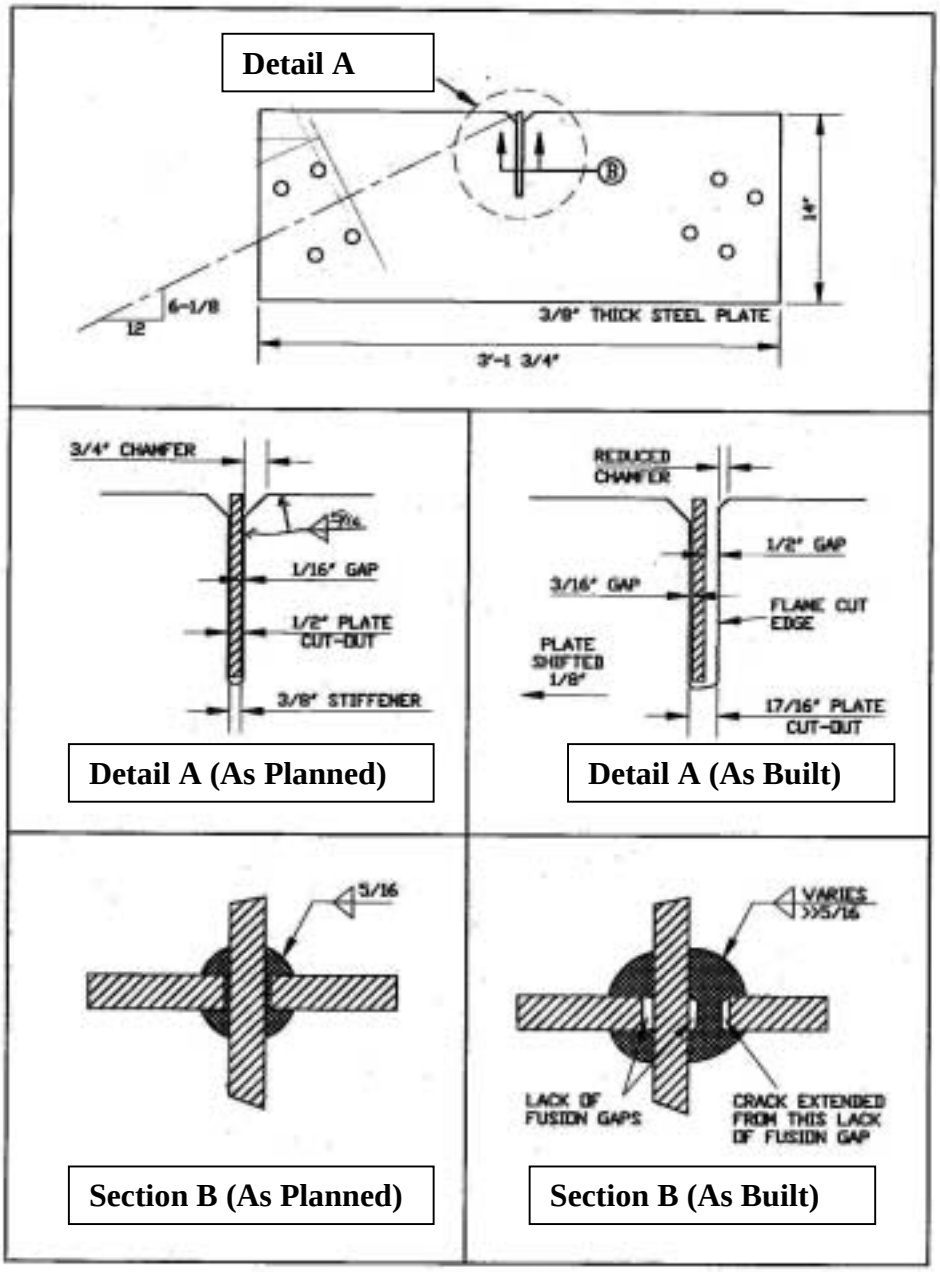

Figure 3.12 Construction aspects of horizontal attachment plate (1 in = 25 mm)

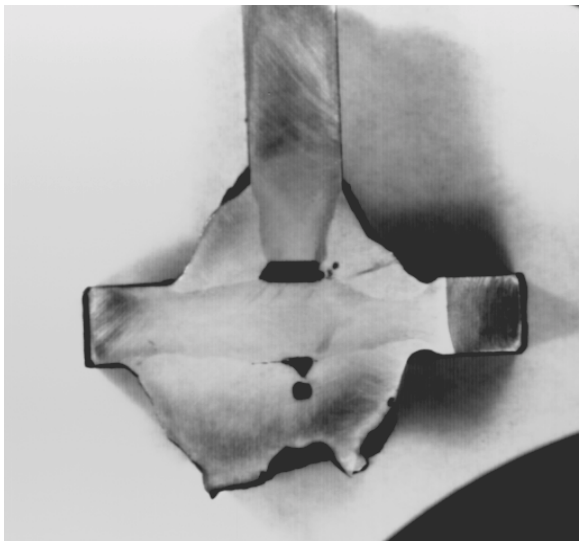

(a) Front side of slice through weld joint

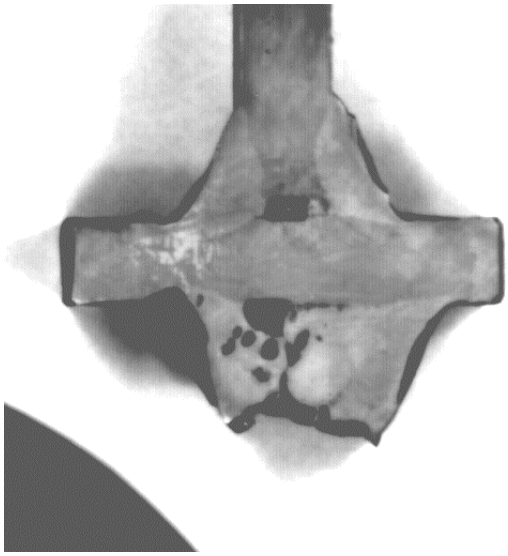

(b) Back side of slice through weld joint

Figure 3.13 View of stiffener to horizontal gusset plate weld

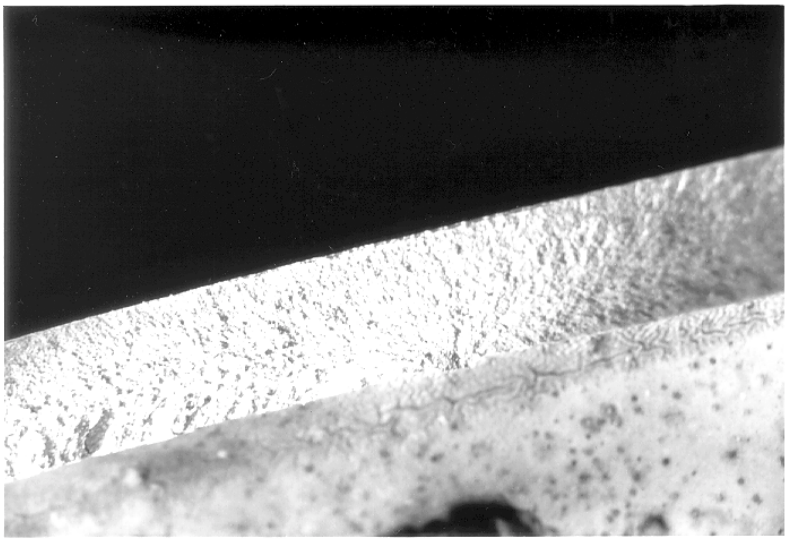

Figure 3.14 View of Part A crack surface

Figure 3.15 View of Part A' crack surface

CHAPTER 4

MATERIAL TESTING

4.1 Introduction

The I-64 Blue River Bridge was designed and constructed in 1969-74 and, consequently, utilized steel that was common during that period. Unfortunately, detailed information concerning the material properties of the Blue River Bridge was not retained by the Indiana Department of Transportation. It was decided, therefore, that a number of materials tests would be conducted to evaluate the physical characteristics of the bridge steel. Tests were performed to evaluate the mechanical, chemical, and fracture toughness properties of the steel used in the web and flange of the bridge.

A 2440 mm (8-ft) wide section of the girder, centered about the fracture, was removed from the bridge and shipped to Purdue University for evaluation and testing. Figure 4.1 depicts the girder section when it arrived at Purdue. This section of the girder was removed when the bridge was repaired. To reinforce the fractured section, and to prevent the fracture surfaces from smashing together during shipping and causing permanent marring that would prevent an effective evaluation of the crack surfaces, splice plates were bolted to each side the web of the section that was removed. These plates, which can be seen in Figure 4.1, were added to protect the crack surface and to reinforce the cracked section during handling and shipping.

The 2440 mm (8-ft) wide girder section was cut apart so that the fracture surfaces could be closely inspected and to facilitate extraction of the material testing samples. First, an oxyacetylene torch was used to cut through the girder web just below the top flange. The cut intersected the end of the brittle fracture and separated the 2440 mm (8-

ft) section into a top flange section and the two web and bottom flange sections shown in Figure 4.2. Next, a 610 mm (2-ft) wide portion was cut off from each end of the two web and bottom flange sections to provide ample material for extraction of the material testing samples.

4.2 Mechanical and Chemical Properties

The purpose in conducting the mechanical and chemical testing of the bridge steel was to define the properties of the steel and to assist in identification of the steel type. A total of six tensile coupons were extracted from the beam web, three from each side of the crack. Four tensile coupons were extracted from the beam bottom flange, two on each side of the crack.

The position of the web and flange tensile coupons that were extracted from the bridge girder is shown in Figure 4.3. Also shown in the figure are the locations for the Charpy V-notch specimens and the fracture specimens; these tests will be discussed in the following section.

The tensile coupons were extracted and tested in accordance with ASTM A370-96 and ASTM E8-93. After extracting the specimen blanks, they were machined to the final dimensions of the tensile coupons as shown in Figure 4.4. The plate-type test specimens were all 38.1 mm (1-1/2") wide. The specimen thickness was the same as the corresponding plate thickness: 12.7 mm (1/2") for the web and 34.9 mm (1-3/8") for the flange.

The tensile coupons were prepared for testing by attaching strain gages and adding gage marks. Two strain gages were bonded to middle of each specimen to record the

strain in the linear region and to capture the yield point. Two gage marks, spaced at 203 mm (8-in.) apart, were punched on the side of each specimen. The gage marks were used to evaluate the ductility of the steel.

The tensile tests were run in stroke control using a 890 kN (200-kip) capacity MTS servo-hydraulic control testing machine. The rate of separation of the cross-heads was controlled such that prior to yielding of the specimen the stress induced was 207 MPa/min (30 ksi/min), and from yielding through rupture the stroke was 25.4 mm/min (1 in/min). The load, stroke and strain values were recorded electronically throughout the test using an Optim MEGADAC data acquisition system. Moreover, the yielding, ultimate load, and rupture load were observed and recorded from the digital indicator on the testing machine.

The stress vs. strain curve is shown in Figure 4.5 for tensile specimen 1TL. The value of Young's modulus, the yield point, tensile strength, rupture stress, and ductility were obtained from these curves. The percent elongation was computed from the change in gage length after rupture by match mating the two pieces of the coupon.

The results of the tensile coupon tests are summarized in Table 4.1 and 4.2 for the web steel and flange steel, respectively. There was little variation in the test results with respect to the measured quantities. It is also evident that the web steel has a greater yield strength and lower ductility than the flange steel, although the tensile strengths are roughly equivalent.

In an effort to further evaluate the web and flange steels, the steel chemistry was determined. Small samples, each measuring about 50 mm (2 in) square, were extracted from the web and flange plates and sent to Sherry Laboratories in Muncie, Indiana for

chemical analysis in accordance with ASTM standards. The results of the chemical analysis are summarized in Table 4.3. The carbon content is listed as 0.2% by weight for the web steel, and 0.17% for the flange steel.

The carbon equivalent provides a measure of the weldability of the steel based upon the steel chemistry, and the influence that it has on the hardenability of the steel. According to the American Welding Society Bridge Welding Code D1.5-95 (1995), the carbon equivalent is computed from the following expression:

$$CE = C + \frac{(M_n + Si)}{6} + \frac{(Cr + M_0 + V)}{5} + \frac{(Ni + Cu)}{15}$$

Use of this equation with the element compositions listed in Table 4.3 results in CE values of 0.39 for the web and 0.36 for the flange. From Appendix III of the AWS Bridge Welding Code (1995), these values of the carbon equivalent would place the steel in Zone II for hardness assessment, but would result in very rapid cooling rates for the desired maximum hardness of 350 VH in the weld heat affected zone. The rapid cooling rates result in a low required energy heat input that can be obtained through conventional welding procedures. It could be concluded, therefore, that the steel has good overall weldability. Moreover, according to the Lincoln Electric Procedure Handbook of Arc Welding (1994), if a carbon equivalent value of less than 0.45 is obtained, then preheat is optional. Consequently, the carbon equivalent assessments by the AWS and the Lincoln Electric methods indicate that the web steel and the flange steel both have good weldability characteristics.

The mechanical and chemical properties of the web and flange plates are compared with those values required by ASTM A7 and ASTM A36/A 36M-96 in Table 4.4. Based upon the comparison, it is evident that the 227.5 MPa (33 ksi) yield strength of the flange steel does not meet the minimum yield strength requirement for A36 steel, but it does match the minimum requirement for A7 steel. The web steel meets the physical property requirements for both A7 and A36 steels. Moreover, both the web and flange steels satisfy the chemical requirements for A7 and A36 steels.

Based upon the measured values of the chemical and physical properties, both the web and flange steels are identified as mild carbon steels. Moreover, it would appear that the web satisfies the requirements for ASTM A36 steel, while the flange satisfies the requirements for ASTM A7 steel.

4.3 Charpy V-Notch Tests

Charpy V-notch (CVN) tests were conducted to evaluate the fracture toughness of the web and flange steels. The CVN is a relatively simple test that can be quickly used to evaluate the notch toughness of steel.

The requirements for preparing the CVN specimens and for conducting the tests are given in ASTM Specifications A370-96 and E23-96. The specimen configuration consists of a 10 mm (0.39 in.) square section x 55 mm (2.16 in.) long blank with a notch machined across the middle of one side of the specimen.

A number of test samples were extracted from the web and flange plates. A total of 64 specimens were extracted from the web, with eight groups of four specimens taken from the web on each side of the fracture – see Figure 4.3. Also, a total of 56 specimens

were extracted from the flange plate, with four groups of seven specimens taken from each side of the fracture. Two different orientations of the notch were used for the flange plate specimens: in one orientation the CVN fracture would simulate crack propagation through the flange thickness, while in the other orientation it models crack growth across the flange plate width

The CVN testing was conducted at two locations: Taussig Engineering and the Purdue University Materials Engineering laboratories. The Charpy machine at Purdue had not been calibrated recently, so a limited degree of testing at a commercial laboratory was conducted to provide a calibrated baseline of CVN results. A total of 24 CVN tests were performed by Taussig Engineering: twelve specimens each from the web and the flange. An additional nineteen tests were performed in the Materials Engineering laboratory at Purdue University: nine specimens from the web and ten from the flange. Consequently, twenty-one CVN specimens were tested from the web plate and twenty-two were tested from the flange plate.

The CVN test results for the web plate steel are shown in Figure 4.6. Excellent agreement is found between the test data collected from the two different Charpy impact machines. For the Taussig Engineering CVN data, three tests were performed at each of the following four temperatures: -28.9, -17.8, 4.4 and 21.1^{o}C (-20, 0, 40 and 70^{o}F). A very low fracture toughness – less than 13.6 Nm (10 ft-lbs) – can be observed for the lower test temperatures.

The CVN test results for the flange plate steel are shown in Figure 4.7. As before, excellent agreement for the test data from both Charpy impact machines was observed for the lower test temperatures. In this case, however, there was a spread in the test data for

(higher) test temperatures above the transition temperature. As before, a low fracture toughness was observed for the low test temperatures.

Charpy V-Notch fracture toughness requirements are given in the AASHTO LRFD Design Specification (1994) for both fracture-critical and nonfracture-critical, welded members. The specification requires that the average CVN energy level for the steel exceed a particular energy level at a given test temperature. Since the Blue River I-64 bridge is located in a Zone 2 environment, with a lowest-anticipated service temperature (LAST) of –34.4^{o}C (-30^{o}F), then the specification requires a minimum fracture toughness energy level of 20 N-m (15 ft-lbs) at a test temperature of 4.4^{o}C (40^{o}F) for nonfracture-critical members. For fracture-critical members, the required energy level is 34 N-m (25 ft-lbs) at 4.4^{o}C (40^{o}F).

The absorbed energy for CVN specimens of the web and flange steels both exceed the minimum energy level required by the LRFD Specification for nonfracture-critical members. Three CVN specimens were tested by Taussig Engineering at the required test temperature of 4.4^{o}C (40^{o}F) for both the web and flange. The average CVN absorbed energy level of the three specimens was 28.9 N-m (21.3 ft-lbs) for the web steel and 50.6 N-m (37.3 ft-lbs) for the flange steel. The web and flange steel both exceed the minimum energy level of 20 N-m (15 ft-lbs) for non-fracture-critical members, and the flange exceeds the 34 N-m (25 ft-lbs) minimum energy level for fracture-critical members. Use of the nonfracture-critical requirements would probably be appropriate because the four girders for the bridge structure clearly provide some degree of redundancy. Therefore, it can be concluded that the web and flange steel used for the welded plate girder had an adequate fracture toughness from a materials standpoint.

4.4 Tensile Fracture Tests

In an effort to complement the Charpy V-Notch fracture toughness test results, a few additional fracture toughness tests were conducted to estimate the specimen tensile fracture toughness at a low test temperature. The fracture toughness was evaluated by estimating the critical stress-intensity factor K_c for a notched (cracked) specimen loaded in uniaxial tension.

The fracture specimen blanks were extracted from the girder web plate material as noted in Figure 4.3. The specimen blanks were then machined to the dimensions shown in Figure 4.8. After machining the specimens to the desired dimensions, then notches were cut into the specimens to assist in the initiation of a crack. Two different specimen types were tested: an edge-cracked specimen and a center-hole specimen. In the edge-cracked specimen, a jewelers saw was used to cut a small notch into one side of the specimen. For the center-hole specimen, shown in Figure 4.9, a 9.5 mm (0.375-in) diameter hole was drilled at mid-width of the specimen and notches were cut on each side of the hole.

The specimens were then placed in a servo-hydraulic testing machine and a small cyclic stress was applied to the specimen to initiate sharp fatigue cracks at the notches. The magnitude of the cyclic stress was selected to be 137.9 MPa (20 ksi), which is a value low enough so that only linear, elastic stresses were applied to the specimen. The cyclic loading was continued until the cracks propagated to a particular desired length.

After pre-cracking, the hydraulic grip for the upper portion of the specimen was loosened and the cross-head raised. An environmental chamber was then lowered onto

the specimen – see Figures 4.10 and 4.11. The specimen was re-gripped and the plexiglass cooling chamber was filled with a mixture of dry ice and ethyl alcohol. Dry ice was added to the mixture for about 15 minutes. During this period of time, the temperature of the pre-cracked steel detail approached that of the mixture, roughly –28.9° C (-20° F). With the environmental camber intact, the specimen was then loaded in uniaxial tension until failure occurred.

A total of five specimens were tested: three edge-cracked specimens and two center-hole specimens. The specimen dimensions, crack size prior to failure, and the failure load are given in Table 4.5. The specimen width and thickness were measured at the location where fracture occurred, and the crack size reported is the average value that was measured on the fracture surface. A brittle type fracture occurred for all of the specimens tested. The appearance of the fracture surface for the edge-cracked and center-hole specimens is shown in Figures 4.12 and 4.13, respectively.

The fracture toughness for the specimens was estimated using linear-elastic fracture mechanics. The following general expression, as given by Albrecht and Yamada (1977), was used to compute the stress-intensity factor:

$$K_I = \sigma\sqrt{\pi a}\ \ F_s\, F_w\, F_g\, F_e$$

where σ is the applied remote tensile stress, a is the appropriate crack size, F_s is a crack-edge correction factor, F_w is a finite-width correction factor, F_g is a geometric detail correction factor for non-uniform opening stresses, and F_e is an elliptical crack front correction factor. Based upon the above equation, the K_I value that corresponds to fracture (K_c) was computed.

The correction factor for an elliptical crack front was taken as 1.0 since the cracks were through-thickness for both specimen types. For the edge-crack tensile specimen, the crack edge and finite width correction factors were obtained from a solution given by Bowie (1964) for a tensile sheet with edge cracks. For the center-hole tensile specimen, the correction factors for finite width and free edge given by Albrecht and Yamada (1977) were used. For the non-uniform stress caused by the center-hole, the correction factor was computed using a solution for the stress field near the hole that was given by Timoshenko and Goodier (1970). The computed values of the critical stress-intensity factor K_c that correspond to specimen fracture are presented in Table 4.6. It can be observed that the edge-cracked specimens give a slightly higher K_c value than the center-hole specimen.

4.5 Fatigue Crack Propagation Tests

Three crack growth tests were conducted to estimate the fatigue crack growth rate of the web steel. The test specimens were extracted from the web plate and prepared in the same fashion as the edge-cracked tension fracture specimens described in the previous section. Rather than loading the specimens to failure, however, the cyclic loading was continued to evaluate the propagation behavior of the cracks in the web steel. Stable crack growth was monitored until the specimen fractured in a ductile fashion – see Figure 4.14.

An apparatus was attached to the testing machine to monitor the crack growth during the cyclic loading. The crack monitoring apparatus, shown in Figure 4.15, consisted of a traveling low-powered (10x) microscope attached to a movable base. The base

movement was controlled by a 40-turn per inch threaded rod (1.575 turns per mm). The rotation of the threaded rod was monitored using a 500 point rotational encoder, producing a digital resolution of 787 divisions per mm (20,000 division per inch). A digital readout provided a measurement accurate to the nearest 0.001-in. (0.25 mm).

The crack monitoring apparatus was used to monitor crack size on the specimen surface during the cyclic loading of the edge cracks. A plot showing crack size versus the number of loading cycles applied to the specimen is shown in Figure 4.16 for the three test specimens. The crack growth curves are different because the initial crack size for the first specimen was notably different than that for the other two specimens.

An estimate of the crack growth rate was obtained by computing the range in stress-intensity factor, at a given crack size, and the corresponding slope to the crack size versus number of cycles curve for each of the data samples. In this fashion, a plot of the crack growth rate da/dN, versus the stress-intensity factor range, (ΔK), could be constructed. The plots for two of the three specimens are shown in Figure 4.17. The plot for the first specimen is not shown because it is believed that the data were corrupted by a sudden hydraulic shutdown during testing.

The Paris-type crack-growth equation is given in the following form (Barsom and Rolfe, 1987):

$$\frac{da}{dN} = A\,(\Delta K)^m$$

where $\frac{da}{dN}$ is the crack-growth rate, ΔK is the stress-intensity factor range, and A is the intercept and m is the slope of the best-fit line. Both A and m are material constants which can be determined from test results. As shown in Figure 4.17, a best-fit line was

placed through the data when presented on a log-log basis. The values obtained for the two valid tests are relatively close to the lower-bound crack growth values reported by Barsom and Rolfe (1987) for ferrite-pearlite steels:

$$\frac{da}{dN} = 3.6 \times 10^{-10} \ (\Delta K)^{3.0}$$

This result indicates that it is reasonable to utilize the lower-bound ferrite-pearlite steel crack growth constants for crack propagation estimates of the web steel.

Table 4.1 Tensile Test Results – Web Steel

Specimen	E, 10^3 MPa (ksi)	Yield Point MPa (ksi)	Tensile Strength MPa (ksi)	% elongation (in 203 mm (8 in.))
1TL	208.9 (30.3)	290 (42)	469 (68)	27.8
2TL	209.6 (30.4)	283 (41)	469 (68)	28.1
3TL	206.8 (30.0)	290 (42)	462 (67)	26.7
1TR	217.9 (31.6)	276 (40)	462 (67)	26.6
2TR	208.2 (30.2)	283 (41)	455 (66)	26.8
3TR	198.6 (28.8)	283 (41)	462 (67)	23.3
Average	208.2 (30.2)	284.1 (41.2)	463.3 (67.2)	26.5

Table 4.2 Tensile Test Result – Flange Steel

Specimen	E, 10^3 MPa (ksi)	Yield Point MPa (ksi)	Tensile Strength MPa (ksi)	% elongation (in 203 mm (8 in.))
AT	204.8 (29.7)	234 (34)	462 (67)	33.6
BT	206.2 (29.9)	234* (34*)	469* (68*)	33.9
CT	202.7 (29.4)	214 (31)	448* (65*)	32.7
DT	(28.2)	228 (33)	441 (64)	35.5
Average	202.0 (29.3)	227.5 (33.0)	455 (66.0)	33.9

*Observed directly during test. (i.e. value not computed from stress-strain graph)

Table 4.3 Chemical Analysis of Web and Flange Steels, in Percent by Weight

Element	Web	Flange
Carbon	0.20	0.17
Manganese	0.91	0.92
Phosphorus	0.017	0.010
Sulfur	0.028	0.019
Silicon	<0.05	<0.05
Nickel	<0.05	<0.05
Chromium	<0.05	<0.05
Molybdenum	<0.05	<0.05
Copper	<0.05	<0.05
Aluminum	<0.05	<0.008

Table 4.4 Comparison of Steel Physical and Chemical Properties with ASTM A7 and ASTM A36 Specifications

BLUE RIVER BRIDGE			ASTM REQUIREMENTS	
Property	Web	Flange	A7	A36 (or A709 gr36)
Yield Point (MPa)	284	227.5	228 min	248 min
Tensile Strength (MPa)	463	455	414-517	400-552
Elongation in 203 mm (%)	26.5	33.9	21 min	20 min
E (10^3 MPa)	208	202	--	--
Carbon (%)	0.2	0.17	none	0.25 max
Manganese (%)	0.91	0.92	none	0.80-1.20
Phosphorous (%)	0.017	0.010	0.04 max	0.04 max
Sulfur (%)	0.028	0.019	0.05 max	0.05 max
Silicon (%)	<0.05	<0.05	None	0.40 max

Table 4.5 Tensile Fracture Test Data

Test Specimen[1]	Width (W) mm (in)	Thickness (t) mm (in)	Total Crack Size[2] (a or 2a) mm (in)	Failure Load (P) kN (kip)
1	88.65 (3.490)	12.62 (0.497)	22.48 (0.885)	308.2 (69.3)
2	88.57 (3.487)	12.67 (0.499)	19.84 (0.781)	310.5 (69.8)
3	88.65 (3.490)	12.57 (0.495)	19.99 (0.787)	332.7 (74.8)
4	88.19 (3.472)	12.57 (0.495)	26.31 (1.036)	345.2 (77.6)
5	88.52 (3.485)	12.70 (0.500)	23.44 (0.923)	362.9 (81.6)

Notes: 1. Nos. 1-3 are edge cracked specimens. Nos. 4-5 are center hole type.
2. Crack size averaged over thickness.

Figure 4.6 Computed Fracture Toughness based on Results of Test Data

Test Specimen	Crack Size: Width Ratio	Correction Factor $F_{cor} = F_w F_g F_s$	Failure Stress $\sigma = P/(t \times W)$ MPa (ksi)	Fracture Toughness $K_C = \sigma\sqrt{\pi a} F_{cor}$ $MPa\sqrt{m}$ $(ksi\sqrt{in})$
1	0.254	1.425	275.8 (40.0)	104.4 (94.95)
2	0.224	1.361	276.5 (40.1)	94.0 (85.5)
3	0.226	1.364	298.6 (43.3)	102.1 (92.85)
4	0.298	1.407	311.6 (45.2)	89.0 (81.0)
5	0.265	1.464	322.7 (46.8)	90.7 (82.5)

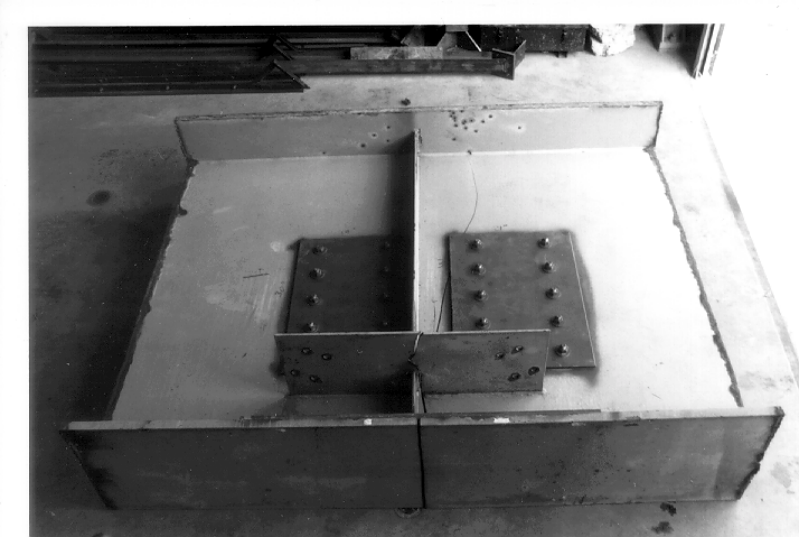

Figure 4.1 View of cracked bridge girder upon arrival at Purdue University

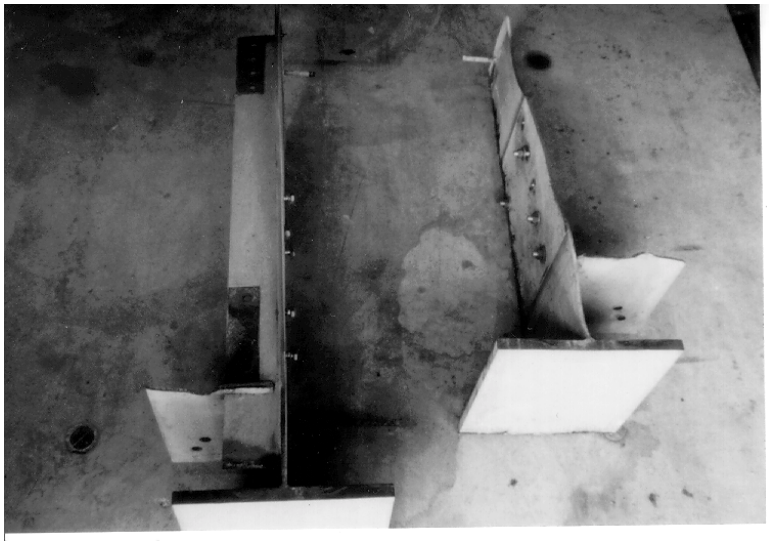

Figure 4.2 View of fracture surfaces after cutting fractured girder

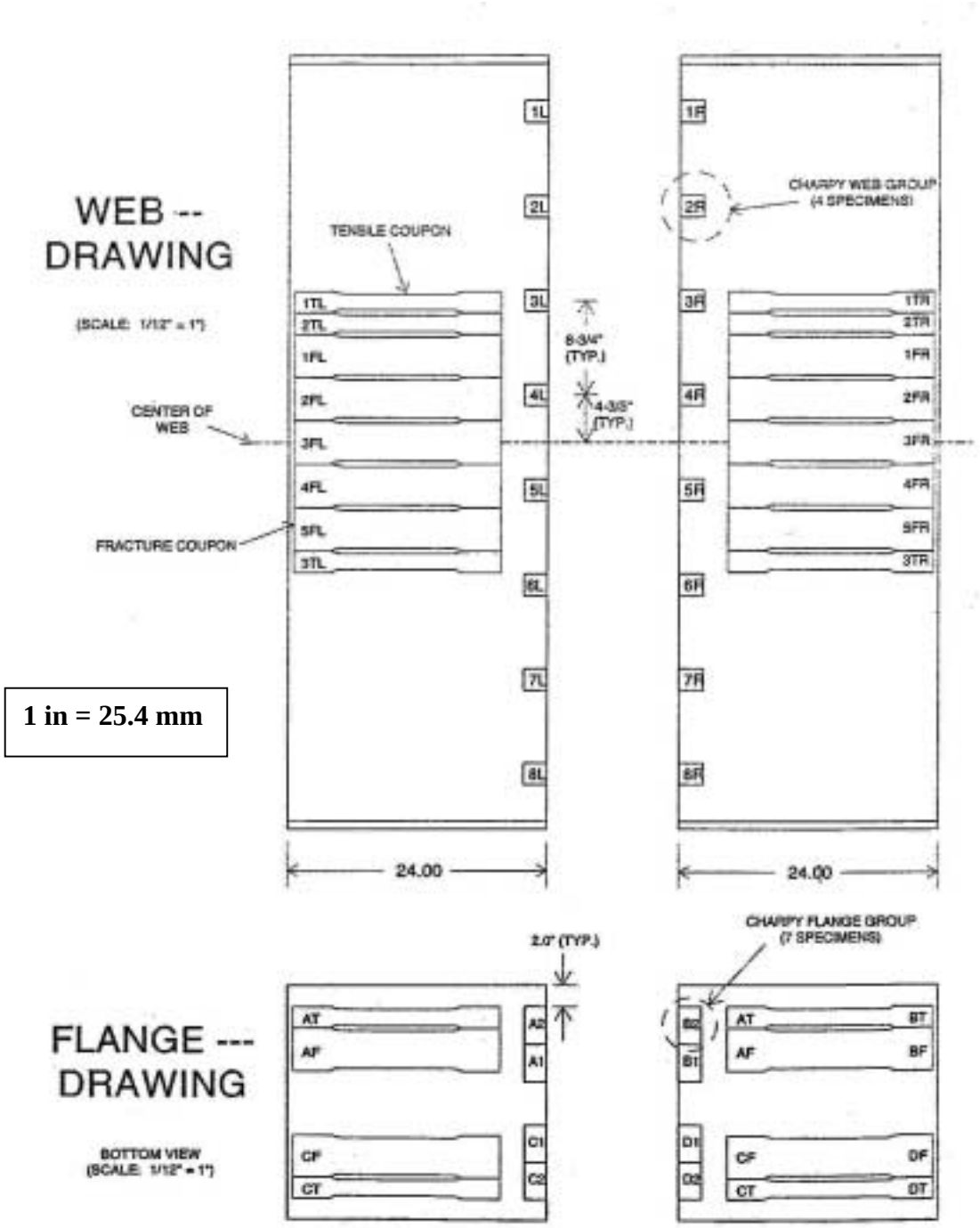

Figure 4.3 Location of flange and web test coupons

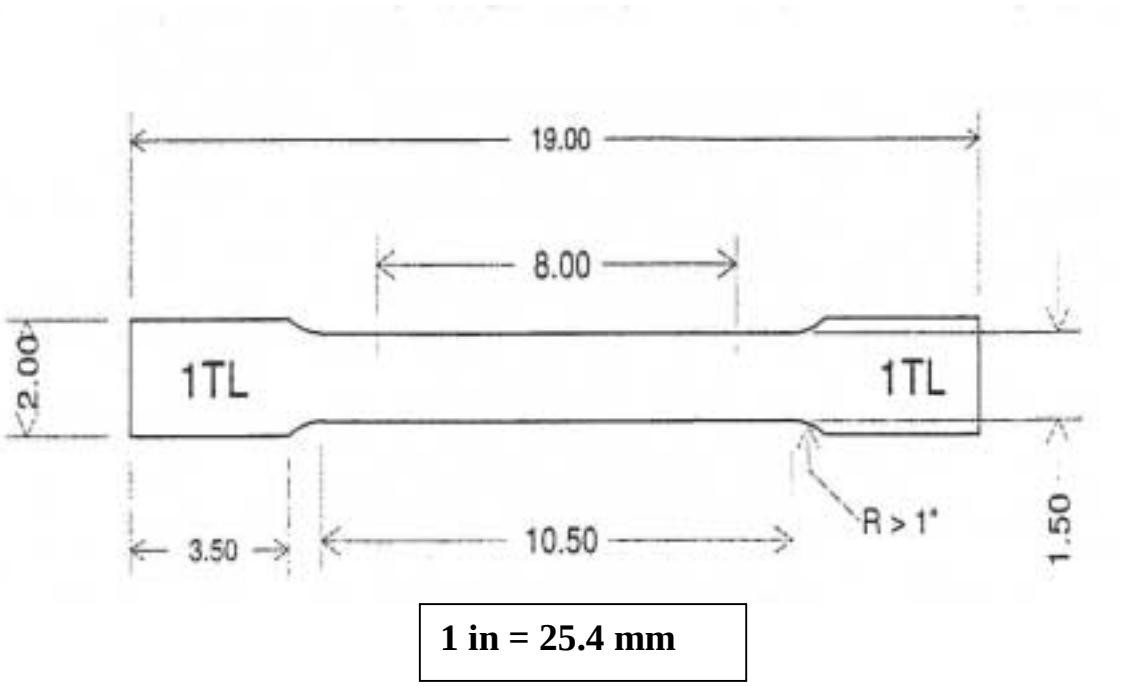

Figure 4.4 Dimensions of tensile test coupon

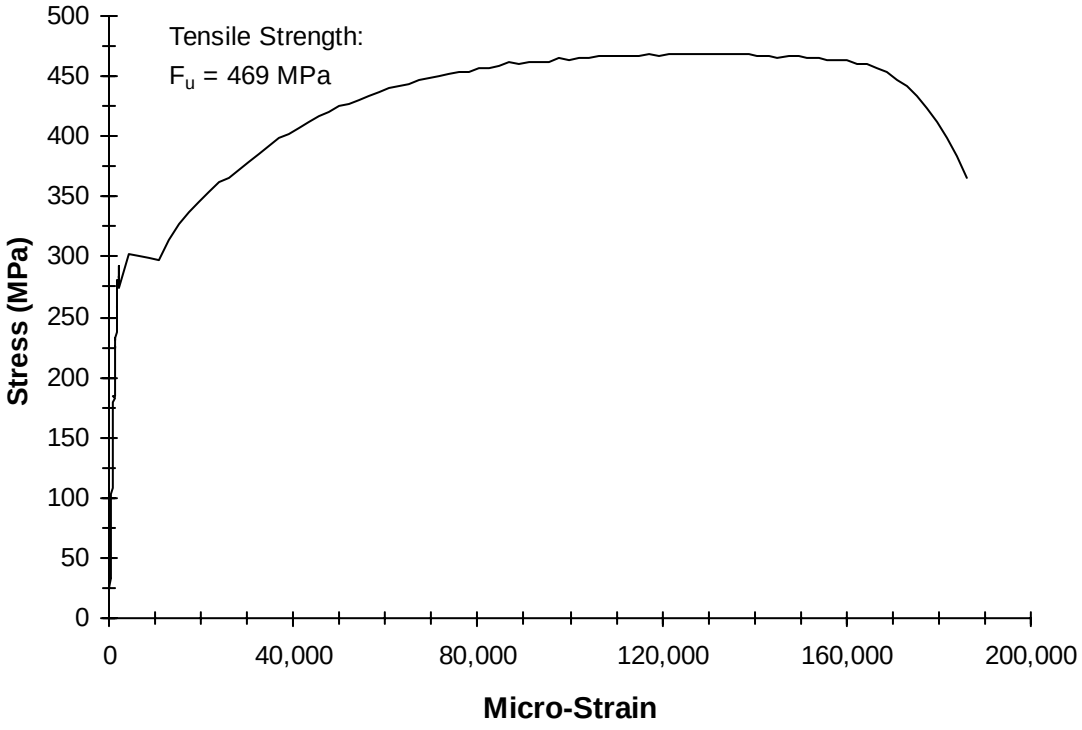

Figure 4.5 Stress versus strain for Specimen 1TL

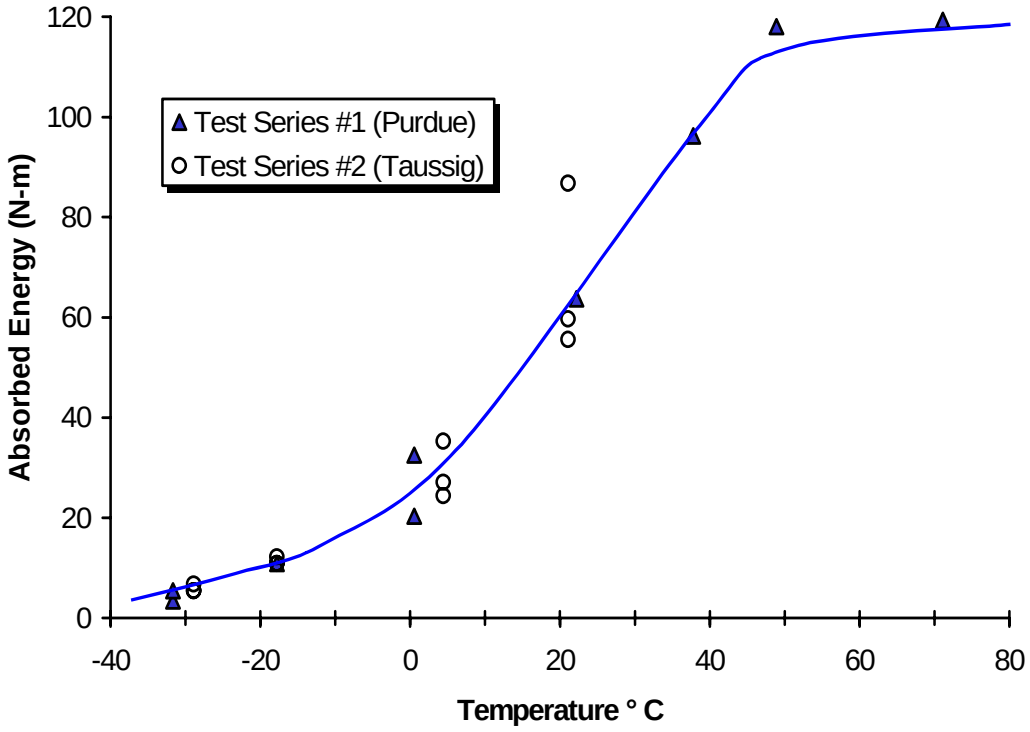

Figure 4.6 Charpy V-notch results for web plate steel

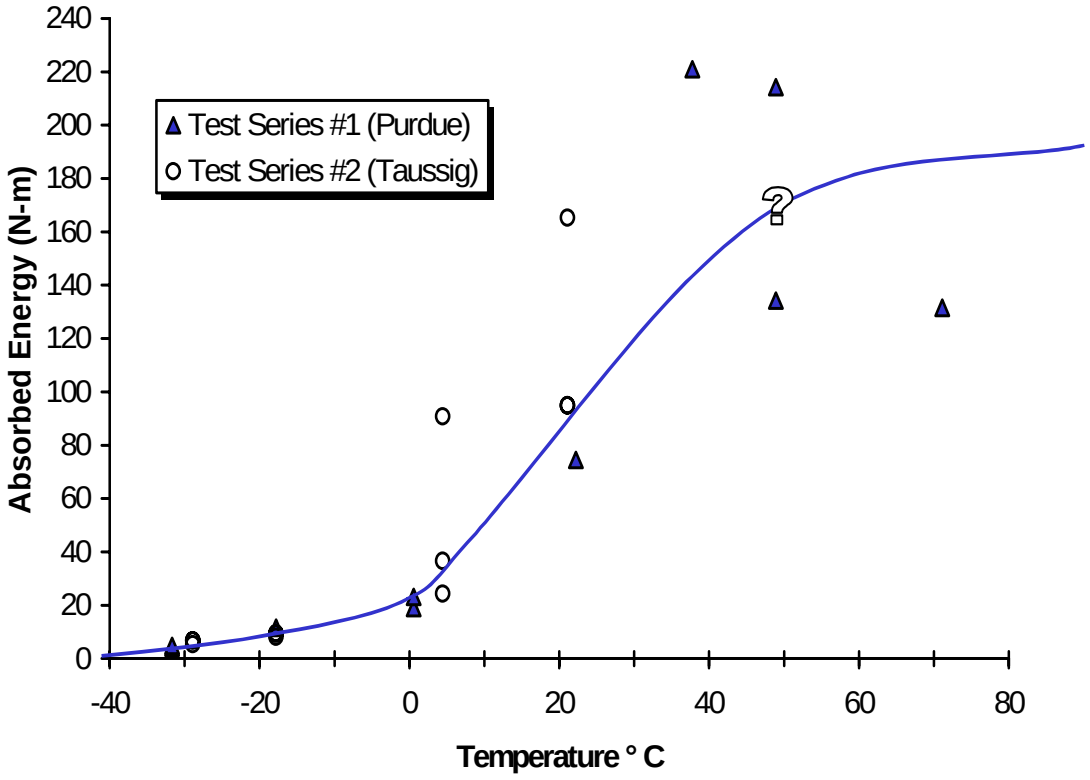

Figure 4.7 Charpy V-notch results for flange plate steel

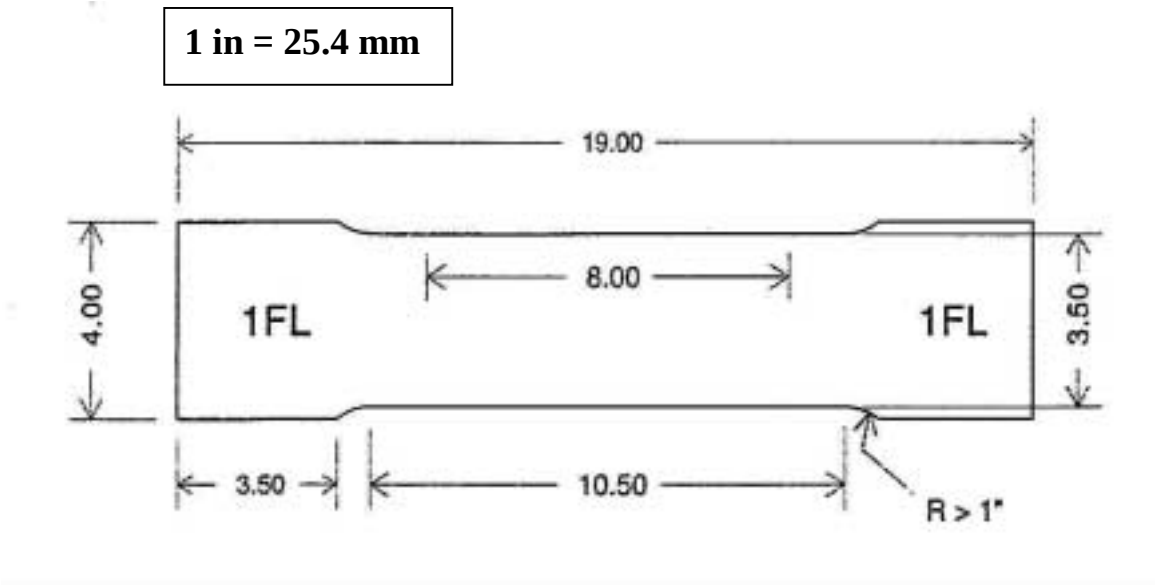

Figure 4.8 Dimensions of fracture toughness test specimen

Figure 4.9 View of center-hole fracture specimen

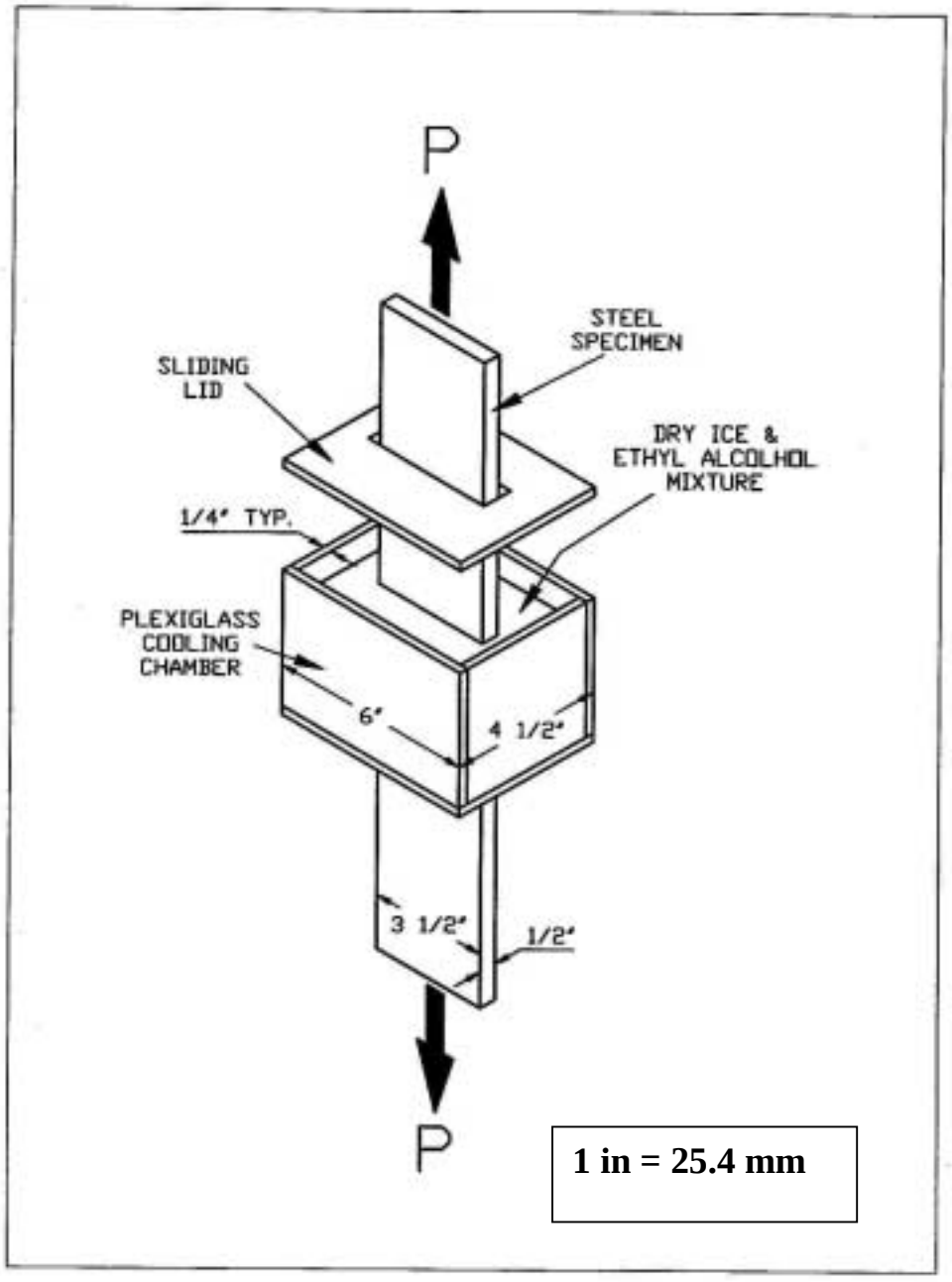

Figure 4.10 Environmental chamber used in brittle fracture test

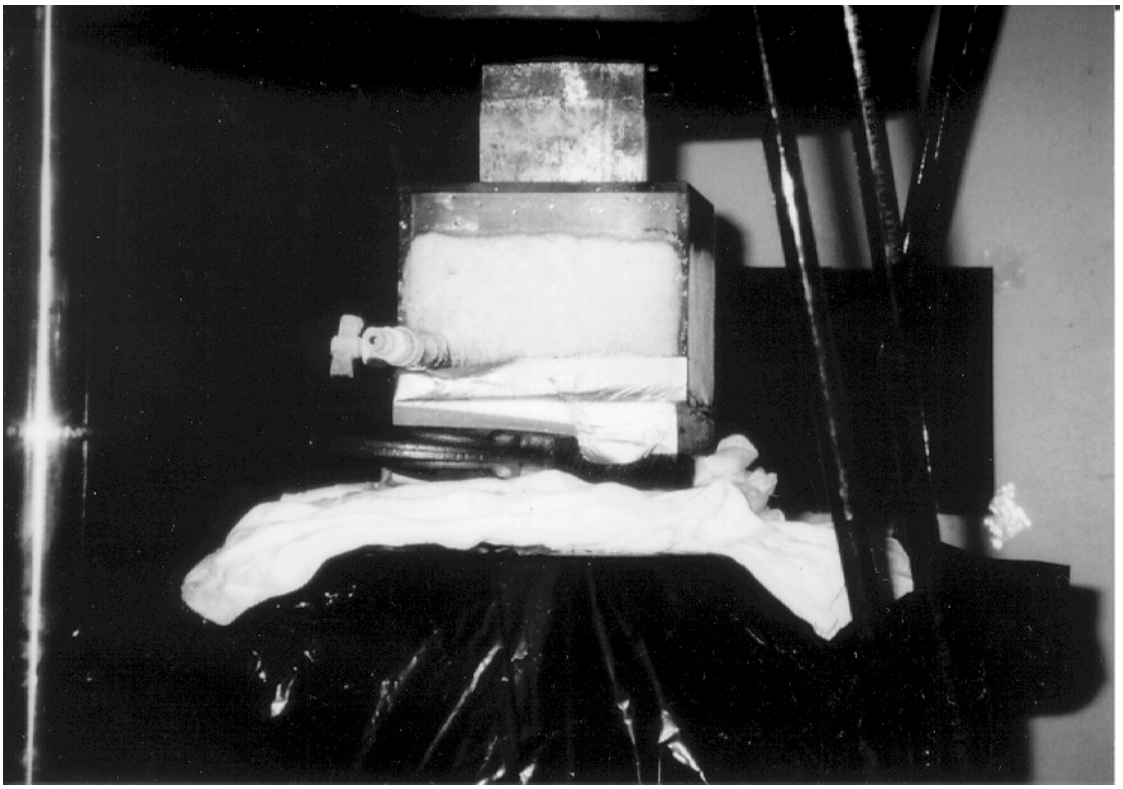

Figure 4.11 View of cooling chamber for fracture toughness test

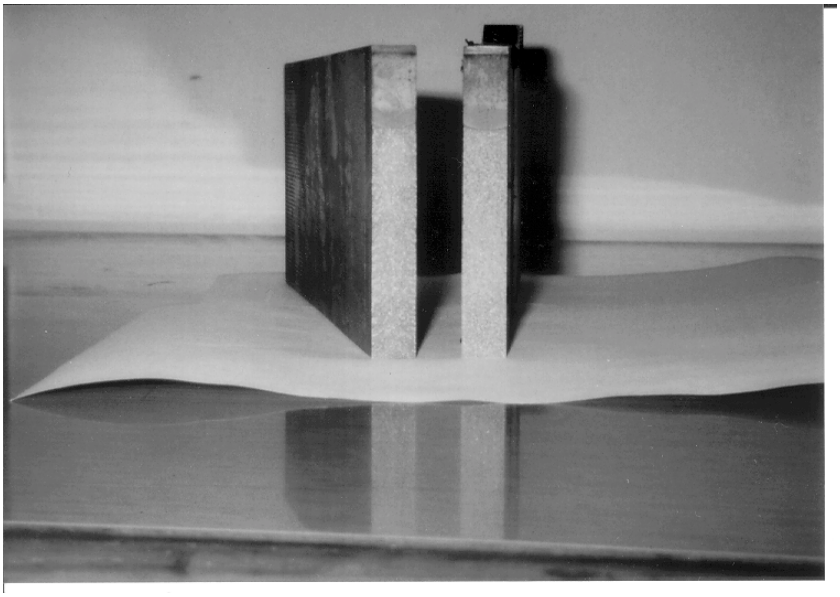

Figure 4.12 View of fracture surface for edge-cracked fracture specimen

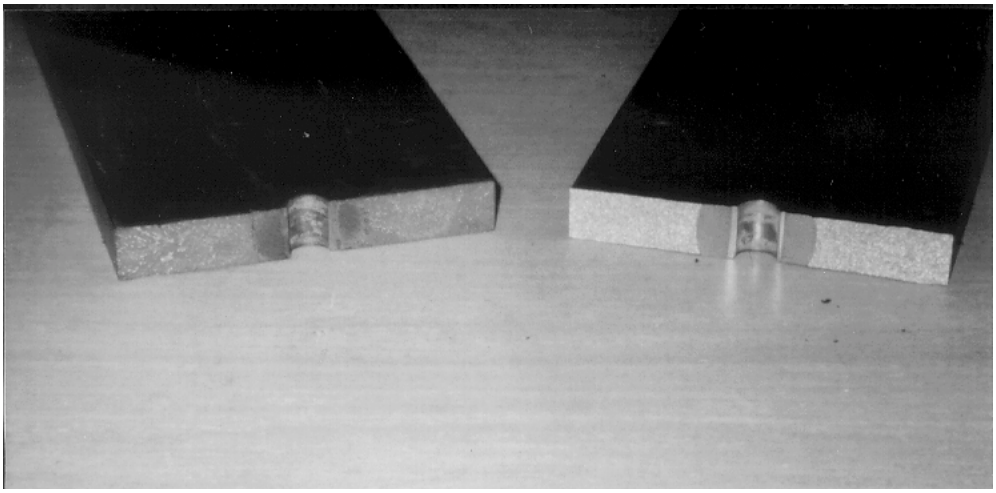

Figure 4.13 View of fracture surface for center-hole fracture specimen

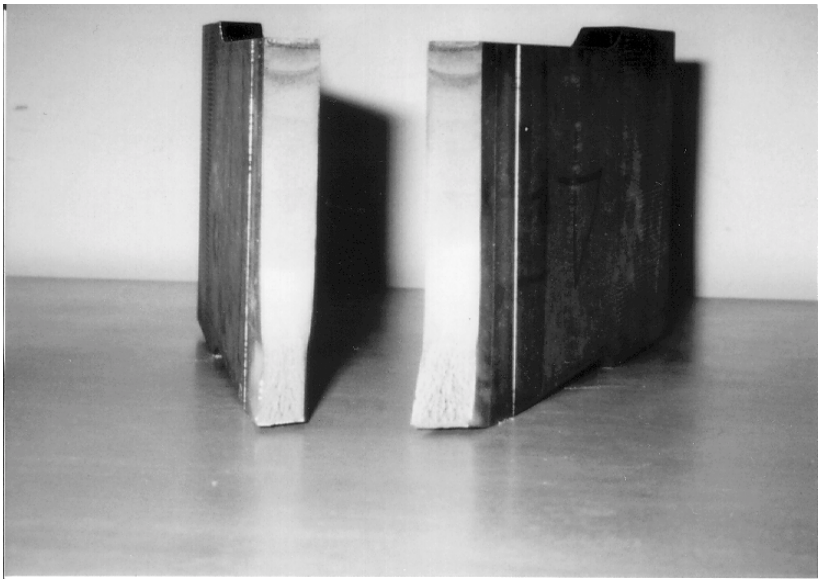

(a) End view of fracture surfaces

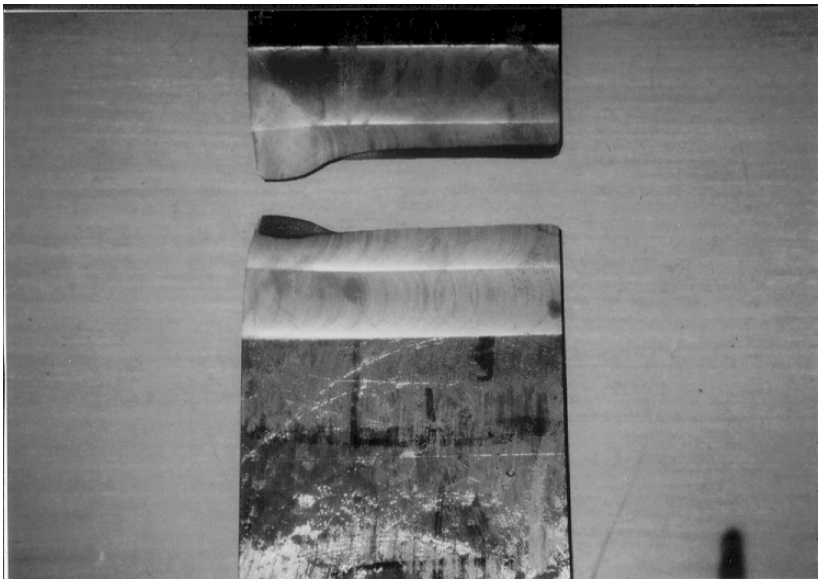

(b) Side view of fracture surface

Figure 4.14 Fracture surfaces of fatigue crack propagation specimen

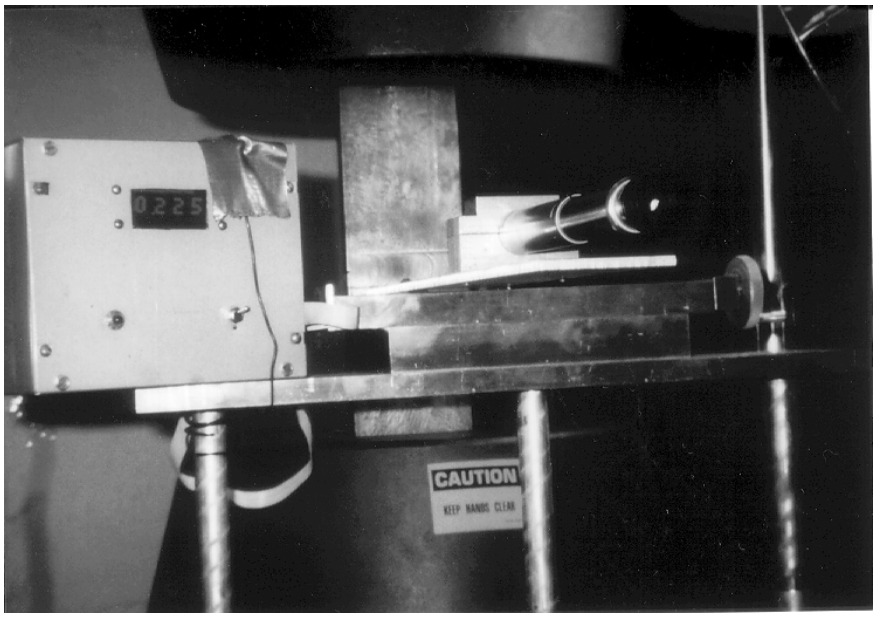

Figure 4.15 Apparatus for monitoring fatigue crack growth

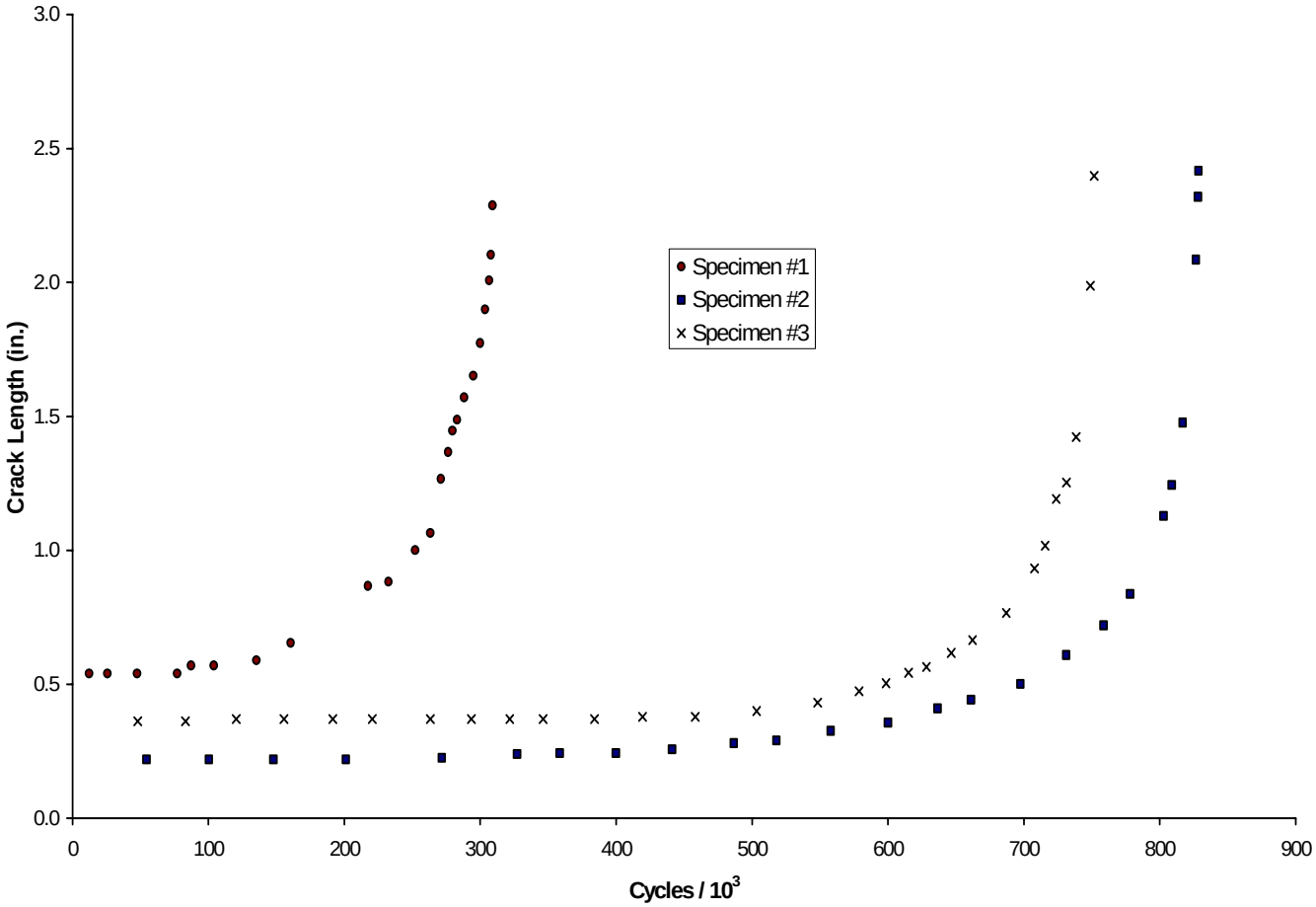

Figure 4.16 Crack Growth Versus Number of Loading Cycles for Three Specimens

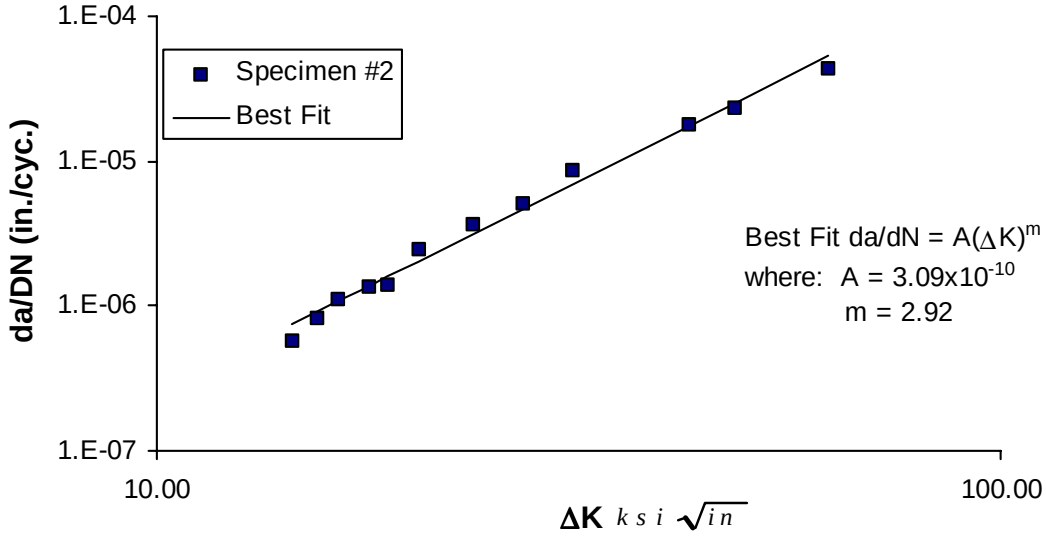

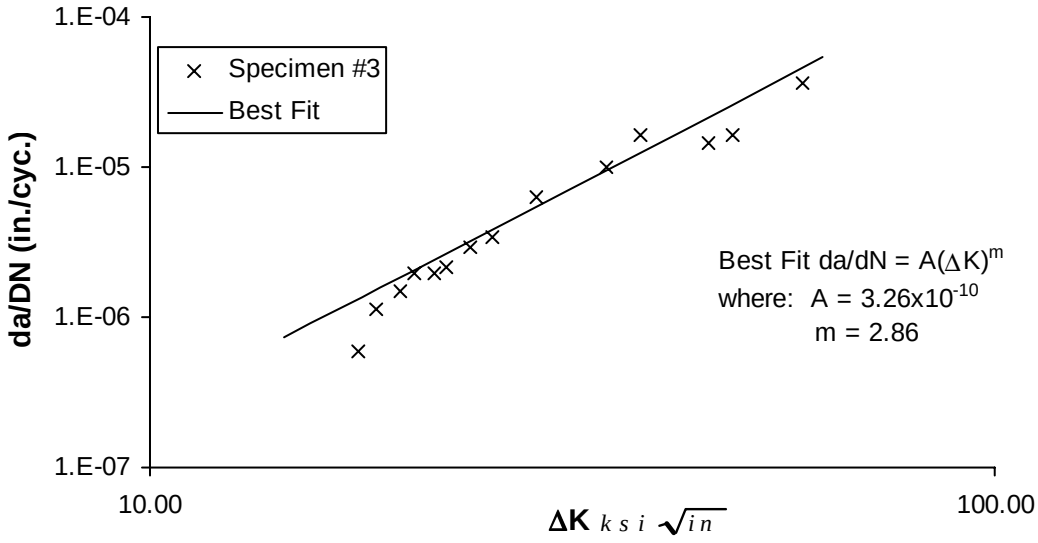

Figure 4.17 Best-fit lines for Crack Propagation Data of Specimens 2 and 3

CHAPTER 5

ANALYSIS OF THE BRIDGE FRACTURE

As stated earlier, a brittle fracture does not generally occur unless several mitigating factors simultaneously work to reduce the resistance of a structural detail to rapid crack extension. Previous chapters have discussed environmental, geometric and material factors for the I-64 Blue River bridge. Estimates of the stress levels developed in the critical bridge girder and possible implications relative to brittle fracture susceptibility of the bridge are discussed in this chapter.

5.1 Stress Levels in the I-64 Blue River Bridge

The stress levels developed in the Blue River bridge were estimated in a couple of different ways. First, an approximate analysis was conducted to estimate the stresses at the location of the critical detail near the middle of the center span. Also, a more refined structural analysis was conducted using SAP2000. The results of these analyses are described below.

5.1.1 Simplified Analysis

A simplified structural analysis was conducted to estimate the stresses in the Blue River bridge superstructure. The analysis is denoted as simplified because a number of simplifying assumptions were utilized to evaluate the stresses developed in the structure. For example, a constant cross section with no change in inertia was assumed. This assumption is not technically correct since the size of the flange plate changes along the

span length of the bridge. A more accurate evaluation of the inertia will typically yield higher bending moments over the interior piers and reduced bending moment values near midspan. Consequently, this assumption tends to be conservative.

Three other simplifying assumptions that were made include the use of the simple "s/5.5" load distribution factor from the LFD version of AASHTO Standard Specifications (1996), the use of a non-composite cross section in the region where the fracture occurred, and the use of routine design impact values as provided in AASHTO. Only two loading cases were considered to compute the bending stress: (a) dead load (due to member and deck weight) plus lane loading and (b) dead load plus truck loading. The HS20 truck and lane loading was utilized for the analysis.

The welded girder section used for the analysis at the critical location involved a 1778 mm x 12.7 mm (70-in. x ½ in.) web plate and 559 mm x 34.9 mm (22-in. x 1 3/8-in.) flange plates. This cross section provides a moment of inertia of 38.02 $(10)^9$ mm^4 (91,354 in^4). The bottom of the horizontal gusset plate was located 285.8 mm (11 ¼-in) above the top of the bottom flange.

The first loading case - for dead load plus lane load - produced a bending moment at midspan of the center span of 4968 kN-m (3665 ft-kips). This value includes an 18.3 percent increase in live load for impact effects, based on the center span length of 45.11 m (148 ft). The second load case – for dead load plus truck load – produced a midspan bending moment of 4815 kN-m (3552 ft-kips). For the two load scenarios considered, the lane loading case produced a slight larger bending moment.

Based upon the bending moment determined in the simplified analysis, the flexural bending stress due to the maximum primary bending moment was determined.

At the center of the horizontal gusset plate, the bending stress was found to be 30.0 MPa (4.35 ksi) for dead load only and 78.2 MPa (11.34 ksi) for dead load plus live load and impact. The corresponding extreme fiber bending stresses for dead load and combined dead plus live and impact load are 46.3 MPa (6.72 ksi) and 120.7 MPa (17.51 ksi), respectively.

5.1.2 Refined Analysis

A more detailed structural analysis was also conducted to provide an improved estimate of the distribution of stresses in the Blue River bridge superstructure. The analysis was performed using SAP2000, a commercial structural analysis program. Frame elements were employed in the two-dimensional analysis. Changes in cross section were modeled appropriately to reflect those locations along the span where a change in the flange plate size occurred. As in the simplified analysis, a non-composite behavior was assumed and the properties of the steel girders only were used. However, to understand the possible influence of composite action on the structural behavior, a composite analysis was also performed using cross sectional properties of the appropriate girder section together with the concrete deck.

Nodes for the frame elements were positioned at locations where changes in the cross section occurred. A 1778 mm x 12.7 mm (70-in. x ½-in.) web plate was used throughout the length of the bridge, but four different thickness values were used for the 559 mm (22-in) wide flange plate: 25.4, 34.9, 44.5, and 63.5 mm (1, 1 3/8, 1 ¾, and 2 ½-in). This involved five flange thickness changes in the two outside spans and seven

thickness changes in the middle span. The moment of inertia of the appropriate cross section was used in the analysis.

The load distribution for the outside girder was computed using the procedures outlined in the AASHTO LRFD Specification (1998). The lever rule provides for a distribution factor of 0.757 times the axle weight. The specification for design then increases this value by 20% to give a value of 0.908. The distribution factor was also computed for two or more design lanes loaded, giving a factor of 0.802 times the axle load.

The stress in the welded girder at the critical location – where the fracture occurred - was computed using the LRFD specification (1998) for each of the given distribution factors. The specification uses a combination of HS20 lane load and truck axle loads. The dead loading caused by the steel girder, concrete deck and wearing surface were also computed. A 15 percent increase in the live load moments for impact effect was included. This impact effect is the prescribed value for dynamic load allowance for the fatigue and fracture limit-states as stipulated in the LRFD Specification (1998). Moreover, to provide a range in behavior for possible involvement of the concrete deck, the stress was computed on the basis of both composite and non-composite cross sectional properties. The results of the stress analysis are summarized in Table 5.1.

5.1.3 Comparison of Analysis Results

A comparison of the stress level at mid-thickness of the horizontal gusset plate generated by using the two analysis methods reveals little difference. It should be pointed

out that the method used to generate the stresses was quite different, although the end result was not significantly different. Use of the simplified analysis produced a stress of 78.2 MPa (11.3 ksi), while the refined analysis predicted a stress level of 72.9 MPa (10.6 ksi) for the lever rule to 80.9 MPa (11.7 ksi) for the modified design value. In the simplified analysis, the controlling load combination was the lane loading, which produced the maximum stress, while the refined analysis utilized a combined load effect. Moreover, a slightly different impact value was used in the two methods: 18.3% in the simplified analysis and 15% for the dynamic load allowance in the refined analysis.

Another point worth noting is that the stresses predicted by the two analysis procedures are design-related values that correspond to the standard design vehicles and the impact corresponding to those vehicles. The actual stresses developed in the bridge at the critical detail may be somewhat different since the actual vehicle axle loads and the impact developed by those vehicles will vary from the design values. Nevertheless, the values predicted by the two analysis techniques provide a basis to examine the performance of the structural detail.

5.2 Fracture Analysis of the I-64 Blue River Bridge

The stresses developed in the simplified and refined analysis are used to examine the fracture resistance and susceptibility of the I-64 Blue River Bridge. Fracture of the horizontal attachment plate and the girder web plate are examined in the following sections.

5.2.1 Fracture Analysis of the Attachment Plate

Fracture of the attachment plate and the general characteristics of the crack pattern were discussed in Section 3.2.1. Fracture mechanics can be used to estimate the fracture strength of the attachment plate if the stress state in the plate, the initial crack size, and the fracture toughness are known. Each of these will be discussed briefly.

As noted earlier, the stresses developed across the width of the attachment plate are not uniform. Stresses are introduced into the attachment plate through the fillet weld that joins the attachment plate to the web of the girder. The force introduced in the attachment plate in this manner is a result of the primary bending stresses. Since the shear transfer is on one side only, and therefore eccentric from the plate centroid, it introduces some bending as well as axial stress. Another factor for non-uniform stress is due to the forces introduced by the horizontal bracing members. The actual stress state is quite complicated and can vary considerably due to thermal effects and impact forces that introduce out-of-plane bending through the horizontal bracing members.

It is likely that a crack in the attachment plate already existed parallel to and on one side of the vertical stiffener. The basis for this statement is the evidence of heavy rust that was found on that portion of the attachment plate fracture surface, compared with the rust found on the remainder of the attachment plate fracture surface. As noted earlier in Section 3.2.1, lack of fusion weld discontinuities caused by extra notching of the attachment plate prior to welding were believed to be responsible for the formation of this pre-existing crack.

The stress-intensity-factor equation for a single-edge-notched specimen is given by Barsom and Rolfe (1987) as:

$$K_I = 1.12\,\sigma\sqrt{\pi a}\;\; k\left(\frac{a}{b}\right)$$

where σ is the remote stress on the plate, a is the crack size, and k(a/b) is a correction factor for finite width. If a crack size equal to the width of the vertical stiffener is used, then the a/b ratio can be used to predict a correction factor, k(a/b), of 1.26. By setting the K_I expression equal to the average value of the fracture toughness determined for the beam web steel with the center-hole fracture test, 89.8 MPa √m (81.75 ksi√in), then the remote stress level at fracture can be determined. This gives a value of 92.4 MPa (13.4 ksi), which is greater than the stress in the girder web at the level of the attachment plate. However, brittle fracture of the girder section would cause significant load transfer to the attachment plate, resulting in a stress greater than that required for fracture.

5.2.2 Fracture Analysis of the Web Plate

The general condition of the web plate fracture surface was discussed in Section 3.2.2. As noted in the earlier discussion, the amount of surface corrosion, and the uniformity of the rust formed on the surface, suggests that a fatigue crack in the web did not propagate very far before the brittle fracture occurred. Also, the change in vertical orientation of the crack emanating from the vicinity of the lateral brace indicates that rapid crack extension occurred when the crack was no more than a short distance away from the region of the lateral brace. On the elevation view, the crack changes from vertical to a slightly slanted position just above and below the horizontal gusset plate region. This may indicate that the crack grew in a vertical plane by stable cyclic crack propagation, before changing direction as crack instability occurred.

Similar to the evaluation of the attachment plate, fracture mechanics can be used to examine the fracture state of the girder web plate. As before, it is important to know the state of stress in the web at the critical location, the initial crack size, and the fracture toughness of the steel.

An estimate of the critical crack size was obtained by using the elastic fracture mechanics expression for the stress-intensity factor in an infinite plate under a constant remote stress loading. The crack can be assumed to be either through-thickness with a crack length of 2a, or an elliptical shaped surface crack that does not extend through the full thickness – see Figure 5.1. The stress-intensity factor expression, K_I, is set equal to the fracture-toughness of the material, K_c, to solve for the half-crack size at fracture. The critical crack size for the the through-thickness stress intensity factor expression solution is given as follows:

$$K_I = \sigma \sqrt{\pi a}$$

$$a_{cr} = \frac{1}{\pi}\left(\frac{K_c}{\sigma_{\max}}\right)^2$$

In the above expression, it is assumed that the remote stress at fracture, σ, is the maximum dead load plus live load stress computed at the level of the horizontal gusset plate: 78.2 MPa (11.34 ksi). Also, the fracture toughness corresponds to the average value of K_c measured in the web steel using the center-hole fracture test: 89.85 MPa√m (81.75 ksi √in). Using these values, the critical half-crack size, a_{cr}, is 420.1 mm (16.54 in). This dimension is clearly incorrect since it is greater than the 325.4 mm (12.81 in) distance from the horizontal gusset plate to the bottom of the lower flange plate.

If a finite-width correction factor, F_w, is included in the K_I expression then the estimate for the critical crack size can be improved. The new expression is given as

$$K_I = \sigma \sqrt{\pi a}\ F_w$$

$$F_w = \sqrt{\sec \frac{\pi a}{W}}$$

where W is the total width of the plate and is taken as twice the distance from the horizontal gusset to the bottom of the girder, or 650.9 mm (25.62 in). Using the same values as before for maximum stress and fracture toughness, then the above expression is found to yield a critical half-crack size of 214.4 mm (8.44-in). While this value is more plausible, it is unlikely that it is correct due to the aforementioned comments of uniformity of corrosion on the fracture surface, as well as the deviation in vertical orientation of the crack.

Possible Modifications of K_I

Further examination of the fracture condition can be conducted by modifying the remotely applied stress, or the fracture toughness, or both of these variables. This should be done, of course, only if there are sufficient reasons to justify such modifications. Modifications of these factors will both be discussed.

One possible modification in the original assumptions is to assume that the stresses in the close vicinity to the horizontal gusset plate are near the yield point of the web plate rather than at a level caused by the summation of the primary dead load and live load bending stresses. Elevated stresses in the vicinity of the horizontal gusset plate are actually very likely due to a number of factors. First, there is a small gap in the web between the toe of the vertical stiffener weld and the end of the fillet weld used to attach

the gusset plate to the girder web. In Fisher et al (1990), the amplification of the primary bending stresses in the web gap region are discussed at length, and it was shown that significant amplification of the stress occurs in this region with the greatest stress occurring at the toe of the vertical stiffener. Another factor to consider is the possible residual stresses that occur in this region since there is considerable constraint present from two welds that nearly intersect. Lastly, there may well have been an increase in stresses in this region due to out-of-plane stresses introduced by the lateral bracing members. Relative to this last point, it should be noted that there was evidence of a loose bolt in one of the lateral braces, meaning that the force may not have been transferred evenly across the two horizontal braces, and may instead have introduced additional bending in the web plate.

The critical crack size is computed assuming that the stress-intensity factor with the secant finite-with correction factor is used along with a remote stress equal to the yield-strength of the web plate and a fracture-toughness for the center-hole fracture specimen. As noted in Chapter 4, the average value of yield strength of the web plate was found to be 284.1 MPa (41.2 ksi). The critical half-crack size is now found to be 31.5 mm (1.24-in). The total crack length would be twice the half-crack length, or 63 mm (2.48 in). As long as the critical crack size remains “small”, then the crack front stress will be influenced by the aforementioned factors and, therefore, the assumption that the stress is equal to the yield strength of the web plate will be reasonable.

A second modification in the computed critical crack size would be to use a reasonable “minimum” fracture toughness of the steel. The K_c values for the center-hole fracture toughness specimens were obtained by using the actual plate thickness, and a

reasonable estimate of the lowest service temperature. However, it is well known that significant constraint at a structural detail will produce a decrease in the fracture toughness, and may cause it to approach the minimum possible K_c value, K_{Ic}. In the region of the horizontal bracing member, considerable restraint in the web gap region did certainly exist due to the small web gap and the nearly intersecting fillet welds. From Barsom and Rolfe (1987), an estimate of K_{Ic} for ASTM A36 steel can be assumed equal to 52.76 MPa√m (48 ksi√in). If the K_{Ic} value is used for the fracture toughness, in conjunction with the secant finite-width stress-intensity factor expression and a remote stress level equal to the yield strength, then the critical half-crack size can be found to be 10.9 mm (0.43 in). The corresponding full crack length would be equal to 21.8 mm (0.86 in). This crack length at instability is short enough so as to not experience a large change in remote stress level as the fatigue crack propagates away from the gusset plate region.

Elliptical Crack Front

Another possible scenario that should be examined is the fracture susceptibility of the crack prior to pop-through on the opposite side of the web. In other words, could fracture have occurred as the crack propagated from a small thumbnail-type initial flaw in the web to an elliptically shaped crack that did not quite propagate through the thickness of the web? Again, linear elastic fracture mechanics is used to examine this possibility. The stress-intensity factor is given by the following expression presented in Barsom and Rolfe (1987):

$$K_I = 1.12\,\sigma\sqrt{\frac{\pi a}{Q}}\;M_k$$

where M_k is a correction factor for finite width, and Q is a factor that accounts for the elliptical crack shape. The constant of 1.12 in the stress-intensity factor solution accounts for free surface effects of a surface crack. The correction factor for finite width is given as follows:

$$M_k = 1.0 + 1.2\left(\frac{a}{t} - 0.5\right)$$

The influence of the elliptical crack shape is represented by Φ_o, the elliptic integral.

$$Q = \Phi_o^2$$

$$\Phi_o = \int_0^{\pi/2} \left[1 - \left(\frac{c^2 - a^2}{c^2}\right)\sin^2\theta\right]^{1/2} d\theta$$

In the elliptic integral expression, a is depth of a surface flaw and 2c is the flaw length dimension on the free surface – see Figure 5.1. The solution for the elliptic integral can be obtained using an expression given by Beyer (1976):

$$\int_0^{\pi/2} \left[1 - k^2 \sin^2 x\right]^{1/2} dx = \frac{\pi}{2}\left[1 - \left(\frac{1}{2}\right)^2 k^2 - \left(\frac{1\cdot 3}{2\cdot 4}\right)^2 \frac{k^4}{3} - \left(\frac{1\cdot 3\cdot 5}{2\cdot 4\cdot 6}\right)^2 \frac{k^6}{5} - \cdots\right]$$

In the expression by Beyer (1976), k^2 is simply the ratio of $[(c^2 - a^2)/c^2]$. The expression converges very rapidly with little significant error after only three terms of the sequence.

The only missing factor in the K_I solution is the influence of a stress amplification along the crack front due to a geometrical stress raiser. This feature was discussed earlier, and it is believed that significant stress amplification occurred due to the small web gap region between the end of the gusset plate fillet weld and the fillet weld of the vertical stiffener. Consequently, an amplification factor F_g is also included in the K_I solution to

represent this effect. This is very similar to the F_g factor described by Albrecht and Yamada (1977) in their approximate method for computing stress-intensity factors. The difference, however, is that in this case it is assumed that the amplification is constant and that the stress does not vary significantly along the path of the crack. Consequently, the stress-intensity factor used in this analysis becomes:

$$K_I = 1.12\,\sigma\sqrt{\frac{\pi a}{Q}}\;M_k F_g$$

The fracture susceptibility was explored using the above expression to determine the crack size at which the stress-intensity factor is equal to the critical fracture toughness, K_c. The analysis was conducted for crack depth to length ratios, a/2c, of 1/6, ¼, and ½. These values represent a reasonable range of surface crack depth to length ratios, with the middle value comparable to the surface crack sizes observed by Hassan and Bowman (1996) in tests conducted on fillet welded cover plate details. The crack size values determined by the surface flaw analysis are summarized in Table 5.2. Most of the values correspond to a fracture toughness equal to the K_{Ic} value of 52.8 MPa√m (48 ksi√in). None of a/2c values examined produced a K_I value as large as the fracture toughness of the center-hole fracture toughness of 89.8 MPa√m (81.75 ksi√in) by the time the crack would have propagated through the thickness of the web. Also, an intermediate fracture toughness value half-way between K_{Ic} and K_c for the center-hole test specimen was also examined. The K_c value for this toughness level is 71.5 MPa√m (65.0 ksi√in).

The values shown in Table 5.2 represent a range of possible surface crack sizes that correspond to various fracture conditions. As noted earlier, it is believed that a crack

depth to length ratio of 0.25 is a likely crack size due to previous observations. Values are also reported for stress amplification values that range from 2 to 3.5. The exact stress amplification is nearly impossible to determine since it depends on both the geometry of the detail as well as the out-of-plane bending effects. However, the stress gradients measured by Fisher et al (1990) in the web gap region of lateral bracing details varied considerably but were often between 2.5 and 3. Consequently, if it is assumed that a/2c is equal to 0.25 and that F_g is between 2.5 and 3.0, then the surface crack size should fall between 41 and 47 mm (1.6 to 1.9 in).

Summary of Crack Sizes for Fracture Models

A summary of the surface crack sizes for the various fracture models discussed is listed in Table 5.3. The appropriate remote stress level and the fracture toughness value utilized to compute the critical crack size that would correspond to brittle fracture are also shown in the tabular listing. The surface crack sizes range from a low value of 22 mm (0.86 in) to an upper value of 429 mm (16.88 in).

The upper value, however, is not believed to be a reasonable estimate since the crack size is large enough that it likely would have been detected during visual inspections of the structure. Moreover, the actual fracture path deviates from a vertical position immediately below the horizontal gusset plate and about 50 mm (2 in) above the gusset plate. The orientation of the crack is shown in the photos of the fracture in Figure 5.2. The crack is believed to have propagated by fatigue to a length no more than about 50 to 75 mm (2 or 3 in) before a brittle fracture occurred. Then, during rapid crack extension the crack turned sharply due to out-of-plane bending stress caused by the differential deformation and the forces developed in the lateral bracing members.

The surface crack size values shown in the last four fracture models are all within the limitations described in the above brittle fracture scenario. However, a through thickness crack with a length of only 22 mm (0.86) is also not likely. The crack probably grew through the thickness from the side of the web that faces the vertical stiffener. A 22 mm (0.86 in) length would mean that the crack length to depth ratio would be about 0.58 or greater, which is unlikely. Consequently, the elliptical crack shape model with a surface crack length of 41 to 47 mm (1.61 to 1.86 in) fits well with the features of the actual fracture surface.

Table 5.1 Flexural tension stresses at critical section

Distribution Factor	Cross Section	f_{BOT} MPa (ksi)	f_{DETAIL} Mpa (ksi)
0.757	Steel	112.4 (16.3)	72.9 (10.6)
0.757	Composite	100.0 (14.5)	72.4 (10.5)
0.908	Steel	124.8 (18.1)	80.9 (11.7)
0.908	Composite	109.6 (15.9)	80.4 (11.7)
0.802	Steel	116.5 (16.9)	75.3 (10.9)
0.802	Composite	102.7 (14.9)	74.8 (10.9)

Table 5.2 Surface crack lengths for fracture of an elliptical crack

K_c, MPa√m (ksi√in)	a/2c Ratio	F_g Amplification	Crack Length, 2c mm (in)
52.8 (48)	0.500	2.0	N/A
	0.250	2.0	N/A
	0.167	2.0	N/A
52.8 (48)	0.500	2.5	N/A
	0.250	2.5	47.4 (1.86)
	0.167	2.5	67.0 (2.64)
52.8 (48)	0.500	3.0	25.1 (0.99)
	0.250	3.0	40.8 (1.61)
	0.167	3.0	57.6 (2.27)
52.8 (48)	0.500	3.5	22.2 (0.87)
	0.250	3.5	35.9 (1.41)
	0.167	3.5	50.6 (1.99)
71.5 (65)	0.500	3.0	N/A
	0.250	3.0	N/A
	0.167	3.0	73.9 (2.91)
71.5 (65)	0.500	3.5	N/A
	0.250	3.5	46.1 (1.82)
	0.167	3.5	65.2 (2.57)

Note: N/A means that the crack did not cause fracture for given K_c value.

Table 5.3 Surface crack lengths for various fracture models

Description of Analytical Model for K_I	Remote Stress MPa (ksi)	K_c Value MPa√m (ksi√in)	Surface Crack Size mm (in)
Center Crack in Finite Width Plate	78.2 (11.34)	89.9 (81.75)	429 (16.88)
Center Crack in Finite Width Plate	284.1 (41.2)	89.9 (81.75)	63 (2.48)
Center Crack in Finite Width Plate	284.1 (41.2)	52.8 (48.0)	22 (0.86)
Elliptical Surface Crack in Finite Width Plate	78.2 (11.34)	52.8 (48.0)	41 (1.61), F_g = 2.5 47 (1.86), F_g = 3.0
Elliptical Surface Crack in Finite Width Plate	78.2 (11.34)	71.5 (65.0)	46 (1.82), F_g = 3.5

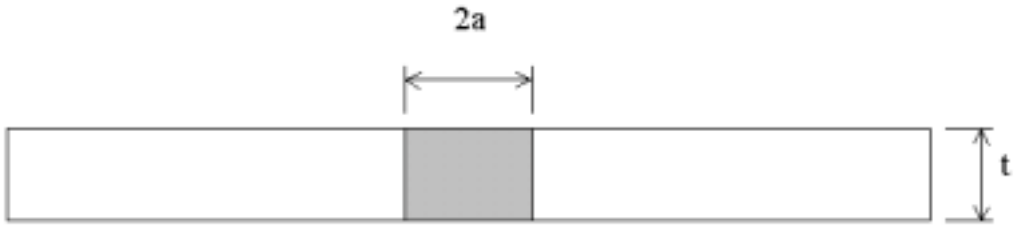

(a) Through-thickness Crack

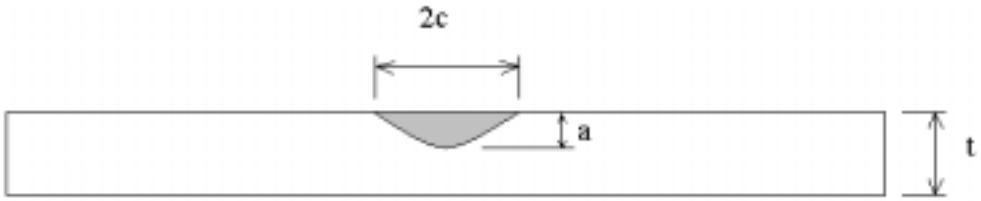

(b) Elliptical Surface Crack

Figure 5.1 Orientation of through-thickness and elliptical crack surface

(a) View of crack above gusset plate

(b) View of crack surface looking down

Figure 5.2 Orientation of brittle fracture crack surface

CHAPTER 6

INSPECTION AND REPAIR

A limited amount of information is available on retrofit and repair guidelines for horizontal gusset plate details similar to the Blue River Bridge. However, based upon the information that is available elsewhere, as well as that which has been gathered from material testing and performance behavior for the horizontal diaphragm detail in question, recommendations were formulated for the inspection and repair of the lateral gusset plate detail.

6.1 Recommendations from Other Sources

A limited amount of information on the repair or retrofit of horizontal gusset plate details is available. One of the primary sources for information on this detail is the NCHRP study that was conducted by Fisher et al (1990). Another source of information that was found is a brief description of repair guidelines issued by the Ohio Department of Transportation.

6.1.1 NCHRP Study 336

Fisher et al (1990) report that the fatigue behavior of web gusset plates appear to be satisfactory for the detail classification assigned by ASSHTO (Category E). In fact, for many of the cyclic tests that they conducted, it was estimated that the total bending stresses exceeded the Category E level. Crack development in the web gaps was found to be compatible with the Category C AASHTO fatigue strength. However, they also noted that fitting a gusset plate around a transverse connection plate without direct attachment

does not appear to be desirable. High stresses were found to occur in the web gap for very small out-of-plane displacements. This situation was observed to result in fatigue cracks at relatively short lives in specimen tests that were conducted as part of the study. Moreover, they recommended that a positive attachment with welds or bolts be made between the horizontal gusset plate and the vertical connection plate. Positive attachment is also mentioned by Fisher et al (1987) as a means to reduce the distortion in web gaps.

Fisher et al (1990) also recommend that the web gap between the toes of the gusset and vertical plate welds should be at least four times the web thickness. An increased gap between the weld toes is known to result in a reduction in the out-of-plane bending stresses. Moreover, they mention in the conclusions to the report that the inability to accurately predict stresses requires positive attachment and a sufficient space between intersecting vertical and horizontal welds. Specifically, they state that, “The horizontal gaps between the intersecting elements should be at least 51 mm (2 in) when welded connections are used and 76 mm (3 in) when bolted connections are used.”

6.1.2 Fatigue Crack Repair

Drilled holes installed at the tips of fatigue cracks that are perpendicular to the primary bending stress are a commonly used repair procedure. Fisher et al (1980) found that fatigue cracks could be prevented from re-initiating at the drilled holes when the following relationship was satisfied:

$$\frac{\Delta K}{\sqrt{\rho}} < 10.5\sqrt{F_y} \qquad \left(F_y \text{ in MPa}\right)$$

$$\frac{\Delta K}{\sqrt{\rho}} < 4\sqrt{F_y} \qquad \left(F_y \text{ in ksi}\right)$$

where ΔK is the stress-intensity factor range for in-plane bending stress, ρ is the radius of the hole, and F_y is the yield strength of the web steel. A simplified expression for the above equations is presented in Fisher et al (1993) by setting the ΔK value equal to the infinite plate expression for stress-intensity factor range. The expression for the required hole diameter, φ, is given as:

$$\phi \geq \frac{S_r^2 L}{35 F_y} \quad \left(for\ F_y\ in\ MPa\right)$$

$$\phi \geq \frac{S_r^2 L}{5 F_y} \quad \left(for\ F_y\ in\ ksi\right)$$

where S_r is the stress-range at the level of the critical detail, and L is the total length of the retrofitted crack. In the above expression, the length of the retrofitted crack is a function of the hole diameter, so the expression must be solved using trial and error or by a simple numerical scheme available in most commercially available math software packages and in many mathematical calculators. Fisher et al (1993) point out that a factor not considered in the above expression is the type of hole preparation and the finish for the hole. They recommend that drilled holes should be ground to a polished finish to remove burrs or other surface irregularities. Also, they recommend that the holes be inspected using dye penetrant to ensure the crack tips were effectively removed.

6.1.3 Ohio Department of Transportation Retrofit

A lower lateral connection retrofit was discussed during a recent meeting of the Midwest Bridge Maintenance Working Group. The retrofit was based on an inter-office communication of the Ohio Department of Transportation. The purpose of the retrofit was to minimize the occurrence of cracking in the positive moment region of girders with

lower lateral connections. The retrofit involves core-drilling through the lateral gusset plates to increase the gap between the fillet weld toes that connect the vertical stiffeners (or connection plate) and the horizontal gussets plates to the web.

Two different core-drilling schemes were available, as shown in Figures 6.1 and 6.2. In one scheme, a large 76 mm (3 in) diameter core is extracted from the horizontal gusset plate, while in the other methods a comparable gap size is accomplished by using three overlapping cores of a 51 mm (2 in) diameter. Both retrofit methods provide for an increased gap between the weld toes and retain the positive connection between the horizontal gusset plate and the vertical stiffener.

The retrofit procedures also require that all remnants of the gusset-to-web/stiffener and excess gusset material must be removed by grinding. Also, they recommend that the ends of the welds should be ground to a smooth, streamline contour, with no rough edges, gouges or surface irregularities. After repair, they require that the region be pencil sandblasted in the corners and checked for cracking by using dye penetrant inspection. Lastly, the requirements indicate that any cracks discovered shall be arrested by drilling 38 mm (1 ½ in) diameter holes at the crack ends and rechecking with dye penetrant.

6.2 Relevant Factors for the I-64 Blue River Bridge

The relevance of the retrofit and repair factors described in the previous section are now discussed in light of the conditions that existed at the time of the brittle fracture of the I-64 Blue River Bridge. A couple of other relevant factors will be reviewed also in this section.

The two primary retrofit features previously discussed are, first, the size of the gap between the weld toes of the vertical stiffener and horizontal gusset plates, and second, the existence of a positive connection between the vertical and horizontal plates. In the case of the I-64 Blue River Bridge, both of these factors were not satisfactorily addressed.

The gap between the weld toes of the vertical stiffener and the horizontal gusset plate was about 11 mm (7/16 in). This dimension is obtained by subtracting the 8 mm (5/16 in) weld size that was used to attach the vertical stiffener to the web of the girder from the 19 mm (3/4 in) chamfer on the gusset plate. The actual as-built chamfer was reduced in size considerably since the gusset plate slot on the side that fractured was flame cut to accommodate the actual position of the vertical plate – see Figure 3.11. While this did not change the relative position of the vertical and horizontal welds, a much larger weld was required to connect the gusset plate to the vertical stiffener on the side that fractured to fill-in the increased gap created by the additional notching. The additional weld undoubtedly resulted in increased residual stresses due to the large size of the stiffener-gusset plate weld and from significant constraint produced by three welds that nearly intersect.

The existing gap size of the weld toes was roughly 11 mm (7/16 in). This dimension is considerably smaller than the 4t gap size recommended by Fisher et al (1990). The I-64 Blue River Bridge had a web thickness of 12.7 mm (1/2 in), which would result in a recommended gap size of 50.8 mm (2 in). Moreover, the gap size produced by the Ohio DOT retrofit recommendations would be roughly 50 to 75 mm (2 to 3 in) depending upon which repair option was selected. An increased weld toe gap would be beneficial because it would decrease the stress amplification effect and reduce the magnitude of the

out-of-plane bending stresses developed in the weld gap region. The reduced bending stress in the weld gap region would, in turn, reduce the likelihood of initiating of fatigue cracks that would eventually propagate to a size that could precipitate a brittle fracture.

The second feature was related to a positive connection between the attachment plate and the vertical stiffener. The initial stiffener-to-gusset plate connection provided for a positive connection. However, it is believed that clear evidence exists to support the notion that the attachment plate fractured prior to the overall brittle fracture – see the discussion in Sections 3.2.1 and 5.2.1. If the attachment plate did indeed fracture prior to the brittle fracture of the overall girder, then a positive connection between the lateral gusset and the vertical stiffener did not fully exist. Fisher et al (1990) discuss the deleterious ramifications of not having a positive connection. They state that, “Fitting gusset plates around a transverse connection plate without a direct attachment …does not appear to be desirable. Relatively high cyclic stresses developed in the web gap at small out-of-plane deformations. This resulted in weld toe stress range levels that exceeded the fatigue limit and resulted in cracks at relatively short fatigue lives.” Although the detail used by Fisher et al (1990) was somewhat different than the gusset detail used in the I-64 Blue River Bridge, the fatigue behavior in the web gap region caused by a lack of positive attachment would have been similar.

It is believed that the premature fracture of the lateral gusset plate was caused by the poor welding procedure that was used to attach the lateral gusset to the vertical stiffener after the plate was notched for fit-up and assembly in the field. Tensile stresses acting normal to the gusset-to-stiffener weld, along with significant welding

discontinuities introduced when depositing weld metal into the large gap created by notching the gusset plate, resulted in a situation that weakened the gusset plate.

Two additional factors may have also contributed somewhat to the brittle fracture. First, there were reports that notable impact was introduced at one end of the bridge as the vehicles came onto the bridge structure. Although it is not known how significant this factor was since it was not examined experimentally, some additional lateral forces certainly could have been introduced through the lateral bracing system and resulted in additional out-of-plane bending in the critical region. The second factor is the presence of loose bolts on one side (the fracture side) of the lateral bracing attachment plate. As noted earlier, a loose connection on one side may have reduced the transfer of lateral bracing forces across the connection and resulted in increased lateral, out-of-plane bending stresses in the critical connection region. While both of these factors may have played some small role, it is not believed that either of them are the primary reasons for the brittle fracture. It is believed, however, that efforts should be taken to minimize their occurrence.

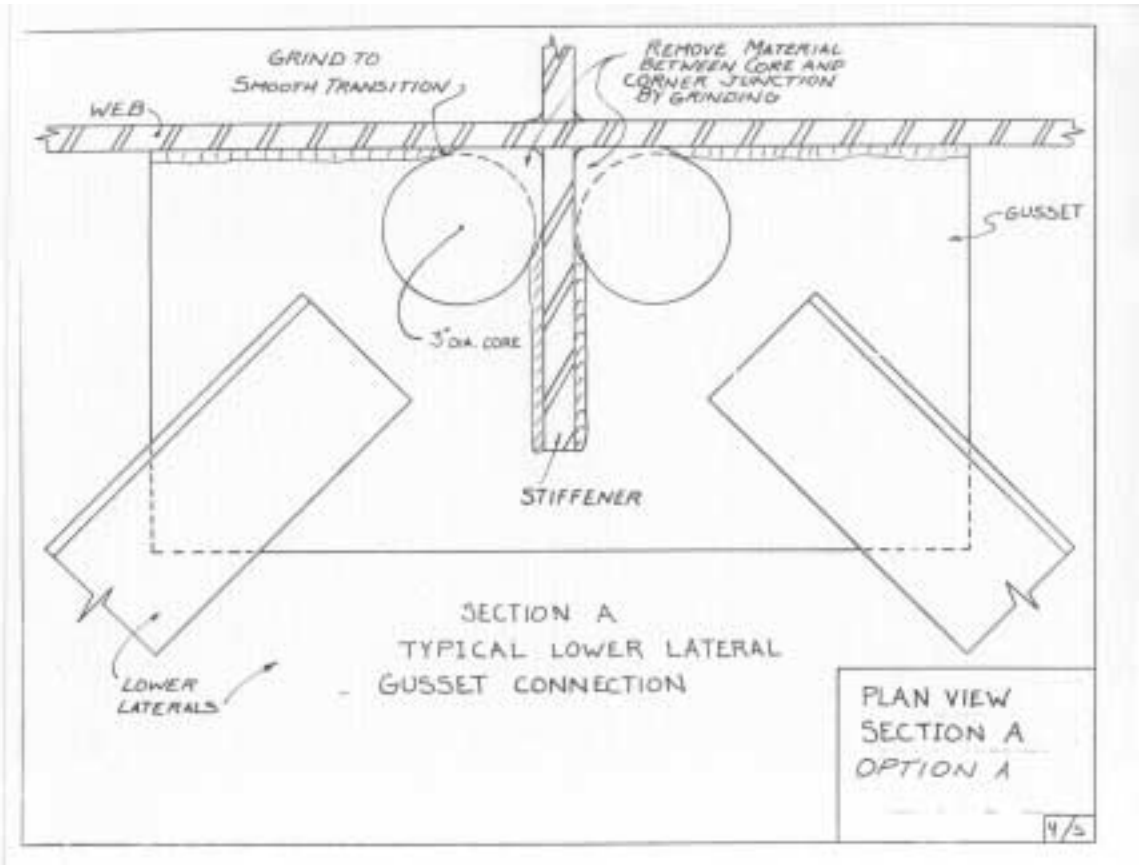

Figure 6.1 Drilled Hole Repair Procedure to Increase Web Gap (Ohio Department of Transportation)

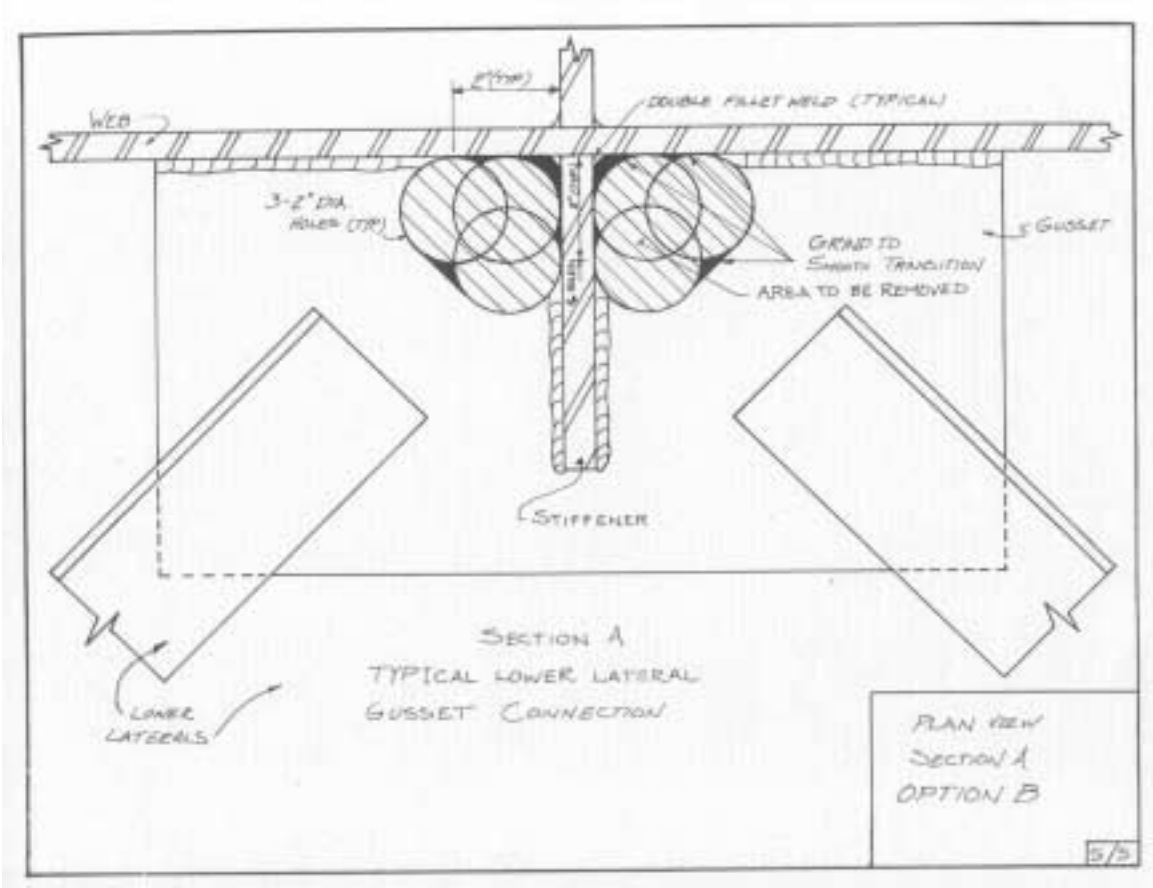

Figure 6.2 Multiple Drilled Hole Repair Procedure to Increase Web Gap (Ohio Department of Transportation)

CHAPTER 7

CONCLUSIONS AND RECOMMENDATIONS

7.1 Summary and Conclusions

The objectives of the research project were to evaluate the brittle fracture that occurred on the I-64 Blue River Bridge in southern Indiana (Harrison County), to develop recommendations for the inspection of lateral bracing details similar to the one that fractured, and to formulate suggestions for retrofit and/or repair of the critical connection detail. The goal was to understand the principal reasons behind the fracture so that measures could be taken to minimize or prevent brittle fractures in other bridge structures that contain a similar structural detail.

The scope of the research involved an examination of the brittle fracture by reviewing several different aspects. A search of the literature was conducted to examine information published on related types of lateral bracing details. Information was gathered on physical and environmental factors related to the performance and behavior of the bridge structure. Also, the bridge response was evaluated by performing experimental tests to examine the behavior of the materials involved and by conducting analytical modeling to understand the range of bending stresses that were acting on the critical detail. Lastly, fracture mechanics principles were also employed to understand various possible rapid crack extension mechanisms for the lateral bracing detail.

A number of observations relevant to the fracture behavior were extracted from the experimental and analytical results presented in previous chapters. A summary of

pertinent observations and the principal conclusions drawn from these observations are noted in the following:

(1) Based upon a visual examination of the fracture surfaces of the I-64 Blue River Bridge girder, it is believed that a brittle fracture initiated in the girder web near the intersection of a vertical connection plate and lateral bracing connection plate. Moreover, it is believed that a fatigue crack initiated in the web plate gap region immediately adjacent to the weld toe of the web-to-vertical stiffener weld. This fatigue crack then grew in a stable fashion due to primary and secondary bending stresses until the crack reached a size sufficient to trigger the brittle fracture.

(2) The brittle fracture occurred in the exterior girder on the northern side of the eastbound structure. The girder that experienced the brittle fracture is located outside of the left lane, which typically carries a lighter volume of traffic. Traffic counts collected in 1994 confirm that the left lane of the eastbound traffic was considerably lighter. The measured average daily traffic in the lane closest to the fracture was 698 vehicles per day, and the average daily truck traffic was only 155 vehicles per day. By rough extrapolation based upon the truck traffic measured, it is estimated that the left lane adjacent to the fracture experienced only 867,000 truck passages for the entire time that the structure had been in service.

(3) A period of extremely cold weather occurred in January of 1994. The lowest temperature recorded during this period was –30 ^{o}C (-22 ^{o}F). This temperature is close to the low end of the Zone 2 lowest anticipated service temperature expected for the bridge structure. Low temperatures are known to result in low fracture

toughness levels in structural steel. It is believed that the brittle fracture occurred during this time.

(4) Testing was conducted to determine the mechanical and chemical properties of the web and flange steel. Mechanical coupon tests indicate that the yield strength of the web steel is over 20 percent greater than that of the flange steel, although they both have comparable tensile strength values. The web satisfies specification requirements for ASTM A36, while the flange plate does not. The carbon equivalent computed on the basis of the steel chemistry for both the flange and the web steel indicates that neither of the steels is susceptible to excessive hardenability and that they are both considered easy to weld.

(5) Charpy-V Notch testing was conducted to evaluate the fracture toughness of the flange and web steel. The testing demonstrated that the average CVN levels for both the flange and the web plates exceeded the minimum energy level required for nonfracture-critical members. Moreover, the flange plate CVN level exceeded the minimum energy level for fracture critical members. Nevertheless, since the number of girders in the bridge provide for some redundancy, then the nonfracture-critical toughness values can be used. On that basis, the flange and web plates used in the Blue River Bridge satisfy the AASHTO fracture toughness requirements.

(6) Examination of the fracture surface of the lateral attachment plate indicates that at least a portion of the plate was fractured well before the brittle fracture occurred. A significant amount of rust was present on the fracture surface in the region immediately adjacent to the vertical stiffener. Further examination revealed that

significant lack of fusion discontinuities were present as a result of the fabrication procedure and likely contributed to the fracture (or partial fracture) of the attachment plate.

(7) Examination of the web fracture surface reveals the presence of a herringbone pattern that points back to the attachment plate region from above and below. There is a small portion of the web plate that is fairly flat and shows no such indications. It is believed that this is the area from which a fatigue crack propagated prior to brittle fracture. The rust product on the web plate is relatively uniform and, consequently, it is believed that this indicates that the fatigue crack did not become very large, and was perhaps not even through-thickness, when the brittle fracture occurred.

(8) Analysis based on elastic fracture mechanics indicates that an elliptical crack with a one-to-four aspect ratio could develop a stress-intensity factor equivalent to the estimated fracture toughness of the steel prior to propagating through the thickness of the web. The surface crack length associated with the critical crack size is about 44 mm (1.75 in). This length is not too different than the size of the flat region observed on the fracture surface.

(9) Four factors are believed to be responsible for elevating the stresses in the gusset-to-stiffener connection welds. First, lack of a positive attachment between the horizontal gusset plate and the vertical diaphragm connection plate (stiffener) resulted when a portion of the attachment plate fractured. Second, only a small lateral gap (less than four times the web thickness) separated the weld toes. Third,

some of the bolts that were used to connect the diagonal bracing members to the gusset plate were loose and likely resulted in increased out-of-plane bending of the girder web. And fourth, impact forces were known to exist at one end of the structure and likely produced additional lateral forces that caused out-of-plane bending. The first three factors are believed to be of primary importance.

7.2 Recommendations for Inspection and Repair

Based upon the findings summarized in this study of the I-64 Blue River Bridge brittle fracture, it is suggested that the following recommendations be considered to improve the performance and behavior of structures with similar lateral bracing details.

(1) Inspect lateral bracing connections to determine if the gusset plate has fractured. If fracture, or even partial fracture, has occurred then the plate must be replaced or repaired. Positive connection between the lateral braces and the vertical stiffener must be maintained through the used of bolted or welded connections.

(2) Inspect the girder web for evidence of fatigue cracking in the immediate vicinity of the regions where the lateral gusset plates and the vertical stiffener intersect. If a fatigue crack is found, then holes should be drilled through the web that remove the tips of the fatigue crack. The diameter of the drilled holes should conform to a size obtained by considering the cyclic stress level at the detail and the length of the crack.

(3) Holes should be drilled through the lateral gusset plate to produce a gap between the welds toes that is at least four times the web thickness or 51 mm (2 in), whichever is larger. The holes should be located adjacent to and on each side of the vertical stiffener.

(4) The bolts that are used to connect the lateral bracing members to the horizontal gusset plates should be checked for tightness. Loose bolts should either be removed and replaced or re-tightened at the discretion of the engineer.

(5) The bridge structure should be inspected to ensure that no conditions exist that are producing excessive impact forces that may introduce damaging longitudinal forces.

7.3 Recommendations for Implementation

A brittle fracture typically does not occur unless a number of factors that are detrimental to the behavior of a structure occur simultaneously. It is believed that a deleterious sequence of events in fact occurred in 1994 on the I-64 Blue River Bridge. However, a number of the factors that led to the brittle fracture can be prevented through corrective maintenance and repair by following the recommendations for inspection and repair as outlined in this report. If these procedures are implemented correctly, then it is believed that the steel structures with gusset-to-stiffener details can be made to be safer and provide for an improved service life.

Structures with gusset-to-stiffener details, especially those along the I-64 corridor in Indiana, should be inspected to detect any evidence of fatigue cracks that have developed in the girder web at those regions where the lateral gusset plates intersect vertical stiffeners. The bridge inspectors should look for fractures that have developed in the horizontal attachment plates, especially in those regions directly adjacent to the vertical stiffener. Also, the bolts used to connect the horizontal bracing members to the gusset plate should be checked to ensure that they are adequately tightened.

Moreover, structures that have gusset-to-stiffener details should be retrofitted to reduce the out-of-plane bending that occurs. Holes should be drilled through the horizontal gusset plate on each side of the vertical stiffener to reduce excessive bending caused by a “small” gap between weld toes. Also, a positive connection between the stiffener and the gusset plate must be maintained through a bolted or welded connection.

LIST OF REFERENCES

"AASHTO LRFD Bridge Design Specifications," (1994). First Edition, American Association of State Highway and Transportation Officials, Washington, D.C.

"AASHTO Standard Specifications for Highway Bridges," (1996). Sixteenth Edition, American Association of State Highway and Transportation Officials, Washington, D.C.

"AASHTO LRFD Bridge Design Specifications," (1998). Second Edition, American Association of State Highway and Transportation Officials, Washington, D.C.

Albrecht, P. and Yamada, K. (1977). "Rapid Calculation of Stress Intensity Factors," *Journal of the Structural Division*, ASCE, Vol. 103, No. ST2, 377-389.

Barsom, John M. and Rolfe, Stanley T. (1987). *Fracture & Fatigue Control in Structures – Applications of Fracture Mechanics.* 2nd Edition, Prentice-Hall, Inc., Englewood Cliffs, N.J.

Beyer, William H. (1976). *Standard Mathematical Tables*. Twenty-fourth Edition, CRC Press, Cleveland, Ohio.

Bowie, O.L. (1964). "Rectangular Tensile Sheet with Symmetric Edge Cracks," *Journal of Applied Mechanics*, ASME, Vol. 31, No. 2, 208-212.

"Bridge Welding Code," (1995). American Welding Society, ANSI/AASHTO/AWS D1.5-95.

Demers, C.E. and Fisher, J.W. (1990). "Fatigue Cracking of Steel Bridge Structures Volume I: A Survey of Localized Cracking in Steel Bridges – 1981 to 1988," Federal Highway Administration, Report No. FHWA-RD-89-166, 342 pp.

Fisher, J.W., Pense, A.W., and Roberts, R. (1977). "Evaluation of Fracture of Lafayette Street Bridge," *Journal of the Structural Division*, American Society of Civil Engineers, 103 (ST7), 1339-1357.

Fisher, J.W., Barthelemy, B.M.., Mertz, D.R., and Edinger, J.A. (1980). "Fatigue Behavior of Full-Scale Welded Bridge Attachments," *National Cooperative Highway Research Program, Report 227*, Transportation Research Board, 47 pp.

Fisher, J.W. (1984). *Fracture and Fatigue of Steel Highway Bridges, Case Studies*. John Wiley & Sons, New York, NY.

Fisher, J.W., Yen, B.T., and Wagner, D.C. (1987). "Review of Field Measurements for Distortion-Induced Fatigue Cracking in Steel Bridges," *Transportation Research Record*, No. 1118, pp. 49-55.

Fisher, J.W., Jin, J., Wagner, D.C., and Yen, B.T. (1990). "Distortion-Induced Fatigue Cracking in Steel Bridges," *National Cooperative Highway Research Program, Report 336*, Transportation Research Board, 43 pp.

Fisher, J.W., Nussbaumer, A., Keating, P.B., and Yen, B.T. (1993). "Resistance of Welded Details Under Variable Amplitude Long-Life Fatigue Loading," *National Cooperative Highway Research Program, Report 354*, Transportation Research Board, 32 pp.

Hassan, Ahmed F. and Bowman, Mark D. (1996). "Fatigue Crack Repair of Steel Beams With Tapered Cover Plate Details," *Journal of Structural Engineering*, ASCE, 122(11), 1337-1346.

Hertzberg, Richard W. (1976). *Deformation and Fracture Mechanics of Engineering Materials*. John Wiley & Sons, New York, NY.

Kulicki, J.M., Murphy, R.E., Mertz, D.R., and Fisher, J.W. (1986). "Fatigue Cracking on I-79 Bridges in West Virginia," *Proceedings*, International Bridge Conference, Pittsburgh, PA, pp. 93-102.

"Procedure Handbook of Arc Welding," (1994). Thirteenth Edition, The Lincoln Electric Company, Cleveland, Ohio.

"Standard Specifications For Highway Bridges," (1986). Sixteenth Edition, American Association of State Highway and Transportation Officials, Washington, D.C.

"Standard Test Methods and Definitions for Mechanical Testing of Steel Products," (1996). ASTM A370-96, American Society for Testing and Materials, Vol. 01.03.

"Test Methods for Notched Bar Impact Testing of Metallic Materials," (1996). ASTM E23-96, American Society for Testing and Materials, Vol. 03.01.

"Test Methods for Tension Testing of Metallic Materials," (1993). ASTM E8-93, American Society for Testing and Materials, Vol. 03.01.

Timoshenko, S.P. and Goodier, J.N. (1970). *Theory of Elasticity*. McGraw-Hill, New York, NY.

GENERAL DISCLAIMER

This document may have problems that one or more of the following disclaimer statements refer to:

- This document has been reproduced from the best copy furnished by the sponsoring agency. It is being released in the interest of making available as much information as possible.
- This document may contain data which exceeds the sheet parameters. It was furnished in this condition by the sponsoring agency and is the best copy available.
- This document may contain tone-on-tone or color graphs, charts and/or pictures which have been reproduced in black and white.
- This document is paginated as submitted by the original source.
- Portions of this document are not fully legible due to the historical nature of some of the material. However, it is the best reproduction available from the original submission.